Resonances in electron scattering by molecules on surfaces

R. E. Palmer

Cavendish Laboratory, University of Cambridge, Madingley Road, Cambridge, CB3 0HE, United Kingdom

P. J. Rous

Department of Physics, University of Maryland Baltimore County, Catonsville, Maryland 21228

This article reviews the discovery, exploration, and application of negative-ion resonances in inelastic electron scattering by molecules adsorbed on surfaces. A major theme of the review is the degree to which the properties of resonances in free molecules are perturbed by adsorption. The influence of the surface upon the energy, lifetime (width), symmetry, and decay channels of molecular resonances is discussed, in the light of both experimental and theoretical studies of a wide range (from diatomic molecules to polymers) of both weakly bound (physisorbed) and strongly bound (chemisorbed) molecules. The metallic image potential, electron scattering by the atoms of the surface, and chemical bonding in chemisorption systems are found to be key factors in determining the energy, width, and symmetry of resonances in molecular adsorbates. In the case of oriented adsorbed molecules, the angular distribution of scattered electrons is found to reflect not only the symmetry of the resonant state (as in the gas phase), but also the orientation of the molecular axis. Coherent elastic electron scattering by the surface can modulate the angular distributions, as well as the shape of the resonance profile. Selection rules that govern the observed resonance behavior are discussed. A further consequence of adsorption is the enrichment of the range of channels into which resonances may decay, and the excitation of both molecule-surface and intermolecular vibrational modes has been established. The article concludes with an evaluation of future prospects for the investigation and application of resonances in adsorbed molecules.

CONTENTS

I. Perspective 384
II. Preliminaries 384
A. Physics of resonance scattering in the gas phase 385
1. What is resonance scattering? 385
2. Classification of molecular resonances 385
3. Overview of the resonance scattering process 387
4. Mechanism of vibrational excitation 387
a. Outline 387
b. Formal treatment 388
5. Signatures of resonance scattering 389
B. Adsorption of molecules on surfaces 389
C. Electron scattering by molecules on surfaces: Scattering mechanisms 390
1. Dipole scattering 390
2. Impact scattering 391
D. Electron scattering by molecules on surfaces: Experimental considerations 392
III. Resonance Scattering by Molecules on Surfaces 393
IV. Resonance Energy and Lifetime 394
A. Effect of the image potential and the short-range surface potential 394
1. Theoretical models 395
a. The image potential 395
b. The short-range surface potential 397
c. The band structure of the surface 399
2. Experimental results and analysis 401
B. Effect of chemical bonding to the surface 405
1. Theoretical models 405
2. Experimental results and analysis 406
C. Effect of interaction with coadsorbed molecules 408
V. Resonance Symmetry and Molecular Orientation 409
A. Angular distribution of scattered electrons 409
1. Theoretical models 410
a. The isolated, oriented molecule 410
b. The molecule on the surface: the image potential 412
c. The molecule on the surface: multiple elastic scattering 415
d. The molecule on the surface: selection rules 417
2. Experimental results and analysis 419
B. Differential capture cross sections 423
C. Apparent shifts of the resonance energy in oriented molecules 424
1. Theoretical model 424
2. Experimental results and analysis 425
D. Selective resonance population in oriented molecules 426
1. Theoretical model 426
2. Experimental results and analysis 427
VI. Resonance Decay Channels 429
A. Theoretical models 429
1. Mode-selective vibrational excitation 429
2. Resonant excitation of molecule-surface vibrational modes 430
B. Experimental results and analysis 430
1. Mode-selective intramolecular vibrational excitation in polyatomic molecules 430
2. Resonant excitation of intermolecular modes 434
3. Resonant excitation of molecule-surface modes 434
4. Resonant excitation of rotational modes 435
5. Branching ratios in resonance decay 435
VII. Future Directions 436
A. Unrecognized resonances? 436
B. Development of the theoretical models 436
C. Applications of resonance electron scattering 437
1. Vibrational states 437
2. Electronic structure 437
3. Geometric structure 437
D. Resonances in electron scattering by atoms on surfaces 438
References 439

I. PERSPECTIVE

The observation of resonances in the cross sections for electron scattering by gas-phase molecules was a well established experimental phenomenon by the early 1970s. Since that time the field of gas-phase electron-molecule scattering has made progress on three fronts: (i) improvements in experimental techniques have allowed more accurate and more comprehensive measurements of molecular cross sections; (ii) the number of molecules in which resonances have been observed has increased substantially, in particular to include many polyatomic as well as diatomic molecules; and (iii) theoretical methods have improved enormously, such that *ab initio* calculations often show remarkable quantitative agreement with the experimental data. Thus the field has continued to mature since the time when George Schulz published his oft cited reviews on resonances in electron-atom and electron-molecule collisions in 1973 (Schulz, 1973a, 1973b). The aim of the present review is to attempt to do for the emerging field of resonances in electron scattering by molecules on surfaces what the Schulz reviews did for the gas phase, that is, to provide both a benchmark enabling researchers to survey the state of the field comprehensively and a foundation on which further work can be built.

Interest in the resonances observed in electron scattering by adsorbed molecules is sharpened by the importance of similar states in a number of electron spectroscopies—photoemission (Plummer and Gustafsson, 1977), x-ray absorption (Woodruff, 1986), and inverse photoemission (Smith and Woodruff, 1986), as well as surface-enhanced Raman spectroscopy (Otto *et al.*, 1989)—and by their postulated role in a whole variety of dynamical processes at surfaces, such as photodesorption (Gadzuk *et al.*, 1990; Zhou *et al.*, 1991), molecule-surface scattering (Haochang *et al.*, 1986; Gadzuk, 1988), and dissociative molecular adsorption (Holloway and Gadzuk, 1985; van den Hoek and Baerends, 1989). These dynamical processes will be the subject of a forthcoming review (Palmer, 1992). Suffice it to say here that electron-scattering experiments provide a vital database for models of these processes, since they elucidate the energy, the lifetime, and the symmetry of the resonant states of molecules on surfaces, as we shall see.

While we are concerned in this article to give an accurate account of the historical development of the field of resonances in electron scattering by adsorbed molecules, our priority is to lay out critically and thematically the physical issues underpinning the work that has been reported to date. With this focus in mind, the article is organized in the following way. In the next section (Sec. II) we lay out a background against which to set investigations of resonance scattering by adsorbed molecules. We discuss the fundamental physics of the resonance scattering process and how it is manifest in the gas-phase studies; we consider the different ways in which a molecule can be bound to the surface of a solid and the various electron-scattering mechanisms that have been isolated in such systems; and we give some attention to the type of experiment that exposes the resonance scattering mechanism in preference to the competing channels of electron-molecule interaction. Section III surveys in outline the factors that modify the nature of resonance scattering in the gas phase when a molecule is adsorbed on a surface. The next two sections take a detailed look at these effects. In Sec. IV we explore the perturbation of the energy and the width (lifetime) of the resonant state due to adsorption. In Sec. V we consider the influence of adsorption on the symmetry of the resonant state, with particular reference to the alignment of the molecular axis because of adsorption and the way this is evident in the angular distribution of scattered electrons. Section VI investigates the various vibrational, rotational, and electronic channels into which resonances can decay and illustrates how adsorption of the molecule enriches the range of possible decay routes. Finally (Sec. VII) we contemplate how the study of resonance electron scattering by molecules on surfaces might develop in the future.

This review is concerned with resonances in electron scattering by molecules on surfaces and does not address itself to the process of dissociative attachment (i.e., molecular dissociation induced by electron attachment) in adsorbed or condensed molecules. A couple of recent reviews by Sanche already provide a quite extensive treatment of this topic (Sanche, 1989, 1990). Again, our main concern is with electron scattering by molecules *adsorbed* on solid surfaces, rather than with condensed molecular solids. For discussions of the latter topic the reader is again referred to the reviews of Sanche.

We aim in this article to review the progress that has been made on both the experimental and the theoretical fronts. In keeping with our aim of focusing on conceptual issues, theoretical models and experiments pertaining to a particular issue are discussed in adjacent subsections within the appropriate section of the article.

II. PRELIMINARIES

In this section we discuss a series of topics as a background to the presentation of detailed studies of resonance scattering by adsorbed molecules in later sections. We begin with a discussion of the basic physical principles of resonance electron scattering, as determined by gas-phase studies. Then we outline the nature of molecular adsorption on solid surfaces, considering in turn weak (physisorption) and strong (chemisorption) molecule-surface bonds. We address the different scattering mechanisms that have been isolated in studies of electron scattering by adsorbates and complete the series of preliminary topics by a consideration of the technical aspects of the experimental exploration of resonance scattering by molecules on surfaces.

A. Physics of resonance scattering in the gas phase

In this section we describe the mechanism of resonance scattering by isolated molecules and summarize the types of molecular resonant state that have been isolated from gas-phase studies; we explore the way in which the short-lived negative ion decays into excited vibrational states of the host molecule when the probe electron is reemitted, and finally outline the experimental signatures of resonance scattering in the gas phase.

1. What is resonance scattering?

In the context of electron scattering by atoms and molecules, resonance scattering is an electron-impact phenomenon which involves the formation of a transient atomic or molecular negative ion. At a particular electron energy, commonly referred to as the resonance energy, the incident electron becomes temporarily trapped in the vicinity of the target molecule. The electron is captured by a quasibound or virtual molecular orbital and is reemitted after a time (typically 10^{-10} to 10^{-15} s) substantially longer than the transit time for unhindered propagation across the molecule. Since the molecule acquires an extra electron during this process, we can regard this electron-scattering phenomenon as the formation of a short-lived negative ion or compound state. From an electron-scattering viewpoint, the formation of the negative ion is manifest as a characteristic peak or resonance in the scattering cross section, thus the term *resonance electron scattering.* For the purposes of this article we regard the terms *resonance, negative ion,* and *compound state* as referring to the same physical entity, and the various terms will be used interchangeably.

A basic description of resonance electron scattering is a familiar part of a number of undergraduate quantum mechanics texts (e.g., Gasiorowicz, 1974), where it emerges as a consequence of the separation of the radial and angular parts of the Schrödinger equation. Consider, for example, the simple square-well potential represented in Fig. 1, where the effective radial potential seen by an electron consists of the superposition of the real attractive potential and a repulsive centrifugal term. The centrifugal term builds a penetrable potential barrier outside the well, which can temporarily trap incident electrons with positive energy. The electron energies at which this trapping occurs are such as to allow the electron to tunnel through the centrifugal barrier and couple into a quasibound level of the well. For a square well, the lowest of these energy levels have approximately the same energies as the bound eigenstates of the square well with infinite walls.

In contrast to this simple model, the origin of the richness of the resonance scattering phenomenon in molecules lies primarily in the number of different channels into which the molecular negative ion can decay. In the case of the simple square well, the electron simply tunnels out of the potential barrier and goes on its way. As

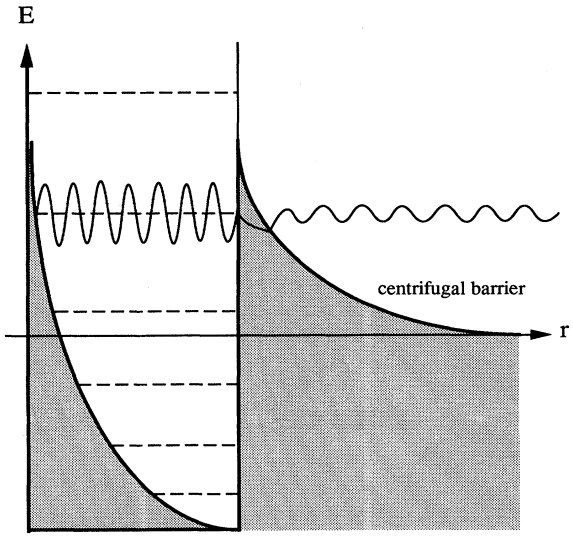

FIG. 1. Schematic diagram of the effective radial potential showing the centrifugal barrier when the real potential is a spherical square well. The dashed lines represent the location of the energy levels of an infinite-depth square well, which are approximately equal to the energies of the resonances above the vacuum level.

Schulz (1973b) has noted, the beauty of molecules is the variety of decay channels available to the negative ion, which may leave the molecule in an excited state. Thus negative-ion formation may result in vibrational, rotational, and electronic excitation or even dissociation of the molecule (dissociative attachment). Resonance electron scattering provides a means of observing such processes in both adsorbed and gas-phase molecules.

2. Classification of molecular resonances

Molecular negative-ion resonances are traditionally divided into two categories, *single-particle* and *core-excited resonances.* When the square well described above is replaced by the potential of a real molecule, the simple picture of resonance scattering outlined in the previous section can be qualitatively preserved. In this case, known as a *single-particle shape resonance,* the incident electron feels a superposition of the polarization, exchange-correlation, and centrifugal potentials, which leads to an electron-molecule potential of the type represented schematically in Fig. 2(a). In a scattering picture, the impinging electron tunnels through the centrifugal barrier into the inner region of the potential-energy curve, where it is confined (in a quasistable state) until it tunnels out again after a time characterized by the resonance lifetime τ. Thus a short-lived molecular ion is formed. The resonance occurs at an electron energy (and therefore wavelength) such that a quasistationary wave is produced in the inner region of the electron-molecule potential-energy curve, a consequence of the constructive interfer-

ence of waves reflected back and forth in that region. The term "shape resonance" reflects the fact that the shape of the potential is responsible for the trapping of the electron.

In contrast to the simple square-well case, resonance electron scattering from a molecule may also occur through a more complex process involving the electronic excitation of the target molecule as the impinging electron approaches. In the case of a core-excited resonance, the probe electron is then trapped in a bound or quasi-bound state of the electronically excited host, represented schematically in Figs. 2(b) and 2(c). Typically, the excitation of the host molecule involves the promotion of a single host electron, leaving a hole in a lower-energy molecular orbital, so that core-excited resonances are typically two-electron/one-hole states.

Core-excited resonances are further classified into two types, *Feshbach resonances* and *core-excited shape resonances.* Feshbach resonances [Fig. 2(b)] arise when the probe electron is temporarily trapped in a bound state of the electronically excited host molecule. The total energy of this type of negative ion is less than that of the electronically excited neutral molecule; in other words, the electronically excited neutral molecule (the "parent" of the resonance) exhibits a positive electron affinity. Thus a characteristic feature of a Feshbach resonance is that it cannot decay back into the (higher-energy) parent state, although this does not preclude decay into the ground state of the neutral molecule or electronically excited states other than the parent. By contrast, core-excited resonances, in which the total energy of the negative ion is greater than that of the parent, electronically excited, neutral molecule [Fig. 2(c)] are called *core-excited shape resonances.* These resonances are similar to simple single-particle shape resonances except that they involve electron attachment to an electronically excited state of the neutral molecule rather than the electronic ground state.

One can also view the formation of a negative-ion state as the occupation by the probe electron of an empty or partially occupied molecular orbital of the host molecule, which, in the case of a core-excited resonance, is accompanied by the promotion of one of the host electrons to an orbital of higher energy. Consider Fig. 3, which shows schematic representations of the electronic configurations of various negative-ion states of the O_2 molecule. Here both the $^2\Pi_g$ state and the $^4\Sigma_u$ state of the O_2^- are single-particle shape resonances, produced by

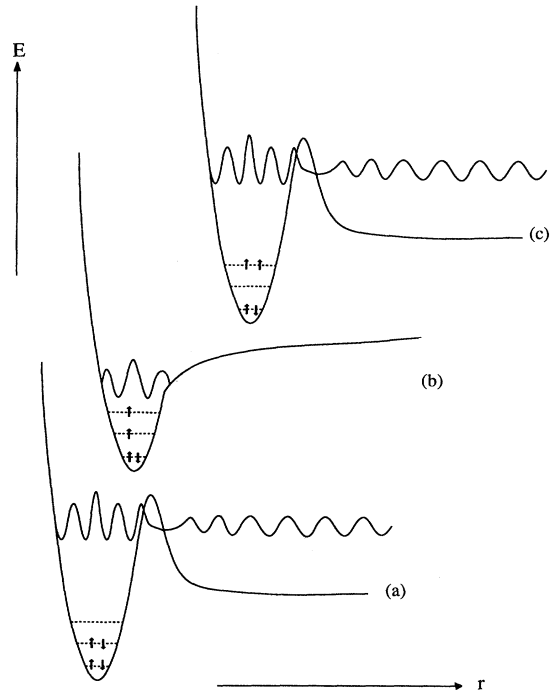

FIG. 2. Schematic diagram showing various types of negative-ion resonances found in molecules: (a) A single-particle shape resonance in which the electron is trapped by the centrifugal barrier of a host molecule in its ground-state configuration. (b) A Feshbach resonance in which the electron is trapped in a bound state of an electronically excited host molecule. (c) A core-excited shape resonance in which the electron is trapped by the centrifugal barrier of a host molecule in an electronically excited state.

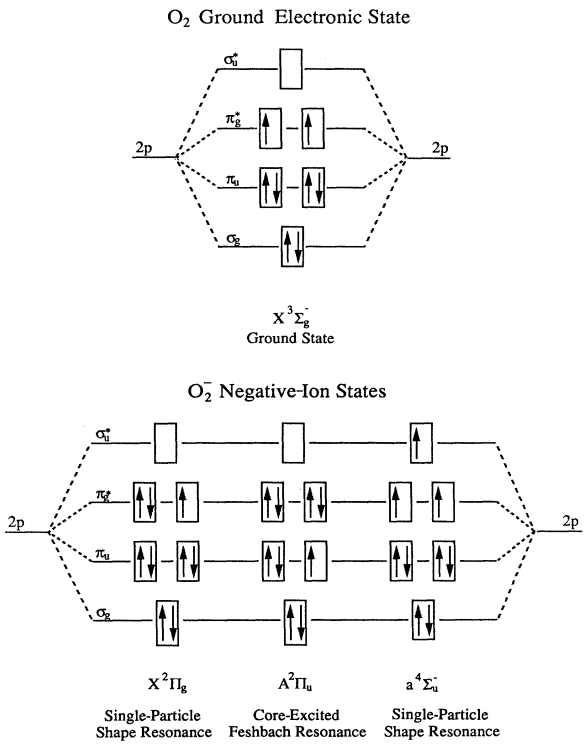

FIG. 3. The electronic configurations of various states of O_2 and O_2^-. The higher-lying molecular orbitals, derived from the atomic $2p$ levels, are shown. The π and π^* orbitals are doubly degenerate ($m_l = \pm 1$). Three negative-ion states identified in gas-phase electron-molecule impact experiments are shown—two shape resonances and a Feshbach resonance.

adding a single electron to the $2p\pi_g^*$ orbital and to the $2p\sigma_u^*$ orbital, respectively. On the other hand, the $^2\Pi_u$ negative-ion state is a core-excited Feshbach resonance. All these resonant states, which are well known in the gas phase, have been identified in electron scattering by physisorbed O_2, as we shall see later in this review.

Apart from the classification of molecular resonant states according to their electronic structure, it is also quite common to divide resonances into categories based on their lifetime (Schulz, 1976, 1979; the latter reference is a reprint of the former). In this case, the reference time scale is the vibrational period of the molecule. When the lifetime of the resonance is substantially longer than the vibrational period, the cross section for vibrational excitation as a function of the probe-electron energy (the *resonance profile* or *excitation function*) exhibits discrete, narrow peaks, attributed to well-formed vibrational levels of the negative-ion state. By contrast, when a resonance is short lived compared with the vibrational period, sometimes known as the "impulse limit," a single broad resonance peak is observed, with a typical width of a few eV. The intermediate case, when the resonance lifetime is comparable with the vibrational period, has been described by the "boomerang" model, and the resonance is therefore sometimes called a boomerang resonance. In this case, the resonance profile exhibits fine structure which shifts according to the resonance decay channel. This fine structure arises from the self-interference of the nuclear wave packet as it propagates over the potential-energy surface of the negative ion and does *not* arise from well-formed vibrational energy levels of the negative-ion state.

3. Overview of the resonance scattering process

For the purposes of our discussion it is convenient to regard resonance electron scattering as consisting of a sequence of three events:

(i) *Capture.* The process by which the incident electron is trapped by an affinity level of the molecule to form the negative-ion state.

(ii) *Dynamics.* The distortion of the intramolecular bonds (or electronic structure) of the host molecule during the lifetime of the resonance. During this process the molecule is in an excited electronic configuration.

(iii) *Detachment.* The process by which the electron is eventually ejected from the negative-ion state, leaving behind it a neutral molecule in, for example, a vibrationally excited state.

In the case of a shape resonance, the capture and detachment processes are governed by the potential barrier that exists between the continuum states of the electron and the resonant state within which the electron is trapped. In the case of shape resonances, this barrier is created by the centrifugal term in the effective electron-molecule radial potential, and it is the height and shape of this barrier which determine the tunneling rate for electron capture from, and electron decay into, the continuum. This, in turn, determines the lifetime and energy of the negative ion.

The *differential* cross section for capture by and emission from the molecular negative ion is determined by the symmetry of the resonant state and is obtained by matching the partial-wave components of the incident and outgoing electron wave field to the quasibound molecular orbital in which the electron is trapped. So, for example, the electron is ejected from the resonant state only into those partial waves which possess the symmetry of the resonant molecular orbital. These partial waves determine the angular distribution of scattered electrons. Similarly, the incident electrons tunnel into the resonant state via the same partial waves, so that the differential electron-capture cross section is the same as the differential cross section for electron emission.

4. Mechanism of vibrational excitation

a. Outline

If we assume that the time required for the capture (and emission) of the incident electron is much smaller than the vibrational period of the molecule, then, according to the Born-Oppenheimer approximation, the vibrational and electronic degrees of freedom are separated, and the electronic state of the molecule determines the potential-energy surface on which intramolecular motion takes place. The capture of the incident electron causes the molecule to make a sudden transition from the ground-state internuclear potential-energy surface of the neutral molecule to the internuclear potential of the negative ion. Immediately after this transition, in classical terms, the nuclei are subject to a force, since they now find themselves in nonequilibrium positions with respect to the potential-energy surface of the negative-ion state. The nuclei respond to this force by moving.

A quantum-mechanical account of this process can be given in terms of the Frank-Condon picture (Gadzuk, 1983, 1987), which is illustrated in Fig. 4(a). Since the negative ion is not an equilibrium configuration of the molecule, the molecular wave function evolves during the time in which the incident electron remains trapped, according to the Hamiltonian of the negative ion. Eventually the negative ion decays (suddenly) by emitting the trapped electron. After emission, the wave function of the neutral molecule is no longer the pure vibrational ground state that was the initial configuration of the molecule prior to the formation of the negative ion. Instead, the molecular wave function corresponds to a superposition of all vibrational eigenstates of the molecule. Thus, from the Frank-Condon viewpoint, the formation of the molecular ion introduces an effective coupling between the ground and vibrationally excited eigenstates of the neutral molecule, which permits the vibrational excita-

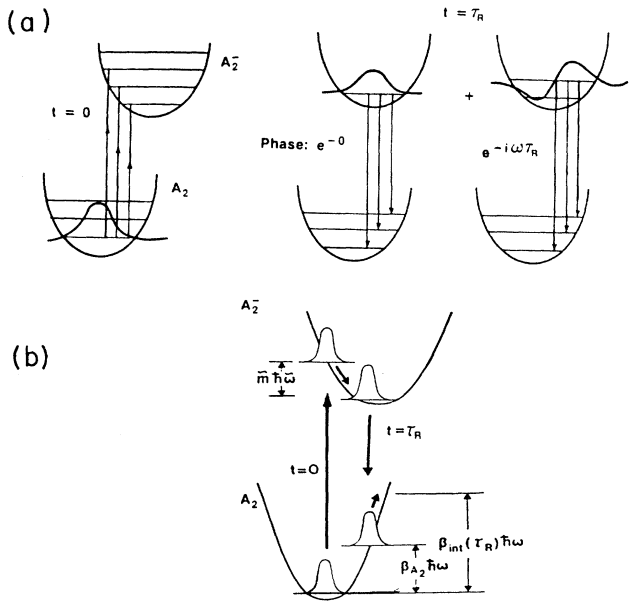

FIG. 4. A schematic diagram of resonant vibrational excitation: (a) Displaced oscillator potentials of the neutral molecule and negative ion showing representative vibrational wave functions and phase factors acquired during the lifetime of the negative ion (the Frank-Condon picture). (b) The semiclassical propagating-wave-packet realization of (a). Gadzuk (1987).

tion of the molecule. In effect, this coupling is mediated by "tunneling" via the vibrational eigenstates of the molecular ion. Thus, after the electron is emitted, there is a finite probability of the neutral molecule's being left in a vibrationally excited state. This excitation is observed, indirectly, as a characteristic energy loss suffered by the resonantly scattered electron. The finite lifetime τ of the negative ion determines the shape of the cross section for resonance scattering as a function of the incident-electron energy (Sec. II.A.2), though there is no simple and general prescription for extracting from the measured resonance profile a width that is equal to the inverse of the resonance lifetime.

b. Formal treatment

When the impinging electron attaches to the host molecule at time $t=0$, the molecule is initially in the vibrational ground state of the neutral molecule $|\chi(0)\rangle$. Whilst the incident electron remains trapped in the molecular ion, the molecular vibrational wave function evolves in time according to the Hamiltonian of the negative ion $\mathcal{H}_{\rm ion}$ (Gadzuk, 1983, 1987):

$$|\chi(t>0)\rangle = e^{-\frac{i}{\hbar}\mathcal{H}_{\rm ion}t}|\chi_0\rangle \ . \tag{1}$$

Eventually the negative ion decays by emitting the trapped electron at a time $t=\tau$. From the viewpoint of the vibrational degrees of freedom, the detachment of the electron causes the molecule to make a sudden transition back to the potential-energy surface of the neutral molecule. After emission, the vibrational wave function of the neutral molecule is no longer the pure vibrational ground state—the initial configuration of the molecule prior to the formation of the negative ion. Instead, the molecular wave function corresponds to a superposition of all the vibrational eigenstates of the neutral molecule, so that the probability of detecting the molecule in the nth vibrational state is

$$P_{0\to n} = |\langle \chi_n | e^{-\frac{i}{\hbar}\mathcal{H}_{\rm ion}\tau}|\chi_0\rangle|^2 \ . \tag{2}$$

This is the Frank-Condon picture of vibrational excitation through resonant electron scattering, shown schematically in Fig. 4(a).

An alternative description of the mechanism of resonant vibrational excitation, in the language of semiclassical wave-packet dynamics, has also been given by Gadzuk (1987, 1988). In this description, the evolution of the vibrational wave function during the lifetime of the resonance $0<t<\tau$ [Eq. (1)] is described by the propagation of a wave packet across the potential-energy surface of the negative ion, as is shown schematically in Fig. 4(b). At $t=0$ the form of the wave packet corresponds to the ground vibrational state of the neutral molecule $|\chi_0\rangle$. At $t=\tau$ the wave packet is returned to the potential-energy surface of the neutral molecule, at which point the excitation probability for each vibrational state may be extracted. In the limit of short resonance lifetime (compared with the vibrational period of the negative ion) the potential-energy curves of the neutral molecule and of the negative ion are approximated by displaced harmonic-oscillator potentials:

$$V_{\rm neutral}(R) = \tfrac{1}{2}kR^2 \ , \tag{3}$$

$$V_{\rm ion}(R) = \tfrac{1}{2}k'(R-R_0)^2 \ , \tag{4}$$

where R_0 is the separation of the well minima and we have assumed that we are dealing with vibrational excitation of a diatomic molecule. In this case the wave packet is subject to a time-dependent interaction potential,

$$V_f(R,t) = V_{\rm ion}(R) - V_{\rm neutral}(R), \quad 0\le t\le\tau \ . \tag{5}$$

From the viewpoint of classical oscillator mechanics, V_f is a time-dependent, temporally localized, forcing function, which is both separable and linear in the normal coordinate R. In the classical limit, the total energy deposited in a classical oscillator by a such a time-dependent forcing function would be

$$\Delta E_{\rm classical} = \frac{|\lambda(\omega')|^2}{2m} \ , \tag{6}$$

where $\lambda(\omega')$ is the Fourier transform of V_f with respect to time, evaluated at the fundamental frequency of the free oscillator ω' corresponding to the molecular ion. In the case under consideration,

$$\Delta E_{\text{classical}} = kR_0^2 \left[1-\cos(\omega'\tau) - \left[\frac{k-k'}{2k} \right] \sin^2(\omega'\tau) \right] . \tag{7}$$

In the quantum-mechanical version of this process, it can be shown (Cohen-Tannoudji, 1977) that the probability of exciting a transition between two vibrational states $P_{m\to n}$ is determined by the quantum analog of ΔE, the so-called Poisson parameter β:

$$\beta(\tau,k,k') = \frac{\Delta E_{\text{classical}}}{\hbar\omega'} = \frac{kR_0^2}{\hbar\omega'} \left[1-\cos(\omega'\tau) - \left[\frac{k-k'}{2k} \right] \sin^2(\omega'\tau) \right] . \tag{8}$$

In the case in which the neutral molecule is initially in its vibrational ground state, we obtain

$$P_{0\to n}(\tau) = \frac{\beta^n}{n!} e^{-\beta} , \tag{9}$$

where if $k = k'$ (and therefore $\omega = \omega'$) then

$$\beta(\tau,k) = \frac{kR_0^2}{\hbar\omega} [1-\cos(\omega\tau)] \tag{10}$$

and the probability of exciting the nth vibrational state through negative-ion formation follows the Poisson distribution. In the more general case in which $k \neq k'$, the distribution of vibrational overtones is not exactly Poisson, reflecting the spreading or contraction of the wave packet as it traverses the potential-energy surface of the negative ion.

Taken together, Eqs. (9) and (10) emphasize the important role played by the resonance lifetime τ in determining, through the Poisson parameter β, the distribution of overtone intensities. For example, from Eq. (10) we see that when $\omega\tau = N\pi$, where N is an odd integer, the probability of resonance excitation of the vibrational overtones is maximized. From a classical viewpoint, this enhancement occurs because temporary formation of the negative ion drives the molecule into a type of mechanical resonance. In contrast, when N is even, the molecule always returns to its vibrational ground state, and the probability of vibrational excitation vanishes.

Gadzuk (1987) has compared this semiclassical wave-packet approach with explicit calculation of the vibrational state distribution from the Frank-Condon picture [Eq. (2)]. For the $^2\Pi_g$ shape resonance in N_2 he showed that there is little difference between the two approaches, demonstrating the utility of the semiclassical approach, which is computationally more desirable, especially when one starts dealing with polyatomic molecules.

As a final note, we need to point out that the negative ion need not decay suddenly, as was assumed when we wrote down the "top hat" form for the forcing function V_f. If the rate of decay of the negative ion is, for example, exponential in time, then one should average the vibrational excitation distribution over time, in which case Gadzuk (1988) has shown that

$$\langle P_{0\to n}(\tau) \rangle = \frac{1}{\tau} \int_{t=0}^{\infty} e^{-t/\tau} P_{0\to n}(t)\, dt . \tag{11}$$

The relationship between the lifetime of the resonance and the distribution of overtone intensities turns out to be rather useful in the analysis of the resonance lifetime on the surface. The rate of decay of the intensities of a sequence of vibrational overtones can be used to obtain a semiquantitative estimate of the lifetime of the resonant state (Sec. IV.A.2).

5. Signatures of resonance scattering

At the experimental level, resonances scattering in the gas phase has three chief phenomenological signatures:

(i) The cross section for molecular vibrational (or electronic or rotational) excitation is enhanced at specific electron-impact energies, perhaps by several orders of magnitude.

(ii) The cross sections for exciting vibrational overtones are also strongly enhanced at the resonance energies; often one is able to detect very-high-order overtones, up to the $v = 0-10$ excitation and beyond.

(iii) The angular distribution of electrons inelastically scattered when the impact energy corresponds to the energy of a resonance is quite different from the angular distributions at other energies; the structure of the angular distribution reflects the symmetry of the negative-ion state.

In the case of polyatomic molecules, one also finds that in many cases only specific vibrational modes are enhanced at the resonance energy, reflecting the shape of the charge distribution in the negative ion which perturbs the molecule. Detailed accounts of these features are given in various reviews (for example, Schulz, 1973b, 1976, 1979; Christophorou, 1984; Allan, 1989). The characteristics of gas-phase resonance scattering represent the reference against which claims for resonance scattering by molecules on surfaces must be judged.

B. Adsorption of molecules on surfaces

The types of interaction between a molecule and a surface are conventionally divided into two categories, physisorption and chemisorption (Zangwill, 1988), which classify the type of adsorption according to the strength of bonding between the molecule and the substrate.

In the case of physisorption, the potential well that holds the molecule to the surface results from the attractive van der Waals interaction and a repulsive wall that is due to the shorter-range overlap of the charge densities

of the molecule and the surface. In the case of a (homonuclear) diatomic molecule, it is traditionally held that the van der Waals term favors an orientation of the molecular axis perpendicular to the surface, whereas the repulsive term favors a parallel orientation, and the latter usually wins. The depth of the physisorption potential well is typically only a few tens of meV, with the result that very low temperatures are required to prevent thermal desorption of physisorbed molecules. A characteristic feature of this weak interaction between the molecule and the surface is that the intrinsic properties of the molecule, such as electronic structure and vibrational frequencies, are virtually unchanged from those of the free (gas-phase) molecule.

In chemisorption a chemical bond is formed by charge transfer between the adsorbed molecule and the surface. The electronic structure and, consequently, the vibrational spectrum of the molecule are always measurably perturbed. The depth of the chemisorption potential well is of the order of 1 eV, although, as in physisorption, the precise bond energy varies considerably from one adsorption system to another. One might wonder whether there are cases in which the distinction between chemisorption and physisorption becomes blurred. One test of the type of bonding is to compare the values of the intramolecular vibrational frequencies on the surface with those found in the gas phase, and one finds that in some cases these frequencies are shifted by no more than 1% or so (physisorption), whereas in other cases substantial frequency shifts are observed, of the order of 10% and sometimes even more (strong chemisorption). There are, however, cases (such as the adsorption of CO on copper surfaces) in which intermediate frequency shifts are found, of the order of a few percent, so we do need to be careful of drawing too sharp a distinction between physisorption and chemisorption.

C. Electron scattering by molecules on surfaces: Scattering mechanisms

While it is not our purpose in this article to review the entire field of inelastic electron scattering by molecules on surfaces, it seems worthwhile, in setting the topic of resonance scattering into context, to discuss briefly their other mechanisms that lead to molecular vibrational excitation in high-resolution electron-energy-loss spectroscopy (HREELS) studies of surface systems. In principle, it ought to be possible to write down a function describing the differential inelastic-scattering cross section by an adsorbate that incorporates all the various contributions to the electron-molecule interaction potential. However, the complexity of the scattering process and, in particular, the coupling of electronic and vibrational degrees of freedom means that such an expression has not yet been derived (indeed, it is questionable whether it would provide very much direct physical insight even if it did exist). Therefore the interaction is conventionally separated into three classes: dipole, impact, and resonance scattering. In this section we give a short account of the chief characteristics of dipole and impact scattering, in comparison with the chief subject of this review, resonance scattering. For a more detailed treatment of these two scattering mechanisms, the reader is referred to the book by Ibach and Mills (1982) and the reviews of Avouris and Demuth (1984), Gadzuk (1987), and Thiry *et al.* (1987).

1. Dipole scattering

Dipole scattering is the term used to describe the scattering of an incident electron by the long-range dipole fields produced by elementary excitations of the surface. These excitations include, for example, electronic excitations and plasmons, as well as vibrational excitations, to which this discussion is addressed primarily. There are a number of equivalent theoretical approaches to the dipole scattering phenomenon (Ibach, 1990); here we discuss a treatment that rather easily describes dipole scattering by molecular overlayers on a metallic surface.

As the probe electron approaches the surface, an adsorbed molecule sees both the electric field of the moving electron and the electric field produced by the redistribution of charge induced in the solid by the field of the probe electron (i.e., screening), the "image" charge in the case of a metal. Since the electron is moving, the molecule sees a time-varying field, and consequently there is a dynamic dipole interaction between the probe electron and the molecule,

$$V_f(\mathbf{r},t)=\frac{2ep_z(t)z(t)}{[r_{\parallel}(t)^2+z(t)^2]^{3/2}}\ , \tag{12}$$

where $\mathbf{r}\equiv(r_{\parallel}(t),z(t))$ is the position vector of the probe electron, expressed in components parallel and perpendicular to the surface, and $p_z(t)$ is the dynamic dipole moment of the molecule *perpendicular* to the surface. If we imagine the molecule as an harmonic oscillator, then we see that, because of the dipolar field provided by the incident electron, the adsorbed molecule experiences a time-dependent forcing function V_f, which may induce vibrational excitation. Clearly the semiclassical analysis of Gadzuk, discussed in Sec. II.A.4, is immediately applicable to this situation, the difference being that the forcing function is now the consequence of a long-range interaction, rather than the sudden change of the molecular potential-energy surface due to negative-ion formation. In particular, one can derive an effective Poisson parameter β, which describes the cross section for vibrational excitation by this long-range dipolar interaction. Such details will not detain us here, since they are not directly relevant to the focus of this review. However, the principal characteristics of dipole scattering are worth mentioning.

The first salient feature of dipole scattering is that the mechanism favors energy-loss events involving small-momentum transfer. This is because, from a classical

viewpoint, the excitation of a vibrational mode transfers an amount of momentum to the incident electron that is small compared with the amount of linear momentum it has when approaching the surface (typically $\Delta k = 0.05$ Å^{-1} compared with $k = 1$ Å^{-1} for an electron approaching with 2 eV of kinetic energy; see Ibach and Mills, 1982 for further discussion). Thus inelastic dipole scattering occurs predominantly in the *forward* direction, the inelastic event being followed by elastic backscattering from the substrate, which provides the momentum transfer to reflect the electron back towards the detector. Therefore the intensity of the observed loss features is concentrated near the specular direction (Fig. 5) and, given the finite acceptance angle of a real electron analyzer, often appears as a single peak in that direction. A practical consequence of this result is that many HREELS studies have been confined to the measurement of spectra in or near the specular direction. The second feature of dipole scattering is that, on a metal surface, vibrational modes with a nonzero dynamic dipole moment perpendicular to the surface are preferentially excited. This occurs because the dynamic dipole moment of vibration parallel to the surface is screened rather effectively, so that the intensity of these modes is extremely weak compared with those polarized normal to the surface. A third characteristic of dipole scattering is that the cross section for vibrational excitation is rather a smooth function of electron-beam energy. Finally, the cross section for the excitation of vibrational overtones, compared with excitation of the fundamental mode, is small in dipole scattering (Ibach and Mills, 1982).

2. Impact scattering

Electrons may also induce elementary excitations within the surface through a much-shorter-range interaction with the atoms in the surface; this is the mechanism known as impact scattering. In the case of molecular adsorbates, vibrational excitation occurs through direct scattering of the incident electron from the ion cores of the molecule. As a consequence of multiple elastic scattering of the probe electron, both before and after the relevant energy-loss event, the impact scattering cross sections show oscillatory structure, as a function of both electron-impact energy (Fig. 6) and scattering angle (Xu *et al.*, 1985). These oscillations are typical of a coherent interference effect, so the cross sections are quite distinct from their dipole scattering counterparts. Thus the specular direction has no particular significance in impact scattering (indeed, the question of whether the intensity of a mode holds up away from the specular direction is the main test used, in practice, to distinguish between impact scattering and dipole scattering). Again, since impact scattering, in contrast with dipole scattering, proceeds through a short-range interaction, modes of vibration both parallel and perpendicular to the surface may be excited. Impact scattering does, however, have its own selection rules (Ibach and Mills, 1982; Thiry *et al.*, 1987); for example, if electrons are collected in the plane that contains the direction of the incoming electrons and the normal to the surface, then modes of vibration (in an ordered surface system) polarized perpendicular to this plane cannot be excited. A final characteristic of this short-range scattering mechanism is that overtone excitation is enhanced in the impact scattering regime (Ibach and Mills, 1982).

Resonance scattering can be viewed as a particular case of impact scattering, in which the energy-loss event itself occurs via electron *capture* into a molecular orbital to form a transient negative ion. We shall see later that one consequence of adsorbing a molecule on a surface is to introduce modulations of the molecular resonance scattering cross sections, which arise from the same type of multiple elastic scattering (occurring before the resonance is formed and after it decays) that is evident in the impact scattering cross sections.

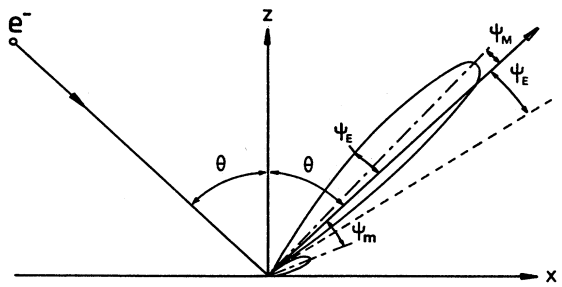

FIG. 5. Schematic plot of the kinematic factor in the dipole scattering probability function, showing that the inelastically scattered electrons are confined to two lobes near the specular reflection direction, i.e., that the momentum transfer parallel to the surface is small. From Thiry *et al.* (1987).

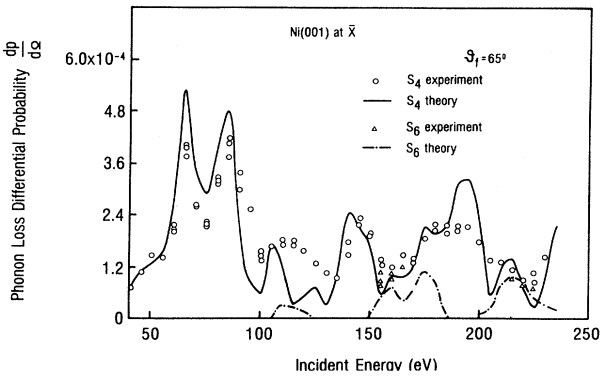

FIG. 6. Probability of phonon excitation via impact scattering as a function of incident-electron energy, showing the oscillatory structures typical of impact scattering cross sections. Experimental results from the Ni(001) surface are shown, together with theoretical calculations. Xu *et al.* (1985).

D. Electron scattering by molecules on surfaces: Experimental considerations

While many HREELS spectrometers with various designs are in use around the world, the basic principles of operation of most of these instruments are rather similar. Figure 7 shows a schematic representation of a typical spectrometer. The electron source is generally a hot thermionic emitter, and electrons boiled off this source are injected by an electrostatic lens system into an electron-energy monochromator (Ibach, 1991) based on electrostatic dispersing elements—typically cylindrical or hemispherical sectors. Some spectrometers feature two successive sets of dispersing elements—a "double-pass monochromator." The electron beam is then accelerated to the desired impact energy and projected at the target surface by a further set of electrostatic lenses. Electrons scattered by the surface system are analyzed by an electron-energy analyzer very similar in design to the monochromator and are subsequently detected with a channel-electron multiplier, or occasionally a multichannel detector array. A scan over the energy of the scattered electrons is generally achieved by ramping the baseline upon which the analyzer voltages sit, so that the resolution of the analyzer remains constant as the energy loss is scanned. The overall energy resolution of such spectrometers has to be traded off against signal levels. The highest resolution reported to date is around 1 meV (Ibach, 1991), but the studies of resonance electron scattering that have been reported so far have rarely featured a resolution much better than 10 meV. In some cases, particularly when one is interested in the high-frequency (a few hundred meV) modes of adsorbed molecules, one might choose a resolution of 10 meV or 20 meV in order to maximize signal levels, provided one were not aiming to explore vibrational line shapes. In other cases, a resolution of around 10 meV might represent a realistic limit on the performance of the spectrometer, with signal levels dropping drastically beyond that point. For whatever reasons, it is the case that few studies of resonance electron scattering have explored the excitation of low-frequency vibrational modes, where high resolution is a necessity.

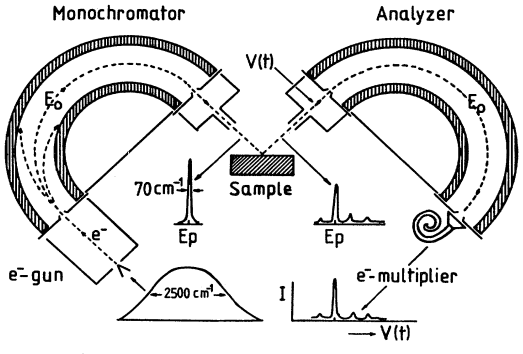

FIG. 7. Schematic diagram of a high-resolution electron-energy-loss spectrometer for surface studies. Typical energy distributions of the electron beam are plotted at various points of the system. From Thiry *et al.* (1987).

The measurement of the cross section for excitation of a particular loss feature in the HREELS spectrum as a function of electron-impact energy (the excitation function), which is central to the study of resonances, imposes constraints on the operation of the spectrometer that are not so commonly encountered in HREELS studies aimed primarily at mapping out vibrational spectra. The ideal spectrometer would doubtless feature a monochromator with a signal output and an analyzer with a transmission function which were each independent of the impact energy; the energy resolution and focal lengths of the system would also be invariant. In practice, excitation functions are accumulated in one of two ways. In most spectrometers, the practice is to choose a particular electron-beam energy, tune the spectrometer for maximum signal transmission at a chosen (nominal) resolution, record a HREELS spectrum, and then select another beam energy and repeat the cycle. This process is certainly time consuming, but has the benefit that at least one obtains a complete energy-loss spectrum at each impact energy, so that internal normalization of the intensities of a particular loss mode is possible. Alternatively, certain spectrometers feature programmable "zoom" lenses (Roy and Tremblay, 1990; zoom lenses have focal properties that are invariant with electron-beam energy), with the aim of approaching the behavior of the ideal spectrometer described above. With such an instrument one is able to sit on a particular energy loss and scan through the impact energy to record in rapid time the excitation function of that mode. Of course, in the real world these spectrometers need to be calibrated. Calibration is a somewhat problematic issue, because one really needs to know the reflectivity of the surface as a function of electron-beam energy, and independent records of the reflectivity functions are not widely available. On the positive side, programmable spectrometers can be used to obtain complete HREELS spectra as a function of impact energy, acquiring excitation functions at a very rapid rate. One particular constraint common to all spectrometers used to acquire excitation functions is the requirement that the transmission function of the analyzer be independent of energy loss, otherwise the possibility of normalizing the excitation function of a particular mode against those for other modes or for the elastic or background intensity is lost. This is a matter of good design—it is hard to calibrate out deviations—and in practice is not usually too great a problem if the range of energy loss which is of interest is a small fraction of the electron-impact energy. If, for example, one were looking at the high-energy overtones of a molecular stretch mode at very low impact energies, one might run into problems of this type.

Two particular details in the interpretation of reported excitation functions seem to be worth highlighting: (i) In many cases the quoted electron-beam impact energies

need ideally to be corrected for the difference in work function between the monochromator slit and the sample, a correction that could be up to about 1 eV. Of course, the relevant work functions may not be known, especially that of the monochromator slit, so experimental calibration of the beam energy at the sample using, for example, the retarding potential technique (Sporken *et al.*, 1985) has much to commend it. (ii) Most of the excitation functions in the literature are normalized, usually to the intensity of another feature in the HREELS spectrum, such as the elastic peak intensity. While, on the whole, normalization seems to us to be a healthy practice, one has to be very careful that the procedure used does not introduce spurious structure into the excitation function that is obtained. One possibility in exploring this effect is to normalize a given set of loss peak intensities by various different methods (using, for example, the energy-loss background intensity in addition to the elastic peak intensity) to see if the chief features of the excitation function remain unaltered.

The measurement of the angular distribution of electrons scattered via a resonant state also requires of a HREELS spectrometer features that are not demanded by vibrational band mapping. In particular, some spectrometers have a fixed monochromator and analyzer, so that, even if the sample can be rotated, the angles of incidence and detection with respect to the surface cannot be varied independently. Again, if the sample is fixed and only one of the monochromator and analyzer is rotatable, one is not able to vary (say) the angle of incidence for which scans over emission angle are performed. What one ideally wants in order to obtain angular distributions is a system that allows two out of the monochromator, sample, and analyzer to rotate. In that way one can obtain scans over the emission angle for a set of angles of incidence or vice versa. We are presuming in this discussion that the direction of the incident beam, the normal to the surface, and the direction of the detected beam define a fixed scattering plane. In fact, it would be very interesting to go out of plane too, because in scattering by surfaces (unlike the gas phase) azimuthal symmetry will typically be broken. No such studies have been reported yet. Compared with the gas phase, angular distribution measurements are restricted by the presence of the surface itself; one has access, in principle, only to 2π steradians of space. Given that the monochromator and analyzer are competing for this space, the practically accessible range is further limited. The widest (one-dimensional) angular scans reported (Sec. V.A.2) have covered a range of about 90 degrees. In practical terms, the measurement of wide-angle distributions would be possible with many more spectrometers than at present with really rather modest changes in design.

III. RESONANCE SCATTERING BY MOLECULES ON SURFACES

When a molecule is adsorbed upon a surface, the picture of resonance scattering in the gas phase that was given in Sec. II.A is altered significantly. Perhaps the simplest of these changes is purely geometrical; the molecules may become oriented, the surface serving as a template to align the molecular axes preferentially in specific directions. Thus, in contrast to resonance scattering in the gas phase, the differential cross sections for both emission and capture are not the orientational average. This, as we shall show later (Sec. V.A), gives us the ability to determine, in a relatively straightforward manner, both the resonance symmetry and, in some cases, the orientation itself.

As far as the resonance electron-scattering process itself is concerned, the surface interacts with both the molecule and with the electron that populates the negative ion. It is therefore convenient to separate the net effect of the surface upon negative-ion formation into two components. The first is the molecule-surface interaction. This is an intrinsic distortion of the electronic structure of the molecule and the molecular negative ion caused by electronic interactions between the surface and the molecule. These distortions may, at least in principle, be so great as to destroy (completely quench) the resonance. On a metallic surface the molecular negative ion experiences an attractive potential produced by its "image" in the surface, and in the case where new chemical bonds are formed between the surface and the molecule (i.e., chemisorption) the electronic structure of the isolated molecule will be altered. The electron-surface interaction is possibly a more subtle, but nevertheless crucial, effect, and arises as a consequence of the fact that in order to observe a resonance in an electron-scattering experiment it is necessary to supply the molecule with an electron and to detect that electron after emission. In gas-phase scattering the electron proceeds to and from the molecule in an unhindered fashion because it is propagating through the vacuum. However, on its path to and from an adsorbed molecule in a surface experiment the electron is scattered by the electron-surface interaction, i.e., it is scattered both by the atoms in the substrate and by other molecules in the molecular overlayer. In consequence, a scattering experiment does not probe simply the intrinsic properties of the adsorbate negative ion.

The effects discussed above can, in principle, change all of the observable properties of a molecular resonance. Compared with the molecule in the gas phase the surface may change in several ways:

(i) *The resonance lifetime.* Deformation of the molecular potential by the molecule-surface interaction may alter the tunneling rate for both capture and emission. This may occur by a direct change in the potential barrier that confines the electron within the negative ion or as a consequence of a change in the resonance symmetry, which opens up new angular momentum channels by which the electron may be captured or emitted. In the case of a shape resonance, the presence of additional partial waves having lower angular momentum may allow the trapped electron to "leak out" more rapidly through an effectively lower centrifugal barrier than in the gas

phase, thus decreasing the resonance lifetime.

(ii) *The resonance energy.* Deformation of the molecular potential by the molecule-surface interaction perturbs the quasibound energy levels of the electron-molecule potential. This change manifests itself as a shift of the resonance energy. The measured resonance energy may also be altered by the scattering of the probe electron before and after capture, which introduces an additional energy-dependent population and depopulation of the resonant state. The latter effect is quite independent of any intrinsic molecular shift introduced by changes in the molecular potential induced by, for example, the image potential or the formation of chemical bonds with the substrate.

(iii) *The resonance symmetry.* The surface breaks the symmetry of the isolated molecule and modifies the resonance by mixing partial waves into the resonant orbital which are forbidden by the symmetry of the gas-phase molecule. This perturbation of the symmetry of the quasibound molecular orbital in which the incident electron is confined will change the character of the differential cross sections for electron capture and electron emission.

(iv) *The angular distribution of scattered electrons.* The surface orients the molecule producing a characteristic angular emission profile, which is not subject to the orientational averaging of the gas phase. These angular distributions will reflect not only changes in the resonance symmetry on adsorption, but also the (elastic) scattering of the probe electron by the atoms and molecules in the surface before and after the formation of the resonance.

(v) *The resonance decay channels.* The surface cannot only alter the absolute cross sections for various modes of excitation of the molecule (by changing the resonance lifetime, for example), but it can also change the branching ratio between competing resonance decay channels. For example, the shortening of the lifetime of the resonant state alters the relative probabilities of exciting a sequence of vibrational overtones. The perturbation by the substrate of the potential-energy surface over which the intramolecular motion evolves during the lifetime of the negative ion may have a similar effect. Coupling of the adsorbed molecule to the surface also creates entirely new decay channels, such as the excitation of the vibration of the whole molecule against the surface. In addition, a reduction of the resonance energy relative to the vacuum energy may diminish the manifold of observable decay channels.

In the discussion above, we have taken as our starting point the gas-phase molecular resonance and then asked how the properties of the resonance are altered when the molecule is adsorbed onto a surface. This question is a major theme of this review because the resonances explored in experimental and theoretical studies have most often been perturbed gas-phase resonances. However, one should recognize that when a molecule is adsorbed onto a surface the possibility exists that new resonant states, not present in the free molecule, may be formed. For example, a bound state of the free molecule may shift above the vacuum level as the molecule approaches the surface, producing a new resonant state. States like this have been predicted to occur, for example, in the adsorption of alkali-metal atoms on metallic surfaces (Nordlander and Tully, 1990). Such behavior has yet to be observed experimentally or treated theoretically for the case of *molecular* resonances and presents an interesting challenge for future research.

IV. RESONANCE ENERGY AND LIFETIME

We begin our detailed consideration of resonances in adsorbed molecules by exploring the energy and lifetime of the resonant state on the surface. It seems appropriate to consider the energy and lifetime τ of the resonance in tandem because the resonance width ($\propto 1/\tau$) is just the imaginary part of the complex resonance energy. We shall see that a number of factors perturb the energy and width of the resonance on the surface. We consider first the influence of the image potential encountered in adsorption on a metallic surface (most studies of resonance scattering by adsorbates have examined molecules on metal surfaces), together with the perturbation of the molecular potential by the short-range potentials of the surface atoms above which the molecule is adsorbed. Subsequently, we consider the role played by chemical bonding between the adsorbate and the substrate in distorting this same potential.

A. Effect of the image potential and the short-range surface potential

When an electron approaches a metallic surface, its electric field is screened by the redistribution of charge within the metal. This screening produces a potential outside the surface, which resembles that due to a positively charged image of the probe electron located inside the surface—the so-called image potential. The image potential perturbs both the energy and the lifetime of the molecular resonance, because it exists equally when the probe electron is attached to the target molecule to form the negative-ion resonance. Thus, to a first approximation, the potential seen by the electron is the superposition of the molecular potential and the (attractive) image potential. Whilst the electron is trapped within the molecule, the attraction between the electron and its image shifts the "binding" energy of the negative-ion state. In addition, the height of the effective tunneling barrier against electron emission and capture is distorted by the image potential, causing a change in the resonance lifetime. The properties of the resonant state are also influenced by the short-range atomic potentials of the surface atoms in the proximity of the adsorbed molecule: the resonance wave function laps out into the surface and

samples these atomic potentials. In particular, the symmetry of the molecular orbital in which the probe electron is trapped is modified, and in terms of a scattering picture this allows extra partial waves to be mixed into the resonance, which affects the lifetime of the negative ion and therefore the observed width of the resonance, as well as its energy. In this section we describe various theoretical models that have been proposed to treat the image potential and the short-range surface potential, before exploring a number of experimental studies of the energy and width of the resonances observed in electron scattering by adsorbed molecules. In some cases, the theoretical models described have been motivated by, and applied to, the results of these experimental investigations.

1. Theoretical models

a. The image potential

Motivated by the experimental studies of Demuth and co-workers (Demuth *et al.*, 1981, 1983; Schmeisser *et al.*, 1982; see Sec. IV.A.2), Gerber and Herzenberg (1985) studied the energy and width of the $^2\Pi_g$ shape resonance in N_2 physisorbed on a metallic surface. In order to investigate the effect of the image potential, they modeled the N_2 molecule by a spherical square well embedded at the center of a spherically symmetric imagelike potential (Fig. 8). The depth and width of the well were adjusted so as to reproduce the (gas-phase) resonance energy and width in the absence of the image potential.

The calculated width and energy of the resonance as a function of the distance of the center of the molecule from the "surface" are reproduced in Fig. 9. As the distance of the molecule from the surface is decreased, the resonance broadens and is shifted down in energy. The energy shift is simply the result of adding the (negative) image potential through the region where the electron is trapped; in effect, the trapped electron is stabilized by the attraction towards its image. The decrease in resonance lifetime occurs because the image potential reduces the height of the centrifugal barrier, increasing the tunneling rate for resonance decay. However, the image potential also lowers the energy of the electron trapped within the molecular core, an effect that tends to compensate for the reduction in the barrier height. In this model, the net effect of the image potential is to decrease the resonance lifetime. This is because the image potential is stronger in the vicinity of the centrifugal barrier than inside the molecular core, so that the reduction of the barrier height is greater than the (downward) shift of the resonance energy, at least for the model of the spherical imagelike potential.

Recently, a more realistic model of the effect of the image potential upon the resonance energy and width has been developed by Teillet-Billy and Gauyacq (1991). In their treatment the molecule was embedded in a classical image potential, and the coupled-angular-modes (CAM) method employed to evaluate the electron scattering

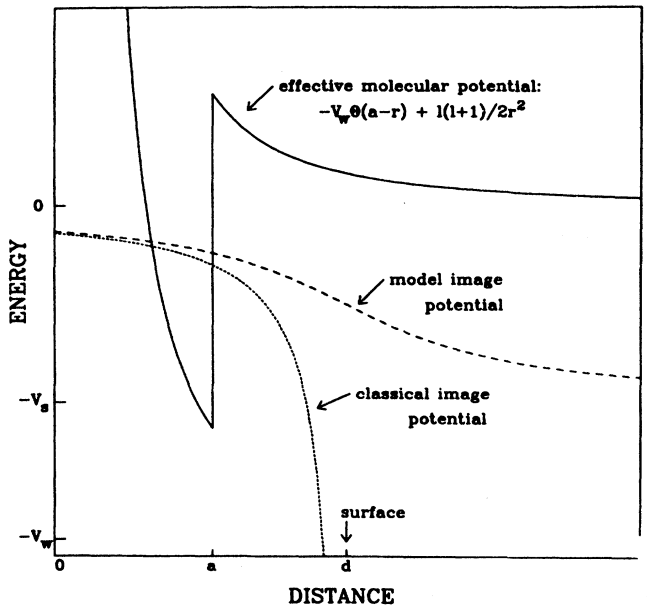

FIG. 8. The model potential employed by Gerber and Herzenberg to simulate the effect of the image potential on the energy and lifetime of a resonance in a molecule adsorbed on a surface. The effective potential seen by the probe electron is the superposition of a spherical square well, a spherically symmetric image potential, and centrifugal potential. The center of the molecule is at $r=0$ and the surface is at $r=d$. Gerber and Herzenberg (1985).

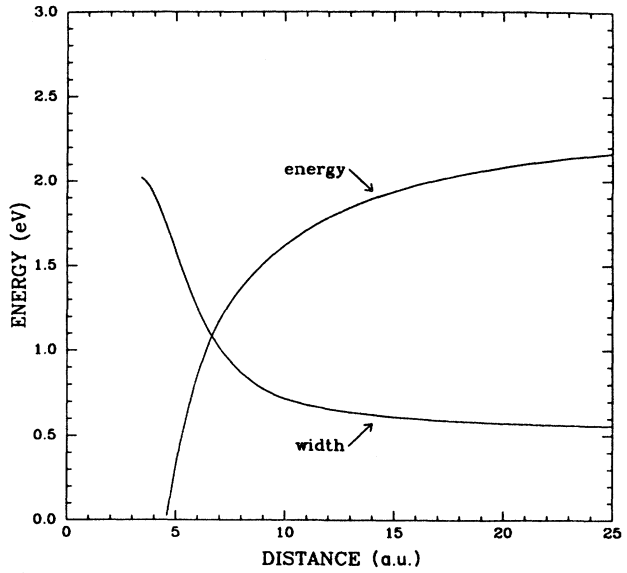

FIG. 9. The resonance pole, $E=E_R+i\Gamma$, for the spherically symmetric image-potential model of Gerber and Herzenberg corresponding to the $^2\Pi_g$ resonance in N_2. E_R is the resonance energy and Γ the resonance width shown as a function of the distance between the molecule and the surface. Gerber and Herzenberg (1985).

close to the resonance energy. The electron-*molecule* scattering is described within the effective-range theory (ERT), in which the potential experienced by the electron that forms the negative ion is partitioned into two regions separated by a sphere of radius r_c centered upon the center of mass of the molecule (Teillet-Billy and Gauyacq, 1990). For the *free* molecule, the potential outside this sphere is taken to be a superposition of the combined polarization and centrifugal potentials of the molecule $V^{\text{ext}}(\mathbf{r})$,

$$V^{\text{ext}}(\mathbf{r})=-\frac{1}{2r^4}+\frac{l(l+1)}{2r^2} \quad \text{(atomic units)} , \tag{13}$$

where it is assumed that the exchange-correlation potential is negligible in this region, a good approximation if the electronic charge density of the molecule is small for $r>r_c$.

In this external region the probe-electron wave function $\psi(\mathbf{r})$ is expanded in a set of spherical harmonics about the molecular center of mass:

$$\psi(\mathbf{r})=\sum_{l,m}\frac{1}{r}R_{lm}(r)Y_{lm}(\hat{\mathbf{r}}) . \tag{14}$$

Inside the sphere surrounding the molecular core ($r\le r_c$), the molecular potential is not explicitly calculated. Instead, the effect of this short-range electron-molecule interaction is described with the effective-range approximation and is modeled by specifying the energy-independent logarithmic derivative of the probe-electron wave function ψ at the surface of the sphere ($r=r_c$),

$$d_{lm}=\frac{1}{R_{lm}(r)}\frac{\delta R_{lm}(r)}{\delta r}\bigg|_{r=r_c} . \tag{15}$$

This set of logarithmic derivatives serves as a boundary condition upon each component of the probe-electron wave function outside the molecular core.

If the external potential is expanded in spherical harmonics,

$$V^{\text{ext}}(\mathbf{r})=\sum_{l,m}V_{lm}^{\text{ext}}(r)Y_{lm}(\hat{\mathbf{r}}) , \tag{16}$$

then the probe-electron wave function can be obtained by solving the radial Schrödinger equation:

$$-\frac{1}{2}\frac{\delta^2 R_{lm}}{\delta r^2}+V_{lm}^{\text{ext}}(r)R_{lm}=ER_{lm} , \tag{17}$$

subject to the boundary condition at $r=r_c$ given by Eq. (15). The solution of this set of equations defines the scattering S matrix of the problem as a function of incident-electron energy. This matrix can be obtained by numerical integration of Eq. (17) to a point well beyond the molecular potential ($r\gg r_c$), where the solutions of Eq. (17) are matched onto their asymptotic forms. The diagonalization of the S matrix yields the time-delay eigenvalues from which the resonant channel can be identified by a large positive eigenvalue whose maximum occurs at the resonance energy. The resonance lifetime τ is obtained from the eigenphase shift $\delta(E)$ of the resonant channel:

$$\tau=\frac{1}{2}\frac{d\delta}{dE} . \tag{18}$$

In order to employ this procedure to determine the resonance electron scattering of a molecule adsorbed on a surface, it is necessary first to determine the ERT boundary condition [Eq. (15)] at the molecular core. This can be done by adjusting the logarithmic derivatives d_{lm} to fit the observed resonance energy (for the resonant channel) and calculated eigenphase shifts (for the nonresonant channels) for the free (gas-phase) molecule. One then regards these derivatives as being transferable between the free and adsorbed molecule. This is an acceptable procedure provided the molecular core is not disturbed, for instance, by the formation of a strong chemical bond between the molecule and the surface. For the weakly bound physisorbed systems this is usually a good approximation.

Thus far, our discussion has concerned the free molecule, whereas we are interested in what happens to the negative-ion resonance when the molecule is adsorbed onto a metallic surface. In order to consider this case one needs to incorporate the electron-*surface* interaction into this theoretical framework. Teillet-Billy and Gauyacq model the electron surface potential as a shifted classical image potential which matches a constant potential V_0 inside the surface:

$$V^s(r)=\begin{cases}-|V_0|, & z\le 0,\\ -\dfrac{1}{4(z+z_c)}, & z\ge 0.\end{cases} \tag{19}$$

This potential, expanded in spherical harmonics, leads to an additional term in the radial Schrödinger equation for the probe-electron wave function in the external region:

$$-\frac{1}{2}\frac{\delta^2 R_{lm}}{\delta r^2}+V_{lm}^{\text{ext}}(r)R_{lm}+\sum_{l',m'}V_{lm,l'm'}^{s}(r)R_{l'm'}=ER_{lm} . \tag{20}$$

In contrast to the radial equation for the free molecule, this equation represents a set of coupled matrix equations for the radial solutions $R_{lm}(r)$. Nevertheless the solutions to this equation may be obtained by numerical integration to determine the scattering S matrix of the molecule adsorbed on the surface. As was outlined above, energy dependence of the scattering matrix eigenvalues yields the resonance lifetime and energy, in this case, of the adsorbed molecule. The corresponding eigenfunction yields the angular distribution of emitted electrons and will be discussed in Sec. V.A.

Teillet-Billy and Gauyacq have used this calculational method to study the energy and width of the $^2\Sigma$ resonance of the CO molecule adsorbed above a surface that was modeled by a simple classical image potential. The presence of atoms within the substrate which provide

elastic scattering centers was ignored. Figure 10 shows the resonance energy as a function of the distance of the molecule from the surface. Compared with the gas-phase value of 19.4 eV (Tronc *et al.*, 1980), the resonance energy is lowered monotonically by the image potential, reaching the experimental value of approximately 18 eV (Jones *et al.*, 1989), for an adsorption height of approximately 2.4 Å. It should be noted that the lowering of the resonance energy is within 0.2 eV of that predicted by a simple image-potential shift, i.e., by the simple addition of the value of the image potential at the center of the molecule to the gas-phase resonance energy. This is in agreement with the results of Gerber and Herzenberg for N_2 and shows that a classical image potential has a rather simple effect on the energy of the resonance over a wide range of resonance energies (2 eV for N_2 and 18 eV for CO).

Figure 11 shows the width of the CO resonance as the molecule is brought towards the surface. As the distance between the molecule and the surface is decreased, the resonance width first decreases and then increases again. Close to the surface, the increase in width, and consequent decrease in resonance lifetime, is associated with the tearing down of the centrifugal barrier and is in accord with the results of Gerber and Herzenberg for N_2. The decrease in width at large distances compared with the gas-phase width is an illustration of the competition between the increased binding of the negative-ion state and the reduction of the centrifugal barrier first noted by Gerber and Herzenberg. The latter effect is small far away from the surface, and therefore the negative ion is stabilized by the image potential there. It should be noted, however, that the results imply that such stabilization effects will be difficult to observe, because the molecule-surface distance required lies well beyond that expected even in physisorption.

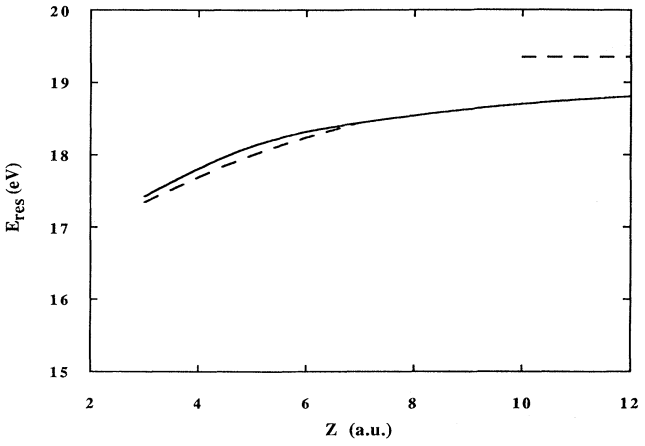

FIG. 10. Resonance energy of the $^2\Sigma$ resonance of CO as a function of the molecule surface distance (heavy dashed line) compared to the image-potential shift (solid line). The thin dashed line gives the location of the resonance in the free molecule, 19.2 eV. Teillet-Billy and Gauyacq (1991).

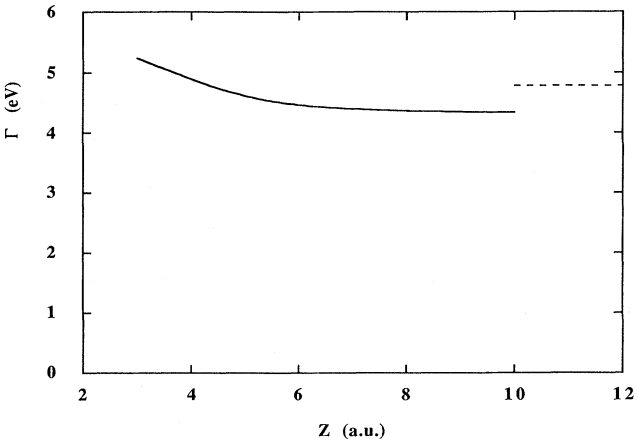

FIG. 11. Resonance width of the $^2\Sigma$ resonance of CO as a function of the molecule surface distance (solid line). The dashed line gives the resonance lifetime in the free molecule. Teillet-Billy and Gauyacq (1991).

b. The short-range surface potential

Far from the surface the molecule sees only the long-range image potential, and the importance of this effect in changing the gas-phase lifetimes and resonance energies has been described in the previous section. However, as the molecule approaches the surface there is another factor that can alter the energy and width of the resonance. This is the short-range interaction between the trapped electron and the short-range potentials of the surface atoms, which in theoretical terms is most easily described within the framework of multiple-scattering theory. From this viewpoint we consider that in the gas phase the negative-ion state consists of an electron trapped in a state described by multiple elastic scattering within the molecular potential. As the molecule is brought up towards the surface, the trapped electron can be elastically scattered by the substrate atoms in addition to the molecule. Thus the distortion of the quasibound state by the surface can be formulated as a multiple-scattering problem in which the trapped electron is multiply reflected between the surface and the molecule. This multiple reflection can change both the resonance energy and the lifetime quite independently of the image-potential effects discussed in the previous section. We note here that the treatment of the image potential by the coupled-angular-modes method described above can also be regarded as a problem of local multiple scattering between the overlapping molecular and image potentials. When we come to consider short-range scattering effects, the multiple-scattering approach becomes particularly transparent since, in the absence of the image potential, the scattering potential can be separated into two nonoverlapping parts, the molecular potential and the surface potential, between which the electron scatters.

Gerber and Herzenberg investigated the effect that multiple scattering between the molecule and a model surface has upon the width and energy of the $^2\Pi_g$ resonance in N_2 at 2.3 eV. They represented the surface by a simple step potential with a height taken to be approximately equal to the sum of the Fermi energy and the work function of the metallic substrate (−9.8 eV for the case of Ag). The scattering by the molecule was evaluated using gas-phase eigenphase sums for the free molecule. In the absence of the surface potential, then, the incident-electron wave function is a plane wave:

$$\psi_{\rm inc}(\mathbf{r})=e^{i\mathbf{k}\cdot\mathbf{r}}=\sum_{lm} A^0_{lm} j_l(\kappa r) Y_{lm}(\hat{\mathbf{r}}) , \tag{21}$$

where $k=\sqrt{2E}$ is the electron wave vector, j_l is a spherical Bessel function, and Y_{lm} is a spherical harmonic.

In the presence of the molecule, the total probe-electron wave function outside the molecular core can be expanded as a set of partial waves about the molecular center of mass,

$$\psi(\mathbf{r})=\sum_{lm} A^0_{lm} j_l(\kappa r) Y_{lm}(\hat{\mathbf{r}}) + \sum_{lm}\left[\sum_{l'm'} M_{lm,l'm'} A^0_{l'm'}\right] h_l^{(1)}(\kappa r) Y_{lm}(\hat{\mathbf{r}}) , \tag{22}$$

where h_l^1 is a spherical Hankel function of the first kind and the molecular scattering matrix $M_{lm,l'm'}$ describes the process by which the probe electron arrives at the molecule in the incoming partial wave (l,m) and is scattered into the partial wave (l',m'). We note that M describes electron scattering by both the nonresonant and resonant channels. The element of M corresponding to the resonant channel has a pole in the complex energy plane at $E=E_R-\frac{1}{2}i\Gamma$, where E_R is the location of the resonance and Γ the resonance width for the *free* molecule. The first term on the right-hand side of Eq. (22) corresponds to a set of incoming waves, and the second term describes a set of outgoing waves.

When the molecule is placed above a surface, the waves leaving the molecule may be reflected by the surface to impinge upon the molecule once again. In an angular momentum representation, centered upon the molecule, the reflectivity of the surface may be written as a matrix $S_{lm,l'm'}$. This matrix describes how an electron that leaves the molecule in partial wave (l,m) can be reflected into an incoming partial wave (l',m'). Multiple reflection between the surface and the molecule alters the spherical wave amplitudes incident upon the molecule. Thus, since the spherical wave amplitudes in the absence of the surface are A^0_{lm}, the spherical wave amplitudes impinging on the molecule above the surface, A_{lm}, are obtained by summing a multiple-scattering series between the surface and the molecule:

$$A=(1+\mathbf{M})(1+\mathbf{SM}+\mathbf{SMSM}+\cdots)(1+\mathbf{S})A^0 = (1+\mathbf{M})(1-\mathbf{SM})^{-1}(1+\mathbf{S})A^0 , \tag{23}$$

which may be summed as a geometric series. The energy and width of the resonance in the molecule above the surface can then be obtained by solving the equation

$$\det(\mathbf{1}-\mathbf{SM})=0 \tag{24}$$

for the complex energy roots $E-\frac{1}{2}i\Gamma$. Thus one obtains the resonance energy E and the resonance width Γ (proportional to the inverse of the resonance lifetime) of the adsorbed molecule.

The advantage of this approach is that it factorizes the problem into two parts. The surface scattering is represented by the matrix S, which, in principle, could be evaluated using a complete model of the scattering potential of both the long-range and the short-range parts of the electron-surface interaction. The molecular scattering is represented by M, which separately contains all the details of the molecular potential. The division between surface and molecular scattering is also a limitation of the approach, since it is assumed that the molecular scattering is unaffected by the interaction between the molecule and the surface (and vice versa). Clearly, this assumption may not be valid if, for example, the resonant state is disturbed by charge transfer between the molecule and the surface.

In Fig. 12 we show the results obtained by Gerber and Herzenberg (1985) in applying this approach to the $^2\Pi_g$ resonance at 2.3 eV in N_2. This figure shows the resonance energy and width as a function of the distance of the molecule above the surface barrier, which was taken to be a potential step of height −9.8 eV. We see that the

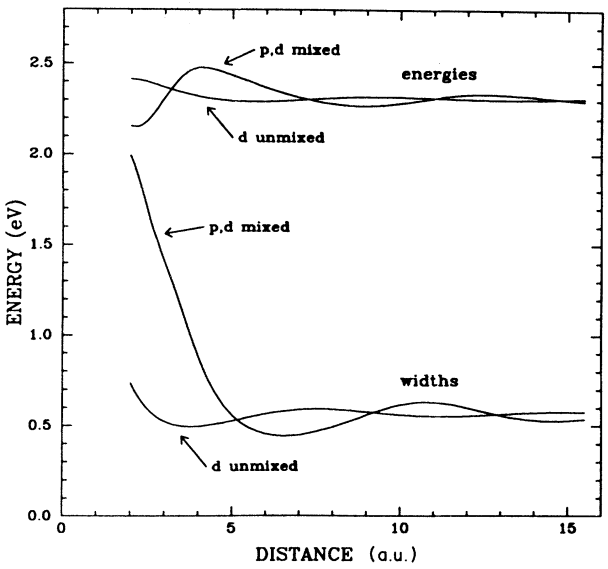

FIG. 12. The resonance pole, $E=E_R+i\Gamma$, calculated by Gerber and Herzenberg for the $^2\Pi_g$ resonance in a N_2 molecule as a function of the distance between the center of mass of the molecule and an abrupt surface barrier of height −9.8 eV. Shown are the resonance energy and width calculated with and without mixing between the $d\pi$ and $p\pi$ partial waves. Gerber and Herzenberg (1985).

resonance width rapidly increases as the molecule approaches the surface. This is a consequence of the breaking of the symmetry of the molecule by the surface potential. This symmetry breaking allows the $^2\Pi_g$ resonant state, which in the gas phase consists of partial waves ($l=2$, $|m|=1$), to acquire a p-wave ($l=1$) component. Since the centrifugal barrier for a p wave is lower than that for the d wave, this coupling allows the resonance to decay more rapidly through the $l=1$ centrifugal barrier, so that the resonance lifetime is reduced as the molecule approaches the surface.

The plot of resonance energy versus distance from the surface shows somewhat less dramatic behavior, with a number of small oscillations and a small (≈ 0.5 eV) drop close to the surface. This suggests that the resonance energy is not strongly affected by multiple scattering, at least for this particular model system. Thus it is the image potential that is responsible for the energy shift in this system, as was verified by these authors and discussed in the previous section.

c. The band structure of the surface

The results presented above were obtained for particular systems and for particular model potentials, and so one is led to ask the question, To what extent do these calculations represent a universal picture of resonance scattering at surfaces? It should be noted, for example, that the work of Teillet-Billy and Gauyacq (1991) and of Gerber and Herzenberg (1985) neglects any modification of the scattering by the molecular core due to the proximity of the surface. Such modifications would be expected to be important if a strong chemical bond were formed between the surface and the molecule, as is the case for chemisorbed molecules. So far, the effects of chemisorption on resonance electron scattering remain unexplored theoretically, although there have been a number of experimental studies of resonances in chemisorbed molecules (Sec. IV.B). However, even in the case of physisorbed molecules, what is missing in the theories outlined above is an adequate treatment of the crystalline nature of the substrate, which influences the resonance through multiple scattering between the surface and the molecule.

Recently Rous (1991b) has used the coupled-angular-modes method of Teillet-Billy and Gauyacq (1991) to reexplore the resonance electron scattering by N_2 on a metallic surface, the case originally considered by Gerber and Herzenberg (1985). In contrast with the approach of Gerber and Herzenberg, the CAM method allows the simultaneous inclusion of both the image potential and the surface barrier. For the model system consisting of an abrupt surface barrier of height -9.8 eV, Rous has demonstrated excellent agreement between the resonance lifetime obtained by the CAM method and the multiple-scattering method of Gerber and Herzenberg.

The results obtained when the surface barrier and image potential are both included are shown in Figs. 13 and 14. We see the characteristic reduction in the resonance energy and lifetime as the molecule approaches the surface, which indicates that, for the expected adsorption height of 4–5 a.u. (2.1–2.7 Å), the resonance lifetime is reduced by 40% to 60% compared with the gas phase.

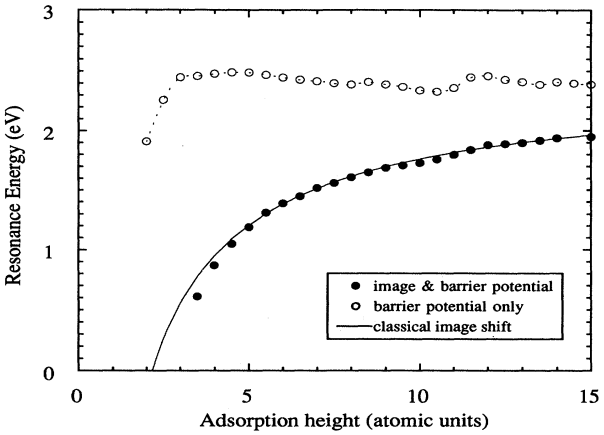

FIG. 13. Energy of the $^2\Pi_g$ resonance in a N_2 molecule as a function of the distance of the molecular center of mass from a metallic surface, calculated using the coupled-angular-modes method: ●, resonance energy with inclusion of the long-range image potential; ○, resonance energy without inclusion of the long-range image potential. Also shown is the classical image shift corresponding to the value of the image potential at the center of mass of the molecule (solid line). The resonance energy tends asymptotically to the gas-phase value of 2.4 eV far away from the surface. Rous (1991b).

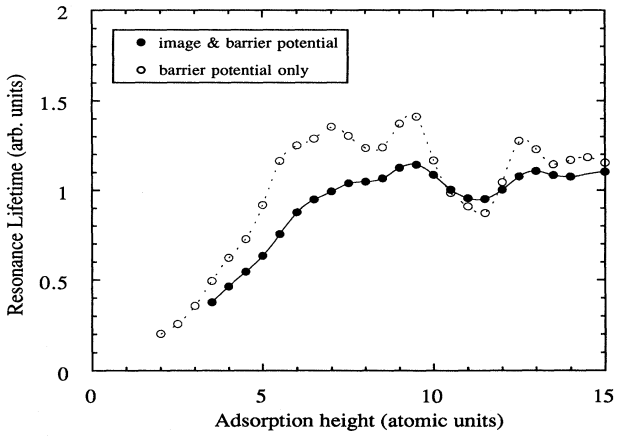

FIG. 14. Resonance lifetime of the $^2\Pi_g$ resonance in a N_2 molecule as a function of the distance of the molecular center of mass from a metallic surface, calculated using the coupled-angular-modes method: ●, resonance lifetime with inclusion of the long-range image potential; ○, lifetime without inclusion of the long-range image potential. The resonance lifetime has been normalized to that of the free molecule ($=1$). Rous (1991b).

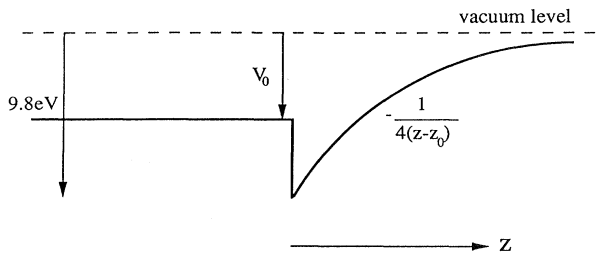

FIG. 15. A schematic diagram of the model potential used to explore the effect of strong substrate reflectivity upon the N_2 resonance. The surface barrier height is adjusted to alter the effective reflectivity of the substrate. As the barrier height approaches the resonance energy the surface becomes perfectly reflecting. Rous (1991b).

The resonance energy drops from 2.4 eV to between 0.9 and 1.3 eV. These values are in reasonable agreement with the observed resonance energy, 1.2 eV, of N_2 on polycrystalline silver (Demuth *et al.*, 1981) and with the resonance lifetime, 40% of the gas-phase value, extracted from the measured overtone intensities (Gadzuk, 1983). Note that, in common with the study of CO by Teillet-Billy and Gauyacq (1991), described above, the reduction of the N_2 resonance energy closely follows that expected from a simple image shift.

Rous went on to explore what happens when the height of the surface barrier potential is changed. The calculations of Gerber and Herzenberg considered the surface barrier height fixed at the sum, −9.8 eV, of the work function and the Fermi energy of the case under consideration (Ag). In the work of Teillet-Billy and Gauyacq, the surface barrier height was taken to be −12.4 eV (the substrate under consideration being Ni) and was matched smoothly onto the classical image potential outside the surface. In reality, the potential inside the surface is not constant but reflects the periodic crystalline nature of the substrate. This periodic potential can strongly affect the reflection of electrons at the surface barrier and therefore strongly modify the lifetime of the resonance as a consequence of multiple electrons scattering between the surface and the molecule. One might expect that the surface barrier approximation would be reasonable if the reflectivity of the metallic substrate were low. This is the case when the energy of the resonant state lies within an unoccupied band of the metallic substrate, because then the electron can easily propagate into the empty electronic states of the metal and the probability of reflection is low. Rous considered what would happen if the resonance energy coincided with a band gap of the metal above the vacuum level. Under these circumstances the electron trapped in the resonance cannot escape into the metal. Instead it is reflected with a probability of unity from the substrate. Rous modeled this case by changing the surface barrier height to alter the reflectivity of the substrate (Fig. 15). In Fig. 16 we show a contour plot of the resonance lifetime as a function of the distance between the molecule and the surface barrier height. As the top of the surface barrier

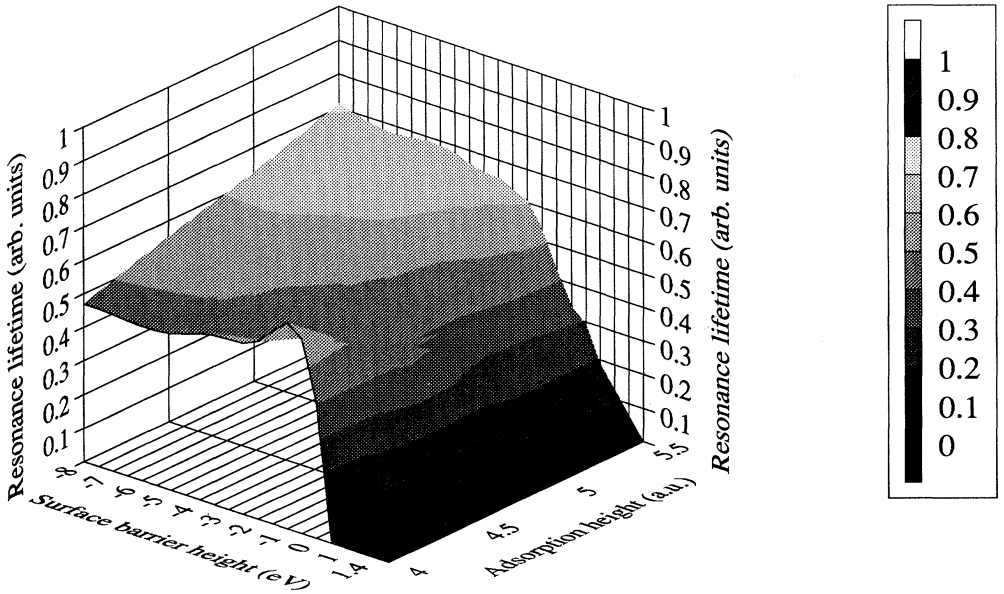

FIG. 16. A contour plot of the lifetime of the $^2\Pi_g$ resonance in a N_2 molecule as a function of both the distance of the molecule from the surface and the height of the barrier potential at the surface (V_0). The surface barrier matches the classical image potential at $z=0$ when $V_0=-9.8$ eV.

is raised towards the value of the resonance energy, the substrate reflectivity rises towards unity and the resonance lifetime is seen to decrease rapidly. For high enough reflectivities the resonance is quenched by multiple scattering.

Whilst this model potential clearly does not adequately reflect the scattering properties of a real metallic surface, the calculation does illustrate an important point, namely, that band structure of the substrate can have a dramatic influence upon the resonance behavior of an adsorbed molecule. In particular, this study shows that negative-ion resonances in adsorbed molecules can be quenched when the resonance energy coincides with a gap in the projected band structure of a metallic substrate. However, we note that whilst dramatic effects can be expected when the substrate reflectivity is high, the quenching of the resonance may be particular to the N_2 system considered here. We might imagine that, for some adsorption geometries and resonant states, the strong scattering from the surface may lead to the opposite effect, the stabilization of the resonance. This would occur when the molecule-surface distance was such that the electron wave field backscattered from the surface constructively interfered with the resonant state. Indications of this type of enhancement can be seen in the large-z behavior of the resonance lifetime shown in Fig. 13. However, for the $^2\Pi_g$ resonance of N_2 on a metallic substrate, only quenching was observed. The further exploration of this phenomenon, based upon a more accurate representation of the scattering properties of a real metallic surface, is clearly necessary.

2. Experimental results and analysis

The first observations of electron scattering by molecules physisorbed on solid surfaces were reported independently by two groups in 1981. Sanche and Michaud (1981a) described HREELS spectra (Fig. 17) and excitation functions for multilayer films of molecular O_2 condensed on the surface of a polycrystalline niobium ribbon. Demuth *et al.* (1981; Schmeisser *et al.*, 1982) reported HREELS spectra and excitation functions for a variety of molecules (N_2, CO, O_2, H_2) adsorbed on a polycrystalline silver surface in both monolayer and multilayer regimes (Fig. 18 shows the HREELS spectrum of a monolayer of N_2). In broad terms one can summarize the results of these papers as follows:

(i) The vibrational frequencies of all the molecules were close to the corresponding gas-phase values; the molecules were physisorbed.

(ii) In some cases a whole sequence of vibrational overtones was excited in addition to the fundamental vibrational mode.

(iii) The intensities of the vibrational modes observed in the HREELS spectra were strong functions of the electron-impact energy; resonances were observed with energies and widths broadly similar to those in the gas phase.

(iv) In the case of condensed O_2, the cross section for the low-lying electronic transition $^3\Sigma_g \rightarrow {}^1\Delta_g$ also exhibited a resonance, with an energy similar to that of the free (gas-phase) molecule.

These results proved conclusively that gas-phase resonances do survive weak adsorption on a solid surface. We shall now examine in more detail some of the more subtle effects that these authors observed, with a view to discussing the perturbation of the energy and lifetime of the resonant states on the surface.

Figure 19 shows the excitation functions obtained by Demuth *et al.* (1981), together with reproductions of the corresponding gas-phase data. Let us concentrate on the N_2 and CO molecules, for which the most extensive data are presented. The data points joined by solid lines correspond to the monolayer regime. One can see that in both cases the peak in the resonance profile is shifted down somewhat compared with the gas-phase case, a shift which Demuth *et al.* attributed to the influence of the image potential created by a metallic surface. It is

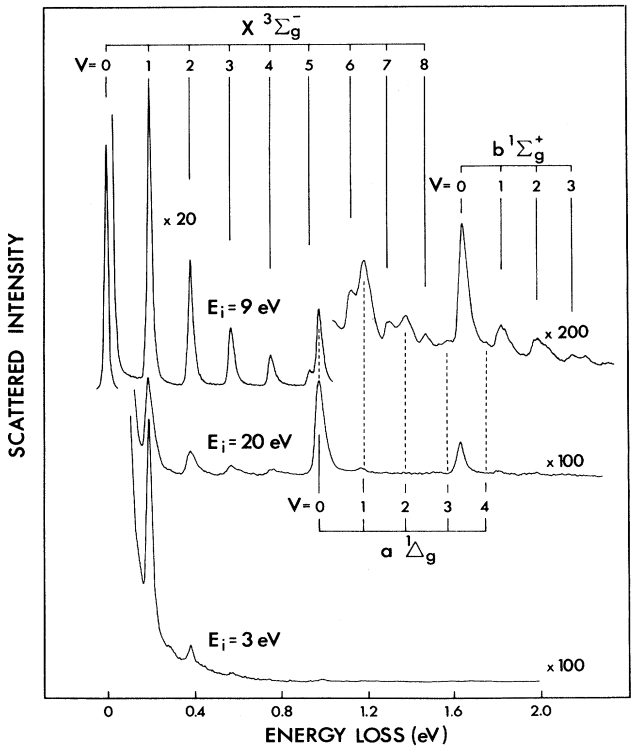

FIG. 17. Electron-energy-loss spectra of a disordered multilayer film of condensed O_2 obtained at various incident-electron energies. At an incident energy of 9 eV, where a negative-ion resonance is formed, the cross sections for both vibrational and electronic excitation are enhanced, and a sequence of vibrational overtones is observed. Sanche and Michaud (1981a).

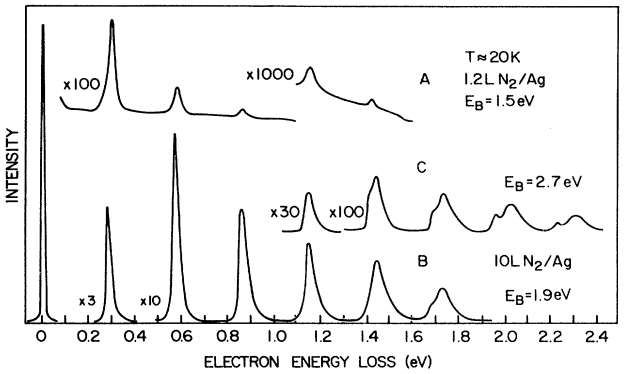

FIG. 18. Electron-energy-loss spectra of N_2 physisorbed on a polycrystalline Ag surface at 20 K. Curve A is obtained with a coverage of about one monolayer; curves B and C correspond to N_2 multilayer films. The incident electron-beam energies are shown in the figure. The strong excitation of the fundamental vibration of N_2 and vibrational overtones is attributed to the formation of a negative-ion resonance. Demuth *et al.* (1981).

noticeable that the downward shift appears significantly larger in the case of N_2, which is somewhat surprising if the image potential is the only factor involved. At higher coverages, corresponding to the multilayer regime, the resonance moves to higher energy in the case of N_2, but to lower energy in the case of CO; a shift to higher energy is anticipated as the molecules move out of range of the image potential. In retrospect, it appears that in addition to the doubtless important role of the image potential, the data may be evidencing the modulation of the cross section due to multiple elastic scattering, which we shall discuss in Sec. V.C. Such a modulation would depend on the existence of ordered patches of oriented molecules, even on a surface with long-range disorder, so that coherent multiple-scattering effects might be evident in the monolayer but washed out at higher coverages where disordered molecular films form. Such an argument might also account for the high-energy wing observed in the monolayer CO excitation function.

Neither the N_2 nor the CO resonances observed by Demuth *et al.* showed the fine structure that is observed in the gas phase and that is attributed, according to the "boomerang" model (see, for example, Birtwistle and Herzenberg, 1971), to interference effects arising from the propagation of the nuclear wave packet over the potential-energy surface of the negative ion (although the discrete electron-impact energies used in the experiment might conceal some structure). The authors thus concluded that the lifetime of the resonance on the surface conformed to the impulse limit, corresponding to a reduction in comparison with the gas phase. In a further and more detailed analysis of the N_2/Ag (polycrystalline) system, the same group (Schmeisser *et al.*, 1982) noted that the intensities of the N_2 vibrational overtones fell away with increasing quantum number at a rate faster than in the gas phase. This observation was interpreted as a further manifestation of a reduced resonance lifetime caused by a perturbation of the molecular potential by the surface.

In an effort to quantify, at least approximately, the reduction in resonance lifetime, Gadzuk (1983) applied the displaced harmonic-oscillator model described in Sec. II.A.4 to the experimental overtone intensities. As shown in Fig. 20, the experimental overtone distribution can be simulated very nicely if the resonance lifetime is reduced to 40% of its gas-phase value. We note that this number is somewhat dependent upon the way in which the decay of the negative ion is described; the result stat-

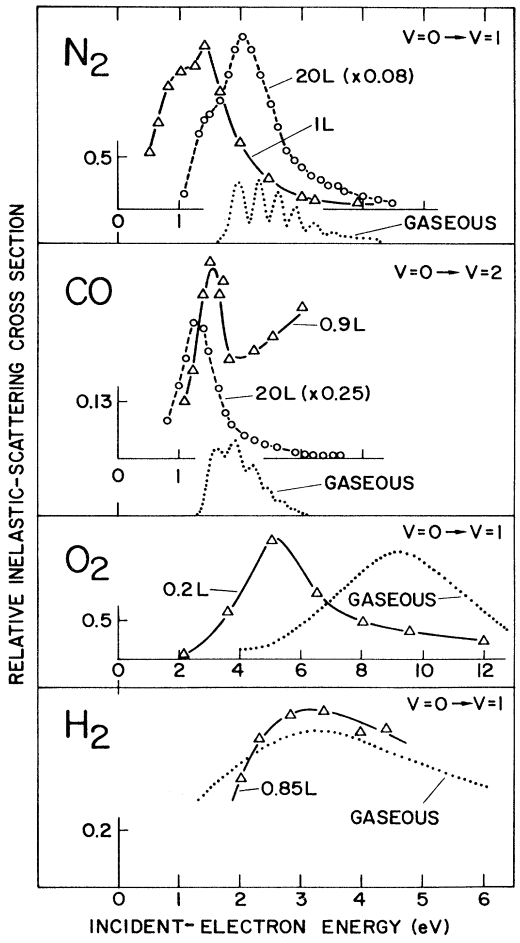

FIG. 19. Cross sections for vibrational excitation of various molecules (v=0–1 modes of N_2, O_2, and H_2; v=0–2 mode of CO) physisorbed on a polycrystalline Ag surface as a function of incident electron-beam energy, normalized by the elastic-scattering intensity. A resonance is seen in each case and attributed to the formation of a short-lived negative ion. In the case of N_2 and CO, shifts in the resonance profile between the monolayer regime (solid lines) and the multilayer regime (dashed lines) are evident. Gas-phase resonance profiles are also shown for comparison. Demuth *et al.* (1981).

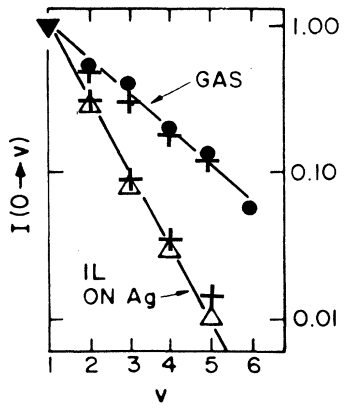

FIG. 20. Normalized intensities of successive vibrational overtones of a monolayer of N_2 physisorbed on Ag (open triangles) at the $^2\Pi_g$ resonance energy, compared with the gas phase (solid circles). Theoretical results embodying a reduced resonance lifetime on the surface are also shown (crosses). Gadzuk (1987).

ed assumes the exponential form of decay discussed in Sec. II.A.4. If, for example, the negative ion is assumed to decay abruptly at $t = \tau$, then a significantly longer lifetime (80% of the gas-phase value) is obtained (Gadzuk, 1988).

The question of whether the absence of fine structure in the resonance profile, in cases where such structure is observed in the gas phase, is an indication of reduced lifetime is a subtle one and warrants some attention. In an early study of resonances in N_2 multilayers, condensed on a polycrystalline platinum ribbon, Sanche and Michaud (1981b) observed four resonances in the energy range 1–25 eV, just as in the gas phase. However, the fine structure observed in the lowest-energy $^2\Pi_g$ resonance in the gas phase was found to be missing. The authors noted, however, that the effect could have been caused by site-to-site fluctuations in the local potential in the film, effectively smearing out the energy resolution of the primary electron beam. In subsequent studies of the same system Sanche and Michaud (1984b) were able to observe fine structure in the resonance, but only in N_2 films with thicknesses of two monolayers and above. However, when submonolayer N_2 was deposited on top of an inert gas (Ar) spacer layer on the Pt substrate, fine structure in the N_2 resonance profile was observed, and this structure became increasingly apparent as the thickness of the spacer layer was increased from one monolayer upwards (Fig. 21; Michaud and Sanche, 1990). One interpretation of these results is that N_2 molecules near the substrate are perturbed, such that the resonance lifetime is reduced, causing the fine structure to be smeared out. Another interpretation, however, is that the (N_2 or Ar) film becomes smoother as it gets thicker (recall that the substrate is rough), so that local potential fluctuations are diminished; in this view the observation of the resonance fine structure is obscured by resolution broadening, and not by lifetime reduction.

Someone might ask "why can't you just extract the lifetime of the resonance from the width of the resonance profile in the excitation function?" The issue is, however, not as straightforward as it might seem. There is, in fact, no simple and general prescription that allows one to extract the lifetime from the measured resonance profile. When a resonance in a gas-phase molecule has a very long lifetime, and the resonance profile consists of a series of sharp peaks (yet to be observed in surface experiments) due to the vibrational levels of the negative-ion state, then one can make a case that the width of the peaks is the inverse of the resonance lifetime. However, Nilsson (1991) has pointed out that, in the case of an adsorbed molecule, there can be a broadening of the peaks in the resonance fine structure even if the resonance lifetime is unchanged. This phenomenon arises from the new low-frequency frustrated translational and rotational modes that are generated when a molecule is adsorbed on a surface. The Franck-Condon transition describing the formation of the negative-ion state may then involve the population of a distribution of these low-frequency and probably unresolved modes, which would manifest itself as a broadening of the vibrational levels of the negative-

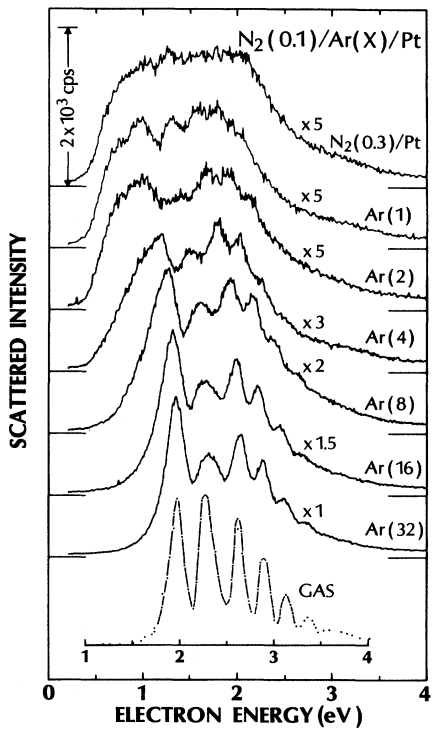

FIG. 21. Excitation function for the $v=0-1$ vibrational excitation of N_2 separated from a polycrystalline Pt substrate by an Ar spacer layer of various thicknesses, given in monolayers. The fine structure visible in the gas-phase resonance profile (also shown) is seen to develop as the N_2 molecules are displaced further away from the metallic substrate. Michaud and Sanche (1990).

ion state. A similar effect is thought to give rise to line broadening in the photoemission spectra of adsorbed molecules (Gadzuk *et al.*, 1982; Nilsson and Mrtensson, 1989). When the lifetime of a resonance is comparable with the vibrational period of the molecule (and the "boomerang" fine structure is observed) or shorter, the simple relation between the resonance profile and the resonance lifetime is again lost, this time even in the case of a molecule in the gas phase.

In the case of the thick films of N_2 where they were able to distinguish fine structure, Sanche and Michaud *estimated* the lifetime from the width of the leading edge of the excitation function, which suggested a decrease of about 15% compared with the gas phase. This figure is in the same ball park as the 40% reduction derived by Gadzuk for the N_2 monolayer on polycrystalline Ag. These numbers represent really rather modest decreases in lifetime compared with what might have been anticipated before the experiments took place, and one would not expect lifetime reductions of this order to prevent the observation of resonances in the physisorbed or condensed phase that have already been seen in the gas phase, especially since the density of the target is much greater on the surface than in the molecular beams used in gas-phase experiments (Ibach, 1982).

At submonolayer coverages of N_2 on a polycrystalline platinum substrate, Sanche and Michaud (1983, 1984b) found that the low-energy $^2\Pi_g$ resonance was shifted down in energy by 0.6 eV compared with the corresponding multilayer film. The resonance in the multilayer was itself shifted down in energy by 0.7 eV with respect to the gas-phase molecule (a similar shift with respect to the gas phase, 0.6 eV, was also found in the energy of the isoelectronic $^2\Pi$ resonance observed in a CO multilayer film; Sanche and Michaud, 1984b). Sanche and Michaud attributed the shift in the multilayer to polarization of the neighboring molecules in the film, and the further shift in the monolayer to the effect of the image potential.

Jacobi and co-workers have made several investigations of resonance scattering by N_2 and CO physisorbed on single-crystal metal surfaces at low temperatures. On Al(111), the cross sections for electron-impact excitation of the molecular stretch modes (measured in the specular direction) differed significantly from one molecule to another (Jacobi *et al.*, 1989). In the case of the N_2 monolayer, a resonance was clearly seen in the excitation function (Fig. 22), centered at about 1.4 eV, a result that coincides nicely with the resonance observed by Demuth *et al.* (1981) in the physisorbed N_2 monolayer on polycrystalline Ag. Demuth *et al.* (1981) attributed this resonance to the gas phase (Schulz, 1973b). In the case of CO, Jacobi *et al.* observed no such clear resonance structure, only a small enhancement near 2 eV superimposed on the smoothly varying dipole scattering cross section (Fig. 22). The predominance of dipole scattering in the case of CO is, however, no surprise, given that the results were obtained in the specular direction; the low-energy CO resonance observed by Demuth *et al.* (1981) for CO

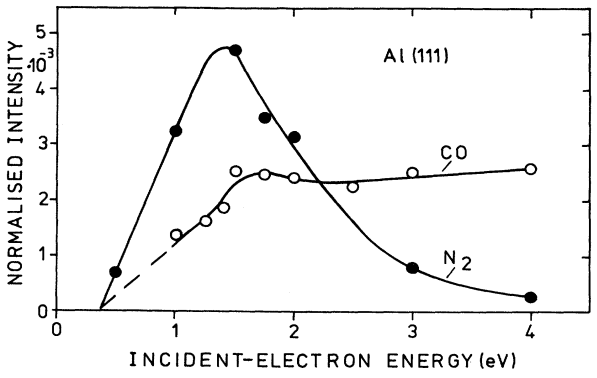

FIG. 22. Excitation functions for the $v=0-1$ vibrational excitation of physisorbed monolayers of N_2 and CO on Al(111), normalized by the elastic-scattering intensity, showing a strong resonance in the case of N_2 but not CO. Jacobi *et al.* (1989).

on polycrystalline Ag was identified from the cross section for excitation of the $v=0-2$ overtone vibration, for which the dipole cross section is negligible. [One might also expect to suppress the dipole contribution in a case like CO/Al(111) by measuring the excitation function of any of the vibrational modes, e.g., the fundamental, with a choice of analyzer angle well away from the specular direction]. Jacobi *et al.* noted that the maximum in the cross section which they derived for N_2/Al(111) was larger than for CO/Al(111) and saw this as manifesting the magnitude of the resonance scattering cross section. It is possible, therefore, that the maximum resonance scattering cross section for CO, which might lie away from specular, exceeds the CO dipole cross section, which peaks on specular.

In subsequent papers, Jacobi and co-workers (Jacobi, Bertolo, and Hansen, 1990; Hansen *et al.*, 1991) claimed that a quenching of the negative-ion resonance could be observed in the case of monolayer CO on the Ag(111) surface. HREELS spectra (Fig. 23), obtained 25 degrees away from the specular direction so that dipole scattering was strongly suppressed, showed negligible CO $v=0-2$ intensity at submonolayer coverages, whereas at multilayer coverages this mode was observed, and with the line-shape asymmetry characteristic of resonance scattering (see Sec. VI.B.3). The overtone was also identified in submonolayer coverages of CO on top of a Xe spacer layer (Fig. 23). The authors concluded that a specific interaction between the CO molecules and the Ag(111) surface was quenching the negative-ion resonance, although a detailed model of this interaction was not proposed. The result seems at first to be at variance with the data of Demuth *et al.* (1981), who, as we discussed above, reported a negative-ion resonance in what was claimed to be monolayer CO on polycrystalline Ag. However, Jacobi *et al.* suggested that three-dimensional CO growth may have occurred on the porous, polycrystalline Ag film, so that Demuth *et al.* were really observing reso-

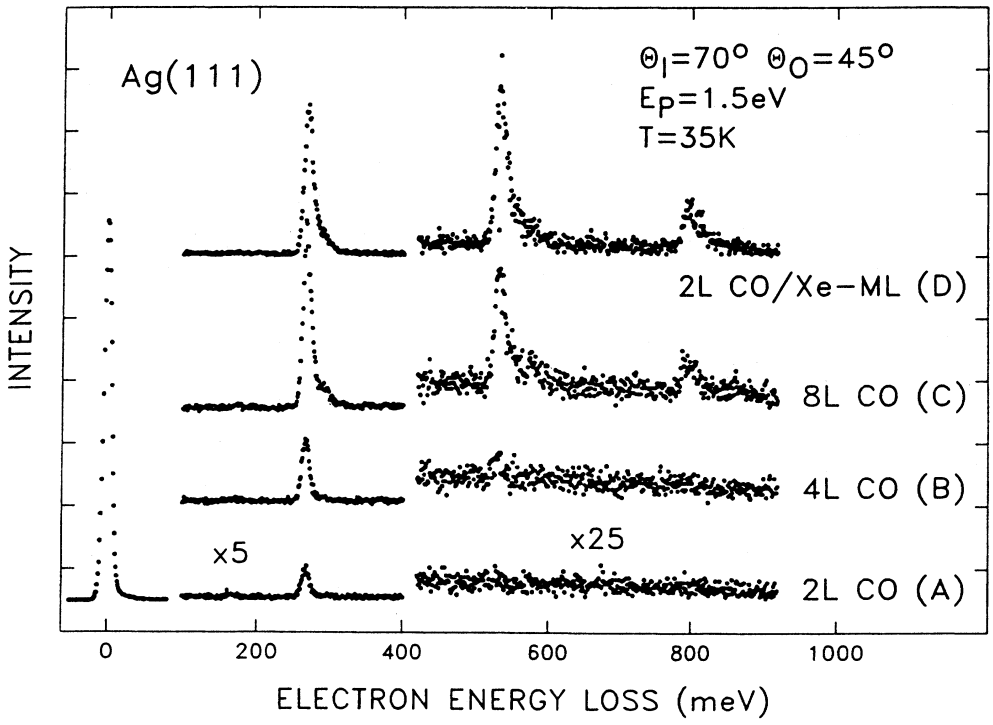

FIG. 23. Electron-energy-loss spectra of CO physisorbed on Ag(111) as a function of coverage. The $v=0-2$ and $v=0-3$ vibrational excitations are not visible at the lowest coverage, 2L (and the $v=0-1$ excitation is weak), unless the CO molecules are displaced away from the metallic surface by a spacer layer of Xe. Jacobi, Bertolo, and Hansen (1990).

nance scattering by those CO molecules remote from the metal surface. Exactly why the CO $^2\Pi$ resonance should be quenched on Ag(111), whereas neither the isoelectronic $^2\Pi_g$ resonance of N_2 (Jacobi, Bertolo, and Hansen, 1990) nor the $^2\Sigma_u$ resonance of H_2 (Demuth *et al.*, 1983) on Ag(111) are quenched, remains enigmatic. As Hansen *et al.* (1991) have recently noted, a reduction of the resonance lifetime in the monolayer (rather than a complete quenching), leading to a reduction in the overtone intensities, may make finding the resonance difficult, because strong dipole excitation of the fundamental vibration of a heteronuclear molecule may obscure the resonant contribution to this mode.

B. Effect of chemical bonding to the surface

If the image potential and the short-range surface potential perturb the energy and the lifetime of the resonance, then one expects that the redistribution of electronic charge resulting from the formation of a chemical bond between the molecule and the surface in the case of chemisorption will produce similar, if not more striking, effects. The theoretical treatment of such effects remains undeveloped, so after some speculations as to the shape which such a theory would need to take, we concentrate on various experimental investigations of resonance scattering by chemisorbed molecules.

1. Theoretical models

The theories regarding the influence of the image potential and of the short-range surface potential on the resonance energy and lifetime, described in Sec. IV.A.1, largely pertain to physisorbed molecules. To date, resonance electron scattering from chemisorbed molecules has received very little theoretical attention. Nevertheless, we may speculate on the physical mechanisms that may play an important role in perturbing the resonant states in chemisorbed molecules.

In the simplest terms chemisorption implies that the molecule-surface interaction is much stronger than in the physisorption case. The work of Gerber and Herzenberg (1985) and of Teillet-Billy and Gauyacq (1991) implies that as the molecule approaches the surface (i.e., the surface-molecule interaction is increased) the effect of the image potential is more pronounced in dragging down the resonance energy and shortening the resonance lifetime. Indeed one expects a very strong distortion of the centrifugal barrier upon chemisorption. These models, however, take no account of the distortion of the electronic structure of the molecule through the formation of the chemical bond between the molecule and the surface, an effect which can be regarded as a modification of the molecular core scattering by the presence of the surface. Particularly dramatic perturbations may be expected

when charge transfer from the substrate to the molecule proceeds through the partial occupation of an affinity level of the molecule associated with the formation of the negative ion. Other strong perturbations may arise from a strong overlap between the resonant orbital and the unoccupied electronic states within the surface. Unoccupied surface states or bands above the Fermi energy of a metallic substrate may provide new routes of escape for the trapped electron, effectively short-circuiting the resonance.

We also note that charge transfer between the chemisorbed molecule and the surface generally results in a perturbation of the vibrational behavior of the molecule, evident, for example, in the shifting of vibrational frequencies relative to the free molecule. Therefore we expect that the potential-energy surface over which the internuclear motion takes place will be altered, perhaps radically, with fundamental implications for the observed resonance scattering cross sections. To our knowledge, no detailed theoretical study of this bonding effect has been performed to date.

2. Experimental results and analysis

The first indication of a resonance in the cross section for excitation of an adsorbed molecular species was reported by Andersson and Davenport (1978), shortly after the publication of the theory paper by Davenport *et al.* (1978) on resonance electron scattering by isolated, oriented molecules, and it concerned chemisorbed species. Andersson and Davenort looked at the chemisorption of CO on Ni(100) and of the OH group on NiO(111). The NiO(111) surface was produced by oxidation of the Ni crystal; the OH groups were produced by exposure to H_2O. The excitation function of the CO stretch vibration conformed to the dipole scattering theory, but the intensity of the OH stretch (and overtone) was substantially enhanced as the beam energy was lowered down to 2.4 eV (Fig. 24), opposing the dipole scattering model. The intensity of the OH overtone (not a double loss) that they were able to observe was also much stronger than expected from dipole scattering. They suggested these effects were due to the formation of a resonance, and, while they were not able to pin down the electronic structure of the negative-ion resonance, they speculated that such a state might arise from adding an electron to the 4-s level of the OH group. In a subsequent analysis of the vibrational excitation of the CO stretch mode on Cu(100), investigated experimentally by Andersson (1979), Persson (1980) found that dipole scattering theory could not entirely account for the observed cross section and postulated a small resonant contribution between 1 and 2 eV assigned to the familiar $^2\Pi$ shape resonance. With the benefit of hindsight one is intrigued to know what the cross sections in the OH/NiO(111) and CO/Cu(100) systems might have looked like had they been recorded away from the specular direction, but thus was born the experimental investigation of resonance scattering by adsorbed molecules.

Another indication of the survival of the $^2\Pi$ shape resonance even in chemisorbed CO was provided by the

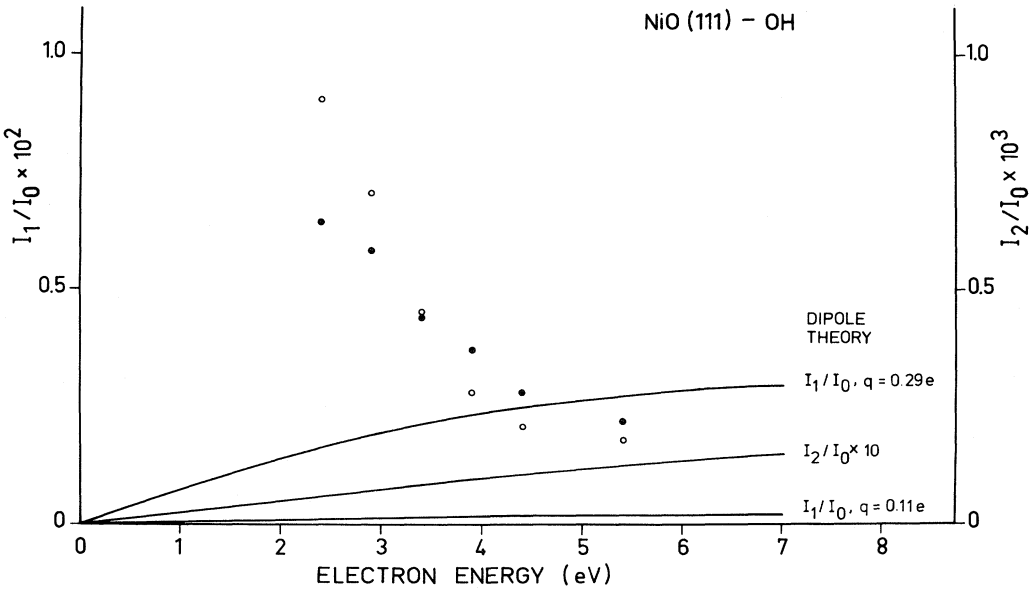

FIG. 24. Cross sections for excitation of the fundamental and first overtone of the stretching mode of OH chemisorbed on NiO(111) as a function of electron-beam energy. In both cases the experimental data deviate radically from the predictions of the dipole scattering theory (solid lines). This deviation is attributed to a negative-ion resonance of the OH group. Andersson and Davenport (1978).

work of Ibach (Ibach, 1982; see also Baro and Ibach, 1981) on the CO/Pt(111) system. Ibach found that the excitation function for the CO stretch mode in the electron-impact energy range 2–9 eV (Fig. 25) looked quite unlike the prediction of the dipole scattering theory but rather resembled a very broad resonance. The large width of the resonance (about 9 eV), compared with the gas phase, indicated a shortened lifetime on the surface. In fact, the resonance was a little broader in the case of bridge-bonded CO than in the case of on-top CO, qualitatively consistent with a stronger interaction between the molecule and the surface in the bridge site, though now that one knows about the modulation of the molecular resonance cross section by multiple-scattering effects (Sec. V.C), one might want to be cautious about this suggestion. Ibach's study also isolated some rather interesting effects relating to mode selectivity in resonance excitation of adsorbates. He showed that weak vibrational features evident in the off-specular HREELS spectra were compatible with the selection rules discussed in Sec. VI.A, as they relate to the on-top and bridge-site point-group symmetries of the CO/Pt(111) system.

The topic of resonance excitation of the chemisorbed OH group, discussed above, was pursued by Stucki *et al.* (1984), who investigated OH/Si(100) (2×1). These authors observed not only the fundamental OH stretch vibration but also first and second overtones of the OH stretch, as well as combination bands involving these

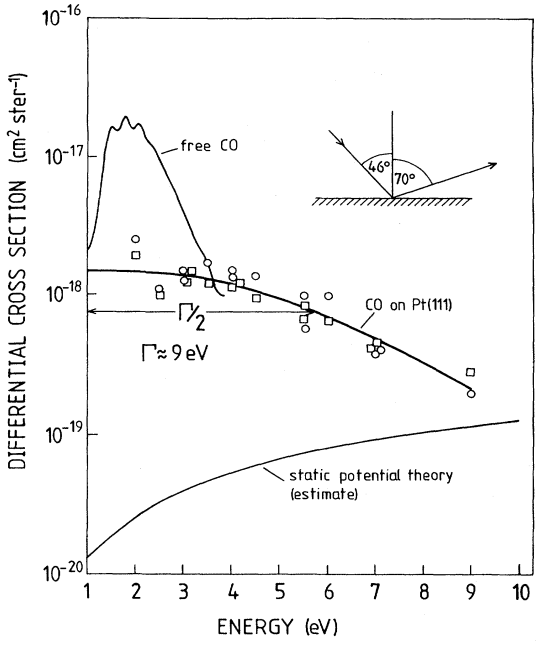

FIG. 25. Cross section for excitation of the stretching vibration of CO chemisorbed on Pt(111) as a function of electron-beam energy (away from the specular direction). The deviation from the prediction of the dipole scattering (static potential) theory is evident and is attributed to a broad negative-ion resonance. The gas-phase resonance profile is shown for comparison. Ibach (1982).

overtones. Similar results were obtained with the OD species. The energy dependence of the mode intensities was not reported, but the authors mentioned that the loss features of interest were more pronounced at low impact energy (1.5 eV) than at higher energy (7 eV). This is consistent with the OH resonance profile in the OH/NiO(111) system reported by Andersson and Davenport (1978), which rises monotonically as the beam energy is lowered towards 2 eV.

A further report of resonance scattering by the hydroxyl group by a HREELS study of OH on the (100) surfaces of Ge_xSi_{1-x} alloys, grown by molecular-beam epitaxy, was given, in summary form, by Farrell *et al.* (1985). First and second overtones of the OH stretch were once more observed with low electron-beam energy. The new feature in this work was the observation of modulations in the cross section for vibrational excitation of the OH fundamental and first overtone as a function of energy, which were sensitive to the scattering geometry. What causes these modulations? One possibility is that they arise from multiple elastic electron scattering (Sec. V). Another possibility is that there might be structure in the elastic peak intensity used to normalize the excitation functions. Farrell *et al.*, however, concentrated on how such an effect might be explicable in terms of resonance scattering by the OH group itself.

Farrell *et al.* modeled the OH group by a pair of shielded Coulombic potentials centered upon the O and H atoms and calculated the matrix element for vibrational excitation as a function of the scattering geometry and the incident-electron energy. It was assumed that the internuclear motion was that of a simple harmonic oscillator. The resulting energy dependence of the cross section for $v \rightarrow 1$ vibrational excitation was found to be strongly dependent upon the scattering geometry. In effect, the modulations derived by Farrell *et al.* may be considered to be due to a mixture of partial waves in the OH resonance; the interference of these partial waves then leads to structure in the cross section as a function of both energy and angle. The resonance behavior of this system is, in fact, analogous to that of CO, studied by Davenport *et al.* (1978), because both OH and CO lack inversion symmetry. This implies that more than one partial-wave component contributes to the resonance. In further experimental investigations of this idea, one would want to study in detail the angular distribution of electrons scattered via the resonance, as a function of the angle of incidence.

A further twist to the story of resonance scattering by the OH group was provided by the work of Nishijima *et al.* (1986), who looked at OH (and OD) chemisorption on the Si(111) (7×7) surface. They found a resonance near 5 eV in the cross section for excitation of the OH stretch mode and the Si-OH bending mode—the first report, to our knowledge, of resonant excitation of a molecule-surface mode (Sec. VI). The authors, following Andersson and Davenport (1978) in the case of OH on NiO(111), speculated that the resonance might have

arisen from electron trapping in the 4*s* orbital of the OH species. On the assumption that this assignment was correct (in both cases), the authors saw the shift in energy as reflecting differences in the electronic structure of the OH group on the two surfaces, though the possible influence of multiple scattering in altering the resonance profile (Sec. V.C) cannot be ignored.

The degree to which the electronic structure of a particular molecular resonance is perturbed as a function of the strength of the molecule-surface bond is nicely highlighted by the study of O_2 adsorption on the Pd(111) surface conducted by Imbihl and Demuth (1986). As a function of surface temperature and treatment, a variety of O_2-derived species can be obtained: physisorbed O_2, atomically chemisorbed O, and a sequence of molecularly chemisorbed species, each species identified by its characteristic vibrational frequency. Imbihl and Demuth found a resonance in the cross section for excitation of the stretch mode of the physisorbed molecule centered at 6 eV under specular scattering conditions (Fig. 26), possibly due to the $^2\Pi_u$ Feshbach resonance of O_2. The cross sections for excitation of the stretch modes of two molecularly chemisorbed species were also measured (Fig. 26); the resonance peak at 6 eV was lost, but the cross sections increased sharply as the beam energy was lowered to the minimum value used, 3 eV. While this substantial shift in resonance energy may involve contributions from multiple-scattering effects (Sec. V.C), it does seem to indicate a striking perturbation of the resonant state due to chemisorption. Indeed, as Imbihl and Demuth discuss, the standard bonding scheme used to describe the molecularly chemisorbed O_2 species, which involves substantial charge transfer from the substrate into the $2p\pi_g^*$ affinity level of O_2, represents a significant perturbation of the electronic structure of the molecule. Since creation of the $^2\Pi_u$ Feshbach resonance in the isolated O_2 molecule involves the addition of two electrons to this level, thereby filling it, one would certainly expect the properties of this resonance to be substantially modified in the molecularly chemisorbed species.

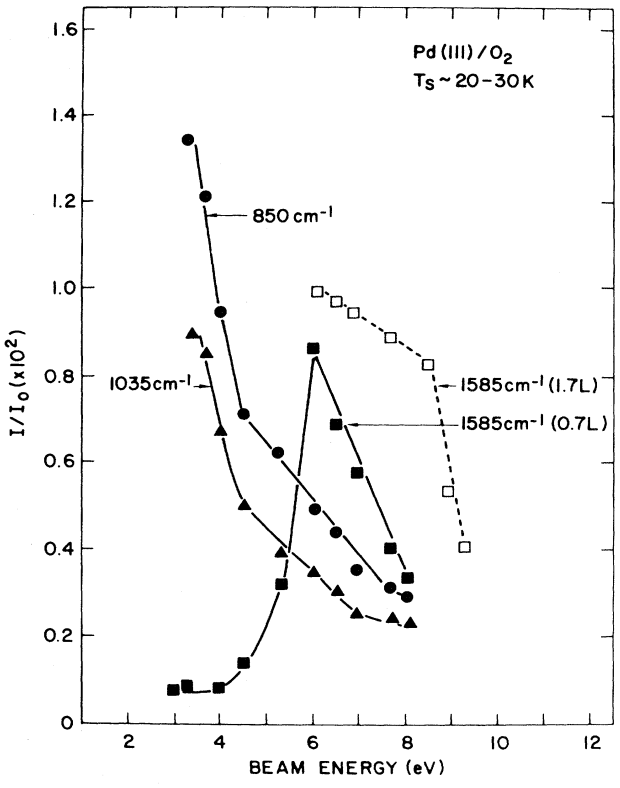

FIG. 26. Cross sections for excitation of the stretch modes of various species of O_2 on Pd(111) as a function of electron-impact energy. The experimental data sets are labeled according to the characteristic frequencies of these species. 1585 cm^{-1} is the frequency of physisorbed O_2 on this surface. 850 cm^{-1} and 1035 cm^{-1} are the frequencies of molecularly chemisorbed O_2 species. The resonance seen in physisorbed O_2 appears to be preserved but is shifted in energy in the chemisorbed species. Imbihl and Demuth (1986).

C. Effect of interaction with coadsorbed molecules

In the previous sections we have seen how the substrate may affect resonances within adsorbed molecules. We now turn to the issue of coadsorption and, in particular, how interactions between adsorbed molecules might affect the formation of resonances.

To date, the only experimental study of resonances in electron scattering by coadsorbed molecules was undertaken by Jacobi and co-workers (Jacobi, Bertolo *et al.*, 1990; Jacobi, Bertolo, and Hansen, 1990). Jacobi's group investigated the influence of the addition of small amounts of H_2O on the low-energy $^2\Pi_g$ shape resonance of the N_2 molecule when it is physisorbed in a monolayer on the Al(111) surface. The results they obtained were rather striking. The intensity of the N_2 stretch mode in the (specular) HREELS spectrum was substantially reduced (Fig. 27), the line shape of this vibration lost the high-energy wing attributed to resonant excitation of the molecule-surface vibrational mode (Sec. VI.B.3), and the angular distribution of inelastically scattered electrons (Sec. V.A.2) came to show a peak in the specular direction. Jacobi *et al.* attributed these dramatic changes to the quenching of the N_2 negative-ion resonance by the coadsorbed H_2O molecules; the residual, weak N_2 scattering was assigned to the dipole mechanism. The authors argued from photoemission data that the H_2O had not displaced N_2 from the surface, which would also have accounted for the suppression of the N_2 intensity. Importantly, Jacobi *et al.* also reported that they had checked that the N_2 resonance had not just shifted in energy due to addition of H_2O, and that they had searched for the N_2 mode at angles away from the specular direction.

What, then, is the origin of this resonance-quenching effect? Clearly some form of interaction between the

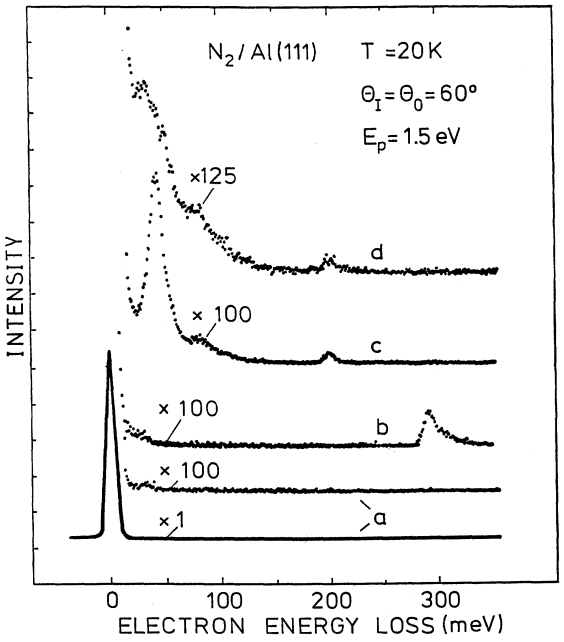

FIG. 27. Electron-energy-loss spectra of N_2 physisorbed on Al(111) and coadsorbed with H_2O: (a) clean surface; (b) 5 L N_2; (c) 0.16 ML H_2O with 5 L N_2; (d) as (c) but after warming sample. The $v=0-1$ vibrational excitation of N_2 at about 300 MeV disappears when water is coadsorbed. Jacobi, Bertolo, *et al.* (1990).

coadsorbates is involved. Jacobi *et al.* speculated that the quenching of the N_2 resonance was due to a *short-range* orbital overlap between the $2p\pi_g^*$ affinity level of N_2 and empty H_2O orbitals. The authors reported that the quenching appeared to saturate at a dose of H_2O corresponding to an H_2O/N_2 ratio on the surface of approximately 1 H_2O molecule to 5 N_2 molecules. If one assumes an intimate mixing of the two surface species, then certainly a direct interaction between the H_2O and N_2 seems possible.

On the theoretical front there are no published theories, although this will not prevent our considering the theoretical issues pertaining to resonance scattering in coadsorbates. If orbital overlap does occur then it may act to "short-circuit" the resonance, allowing the electron to tunnel through an effectively lower centrifugal barrier. Alternatively, charge transfer between the coadsorbates may distort the electronic structure of the host molecule, thus modifying the resonance in a similar manner to the formation of a chemical bond between the substrate and the molecule, as was discussed in Sec. IV.B.1. We note that this type of interaction may also proceed by a more indirect route, namely, by charge transfer between the molecules via the surface.

We must also consider the possibility of a longer-range, electrostatic interaction affecting the resonant state. This form of interaction could be particularly important if the coadsorbed molecule that does not support the resonance possesses a large dipole moment. In this case, the trapped electron feels the dipolar field of the coadsorbate leading to a modification of the potential, which temporarily binds the electron. Under these circumstances, the molecule in which the electron is trapped may also be polarized, an effect that would be expected to alter the potential experienced by the probe electron. Clearly, we are now entering into the realm of speculation because, at present, there are no existing theories of the effect of coadsorption upon the resonance properties of adsorbed molecules. Nevertheless, the theoretical investigation of resonances in coadsorption systems can be expected to be an important component of the future development of resonance electron scattering from adsorbed molecules.

V. RESONANCE SYMMETRY AND MOLECULAR ORIENTATION

The cross sections obtained in electron scattering by molecules in the gas phase average over the random distribution of molecular orientations present. Nevertheless, the angular distributions of electrons scattered via a molecular resonance are not isotropic; they manifest the symmetry of the negative ion that is formed. The differential cross sections for electron capture and electron emission show the same structure; the anisotropy of the capture cross section means that the probability of populating a resonant state is greater in some molecules than in others, so that the average over molecular orientations is weighted rather than uniform; hence the characteristic angular emission profiles that are observed. When a molecule is adsorbed on the surface of a solid, the axis of the molecule is often oriented. The measurement of the angular distribution of scattered electrons then reflects the symmetry of the resonant state (on the surface) *and* the orientation of the molecular axis, and is consequently a probe of both. If a molecule has, say, two resonant states of similar energy but different symmetry, it becomes possible to populate one state in preference to the other by controlling the scattering geometry. Molecules that are *oriented* on the surface of a solid are also often *ordered* in molecular arrays with good long-range order. In this case, the wave function of the electron that impinges upon a given molecule to form a transient negative ion reflects the coherent elastic scattering that occurs *en route* to the molecule; this wave function is no longer the plane wave of the gas-phase experiment. Similarly, the wave field of the electron emitted by the negative ion when it decays will be modified by coherent scattering *en route* to the detector. These coherent scattering effects modulate both the energy and the angular dependence of the cross section for resonance scattering. In this section we give detailed attention to this series of issues.

A. Angular distribution of scattered electrons

In this section we begin by laying out a scheme that can be used to interpret the type of angular distribution

of scattered electrons that has been obtained in recent experiments. We start with the case of the isolated, oriented molecule. We consider the modifications to this picture introduced by the image potential and by the coherent elastic scattering of the probe electron before and after the formation of the resonance, and we describe selection rules which can simplify the interpretation of the angular distributions measured. Subsequently we take a detailed look at the experimental results themselves.

1. Theoretical models

A helpful starting point in a consideration of the angular distribution of electrons scattered by oriented molecules on a surface is the hypothetical case of the isolated, oriented molecule. We describe the angular distributions obtained in this case, and then consider the effect of the surface upon the scattered electron. This can be split into two components, both of which involve elastic scattering of the electron before and after resonance formation. The first is electron scattering by the image potential, and the second is multiple elastic scattering of the electron among the surface atoms and the molecules in the overlayer. The relative importance of these two effects will be discussed below.

a. The isolated, oriented molecule

The simplest quantitative formulation of resonance scattering by an isolated, oriented molecule is given by Davenport *et al.* (1978). This treatment covers single-particle shape resonances, and not core-excited states. The probe electron and target molecule are represented by a single wave function Ψ, which is an eigenfunction of the full Hamiltonian $\mathcal{H}$ of the electron-molecule system with nuclear coordinates $\mathbf{R}$:

$$\mathcal{H}=-\tfrac{1}{2}\nabla_r^2+H_m(\mathbf{R})+V(\mathbf{r},\mathbf{R}) \ . \tag{25}$$

Here H_m is the Hamiltonian of the target molecule, V the electron-molecule interaction potential, and $\mathbf{r}$ the position of the probe electron. If the interaction time is short compared with the vibrational period of the molecule, then, according to the Born-Oppenheimer approximation, $\Psi(\mathbf{r},\mathbf{R})$ can be separated into a product of the vibrational wave function of the target molecule, $\chi_\nu(\mathbf{R})$, and the wave function of the probe electron, $\psi(\mathbf{r})$,

$$\Psi(\mathbf{r},\mathbf{R})=\chi_\nu(\mathbf{R})\psi(\mathbf{r},\mathbf{R}) \ . \tag{26}$$

Outside the range of the molecular potential the electron wave function ψ has the asymptotic form (for a fixed set of internuclear coordinates $\mathbf{R}$)

$$\psi(\mathbf{r},\mathbf{R})=e^{i\mathbf{k}\cdot\mathbf{r}}+\sum_{\mathbf{k}'} f_{\mathbf{k}\mathbf{k}'}(\mathbf{R})e^{i\mathbf{k}'\cdot\mathbf{r}} \ , \tag{27}$$

where f is the amplitude for elastic scattering of an electron from a plane wave with wave vector $\mathbf{k}$ into a plane wave with wave vector $\mathbf{k}'$. This scattering amplitude may be calculated using standard scattering theory. The full transition amplitude F between two states, such that in the first the molecule is in the vibrational state ν and the electron wave function is a plane wave of wave vector $\mathbf{k}$, while in the second the molecule is in the vibrational state ν' and the electron wave function is a plane wave of wave vector $\mathbf{k}'$, is then obtained by integrating over the nuclear coordinates $\mathbf{R}$ corresponding to the two vibrational eigenstates:

$$F_{\mathbf{k}\mathbf{k}'}^{\nu\nu'}=\int\int\int \chi_\nu(\mathbf{R})f_{\mathbf{k}\mathbf{k}'}(\mathbf{R})\chi_{\nu'}(\mathbf{R})d^3\mathbf{R} \ . \tag{28}$$

In an angular momentum representation, outside the range of the molecular potential, the incident-electron wave function can be expanded as a set of spherical partial waves about the center of mass of the molecule:

$$\psi_0(\mathbf{r})=\sum_{lm} A_{lm}j_l(\kappa r)Y_{lm}(\hat{\mathbf{r}}) \ . \tag{29}$$

If the electron excites a vibrational transition $\nu\rightarrow\nu'$, then the outgoing wave field of the scattered electron is

$$\psi_s(\mathbf{r})=\sum_{lm}\left[\sum_{l'm'} F_{lm,l'm'}^{\nu\nu'}A_{l'm'}\right]h_l^{(1)}(\kappa\tau)Y_{lm}(\hat{\mathbf{r}}) \tag{30}$$

where

$$F_{lm,l'm'}^{\nu\nu'}=\int\int Y_{lm}(\hat{\mathbf{k}})F_{\mathbf{k}\mathbf{k}'}^{\nu\nu'}Y_{l'm'}(\hat{\mathbf{k}}')d^2\Omega\, d^2\Omega' \ . \tag{31}$$

Thus the transition amplitude F describes the process by which the probe electron arrives at the molecule in the incoming partial wave (l,m), excites a vibrational transition within the molecule, and then leaves in the outgoing partial wave (l',m').

In order to calculate F, we first have to calculate f, the scattering amplitude for a fixed set of internuclear coordinates. This can be done using a multiple-scattering method (Danese and Connolly, 1974), or by more sophisticated means (Burke *et al.*, 1977). Within the standard multiple-scattering framework, the molecular potential experienced by the probe electron is partitioned into three regions separated by spherical surfaces (Fig. 28). Nonoverlapping spheres centered upon each nucleus are surrounded by an outer sphere. Inside each atomic sphere (region I) and beyond the outer sphere (region III) the potential is spherically averaged. Each atom can then be described by a set of phase shifts. In the interstitial region (region II) the potential is volume averaged to a constant. Inside the outer sphere the exchange-correlation potential can be modeled by a local potential of $X\alpha$ form, which is matched onto the classical polarization potential at the outer sphere.

Davenport *et al.* (1978) used this method to study the differential cross sections for inelastic electron scattering by isolated, oriented molecules. If the molecule is isolated then the electron arrives and leaves the molecule in pure plane-wave states, so that

$$A_{lm}=4\pi i^l Y_{lm}(\hat{\mathbf{k}}) \tag{32}$$

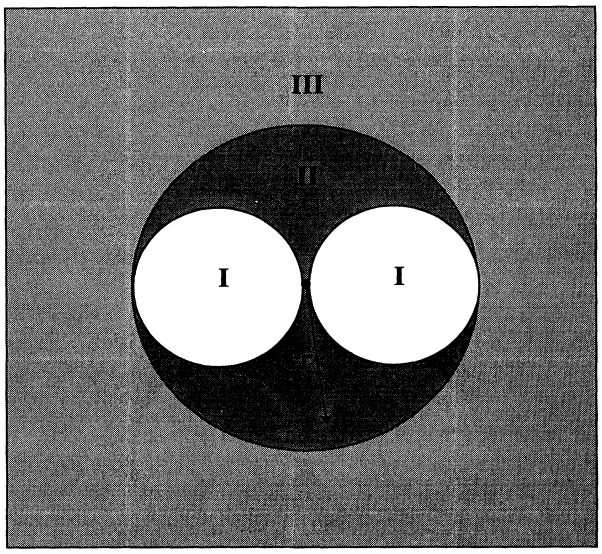

FIG. 28. A schematic diagram of the partitioning of the molecular potential of a diatomic molecule into three nonoverlapping regions, used by Davenport (1978) to evaluate the differential cross section from resonance electron scattering from oriented molecules. Region I, the atomic spheres. Region II, the interstitial potential (averaged to a constant). Region III lies beyond the outer sphere.

and

$$\frac{d\sigma}{d\Omega}=\left|\sum_{lm}\sum_{l'm'}Y_{lm}(\hat{\mathbf{k}})F^{\nu\nu'}_{lm,l'm'}Y_{l'm'}(\hat{\mathbf{k}}')\right|^2 . \tag{33}$$

From this result one can see that the angular distribution of electrons emitted from the negative-ion state of an isolated molecule depends upon two factors. The first is the angle of incidence of the probe electron, appearing through $\mathbf{k}$ in Eq. (33). The second is the symmetry of the negative ion, which is contained in the transition amplitude F. This equation expresses the physics of resonance formation: the differential cross sections for resonance electron scattering by an isolated molecule are obtained by matching the partial-wave expansion of the incoming and outgoing electron waves to the molecular negative-ion state formed when the electron is trapped. The electron is ejected into the partial waves consistent with the symmetry of the resonant molecular orbital, which then determine the angular distribution of scattered electrons. The incident electron tunnels into the resonant state via the same partial waves, so that the differential cross section for electron capture is the same as the differential cross section for electron emission.

A simple case, and one which represents quite a good approximation in a number of instances, occurs when only a single partial-wave component, (l,m), contributes to a resonance. In this case

$$F^{\nu\nu'}_{lm,l'm'}=F^{\nu\nu'}_{lm}\delta_{ll'}\delta_{mm'} , \tag{34}$$

so that

$$\frac{d\sigma}{d\Omega}=|Y_{lm}(\hat{\mathbf{k}})F^{\nu\nu'}_{lm}Y_{lm}(\hat{\mathbf{k}}')|^2 . \tag{35}$$

Thus electrons emerge from the negative ion in a pure partial wave, (l,m), independent of the angle of incidence. The angle of incidence simply changes the prob-

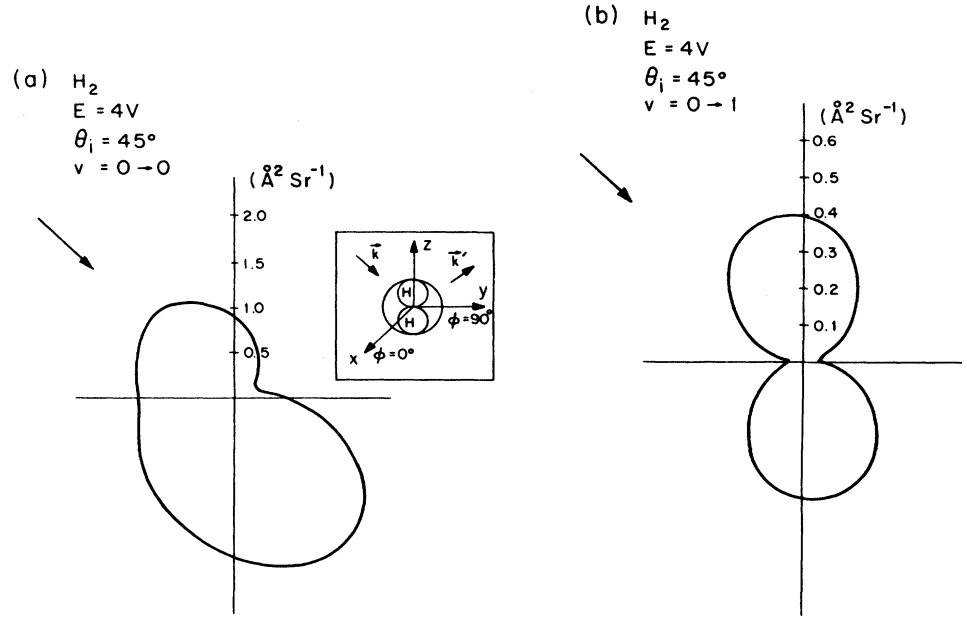

FIG. 29. Polar plots of the angular distribution of electrons emitted at 4 eV after the vibrational excitation of the $^2\Sigma_u^+$ resonance in oriented H_2. Angle of incidence is 45° from the molecular axis: (a) Elastic scattering. (b) Inelastic scattering via the $v=0-1$ vibrational excitation. This resonance decays into a $p\sigma$ partial wave. Davenport *et al.* (1978).

ability of populating the negative-ion state; it has no influence on the angular emission profile.

Davenport *et al.* calculated the angular distribution of electrons scattered via the shape resonances of a variety of oriented molecules. The angular distribution of electrons is inelastically scattered at 4 eV via the $^2\Sigma_u$ resonance of the hydrogen molecule is shown in Fig. 29. The vibrational excitation of the molecule is dominated by the σ_u channel. Thus Eq. (33) becomes

$$\frac{d\sigma}{d\Omega} \propto \cos^2(\theta_{\text{in}})\cos^2(\theta_{\text{out}}) , \tag{36}$$

where the polar angle θ is measured from the axis of the molecule. We see that the $(l=1,m=0)(p_z)$ partial wave dominates the angular distribution of emitted electrons, and this angular distribution is found to be independent of the incident angle. Similarly, the angular distribution of electrons inelastically scattered at an energy of 4 eV via the $^2\Pi_g$ resonance in N_2, [Fig. 30(b)] is dominated by a d wave of π symmetry $(l=2,|m|=1)$. Therefore we can see that, when a single partial wave dominates a resonance, the incident electron effectively "forgets" its initial direction when it becomes trapped in the resonant orbital and loses energy by stimulating a vibrational transition. Thus when, and *only* when, a single partial wave dominates the resonance, the distribution of inelastically scattered electrons is purely determined by the symmetry of the quasibound orbital and orientation of the molecule. This is in strong contrast to the angular distribution of elastic scattering [Fig. 30(a)], which displays a characteristic forward-scattering peak arising from the requirement for the conservation of scattered particles (see also Willis, 1980).

A more complex case occurs when more than one partial-wave component contributes to a resonance. This is the case with the $^2\Pi$ resonance of CO, which is isoelectronic with the $^2\Pi_g$ resonance of N_2. Because CO is a heteronuclear molecule, inversion symmetry is broken, and interference between the $p\pi$ and $d\pi$ partial waves, which both contribute to the resonance, produces the angular distribution of emitted electrons shown in Fig. 31. We note that the *p-d* coupling in the $^2\Pi$ resonances of CO means that the angular distribution of emitted electrons is dependent upon the angle of incidence. This is always the case when more than one partial wave contributes to the resonant state.

The results of Davenport *et al.* concern oriented but isolated molecules. However, this picture changes substantially when a molecule is adsorbed on a surface, as we shall see in the next section.

b. The molecule on the surface: the image potential

As the incident electron approaches a metallic surface it sees the image potential produced by screening in the metal. This is a long-range interaction, which scatters the electrons incident upon and emitted from the negative ion. This scattering process can be regarded as a form of refraction which the electron undergoes as it approaches and leaves the surface.

A particularly simple picture of refraction by the im-

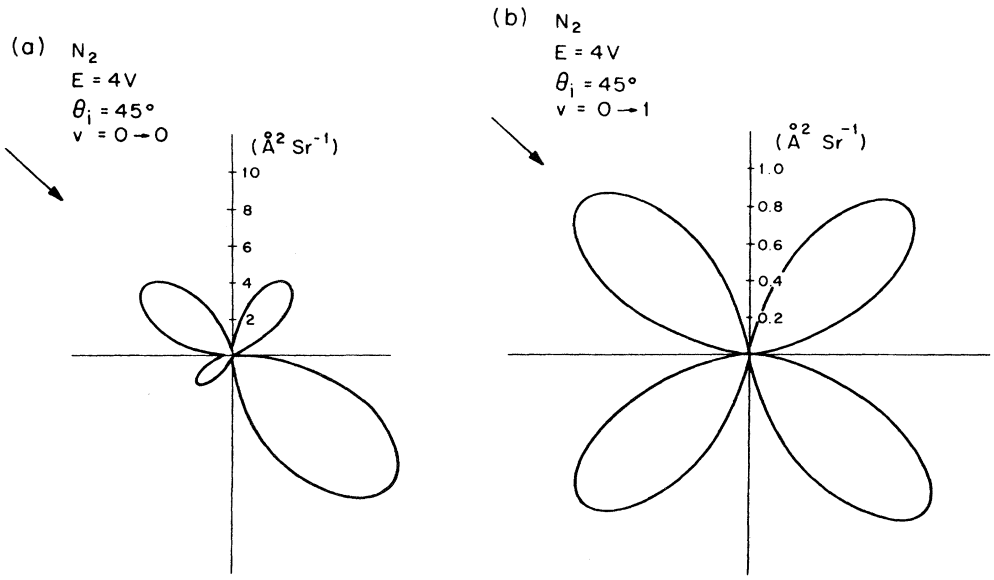

FIG. 30. Polar plots of the angular distribution of electrons emitted at 4 eV after the vibrational excitation of the nearby ($E_H=2.4$ eV) $^2\Pi_g$ resonance in oriented N_2. Angle of incidence is 45° from the molecular axis: (a) Elastic scattering; (b) Inelastic scattering via the $v=0-1$ vibrational excitation. This resonance decays into a $d\pi$ partial wave. Davenport *et al.* (1978).

age potential is provided by Teillet-Billy and Gauyacq (1991), who consider an electron of energy E incident upon an adsorbed molecule whose center of mass is a distance Z from the surface. The approximate trajectory of the electron was found from classical dynamics and is illustrated schematically in Fig. 32. If the electron beam approaches the surface at large distance at an angle of θ_∞ with respect to the normal, then as a result of refraction by the image potential the electron actually strikes the molecule at an angle θ with respect to the surface normal, where

$$\tan\theta_\infty = \left[\frac{\sin^2\theta}{\cos^2\theta - [4(Z+z_0)E]^{-1}}\right]^{1/2}. \tag{37}$$

Similarly, an electron emitted from the molecule at an angle θ_∞ suffers refraction on its way out of the surface and will actually be detected, far from the surface, emerging at an angle θ. Thus the effect of the image-potential scattering is to scatter the incident electron to smaller angles prior to capture and then to larger angles after emission. The amount of refraction is dependent upon the dimensionless parameter

$$\gamma = \frac{1}{4(Z+z_0)E}, \tag{38}$$

which is simply the ratio of the value of the image potential at the molecular center to the incident-electron energy. We see that if the electron energy drops or if the molecule sits closer to the surface, refraction becomes more significant.

In order to quantify the effect of refraction, Teillet-Billy and Gauyacq (1991) have used this classical approach to evaluate the angular distribution of electrons with energy 18 eV emitted into an f wave from a molecule placed with its center a distance of 5 a.u. above a surface modeled by a simple image potential. This model does not include the effect of refraction upon the incident electron. However, when only a single partial wave contributes to the resonance, refraction of the incident elec-

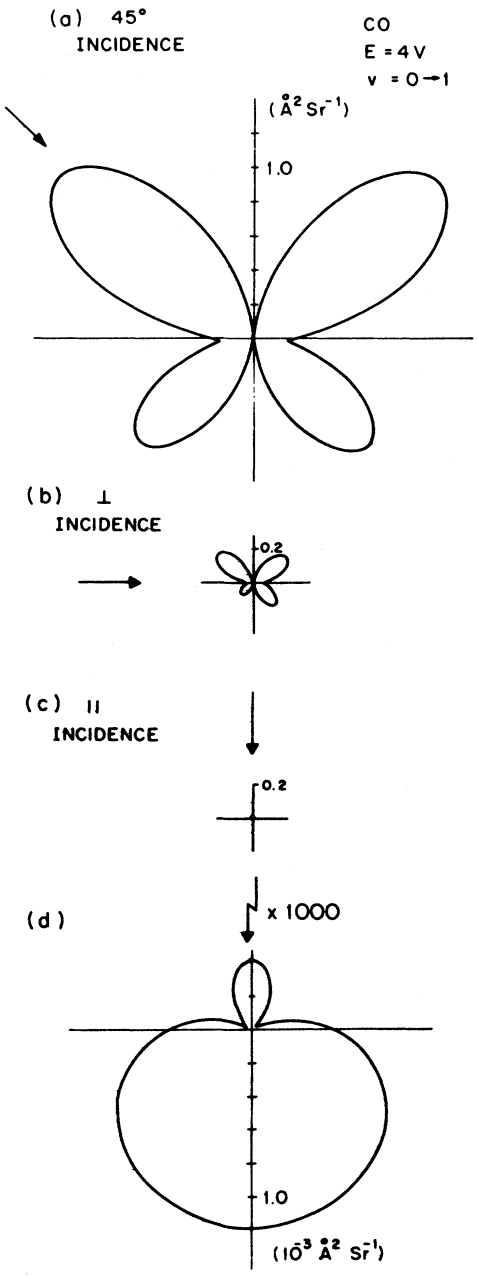

FIG. 31. Polar plots of the angular distribution of electrons emitted from the $^2\Pi$ resonance at 4 eV in oriented CO for the $v=0-1$ vibrational excitation: (a) for an angle of incidence of 45° from the molecular axis; (b) for an angle of incidence perpendicular to the molecular axis; (c) and (d) for an angle of incidence parallel to the molecular axis. The lack of inversion symmetry in CO means that this resonance decays into a mixture of $d\pi$ and $p\pi$ partial waves. Davenport *et al.* (1978).

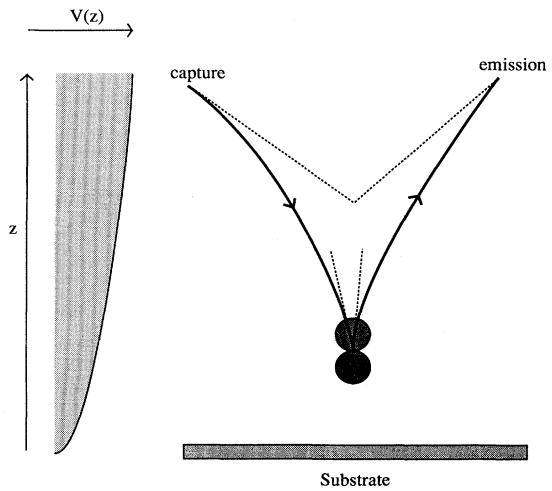

FIG. 32. Schematic diagram of the classical trajectory followed by the probe electron through a classical image potential before and after the formation of a molecular negative ion.

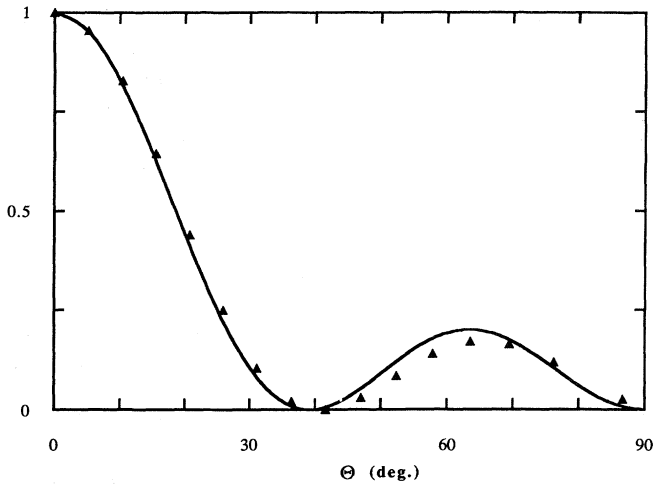

FIG. 33. The angular distribution of electrons with energy 18 eV emitted into an f wave by the adsorbed molecule: ▲, including refraction by the image potential; solid curve, without inclusion of refraction by the image potential. Teillet-Billy and Gauyacq (1990).

tron serves only to alter the rate at which the negative-ion state is populated, i.e., it simply scales the observed angular distribution of emitted electrons. Figure 33, shows a comparison of the angular distribution of emitted electrons with and without the inclusion of refraction by the image potential. Clearly the effect of refraction is weak for this electron energy, as can be understood by considering the value of the dimensionless parameter γ, which is approximately 0.08 in this case.

In Fig. 34 we show the results of extending this calculation to lower electron energies for a $^2\Pi_g$ resonance in which electrons are emitted into the partial waves ($l=2, |m|=1$). From this figure we see that for a resonance energy of 2.0 eV (corresponding, approximately, to the $^2\Pi_g$ resonance in N_2) refraction by the image potential significantly distorts the angular distribution of electrons emitted by this molecule, pushing the peak in the angular distribution by about 20 degrees towards higher angles. If the resonance energy is raised to 10 eV, then, once again, the effect of the image potential is less dramatic.

From this discussion it is clear that the extent to which the image potential plays a role in distorting the angular distributions is a strong function of the electron energy and the adsorption height. However, within the limitations of this model, we can draw some general conclusions. Below about 5 eV one needs to consider refraction by the image potential. Since this energy range includes many low-lying resonant states, there is a clear motivation for development of a complete quantum-mechanical description of refraction by the image potential. Such a theory does not exist at present. For resonance energies above about 10 eV we anticipate that refraction by the image potential is not significant, particularly if the emission profile contains sharp structure at

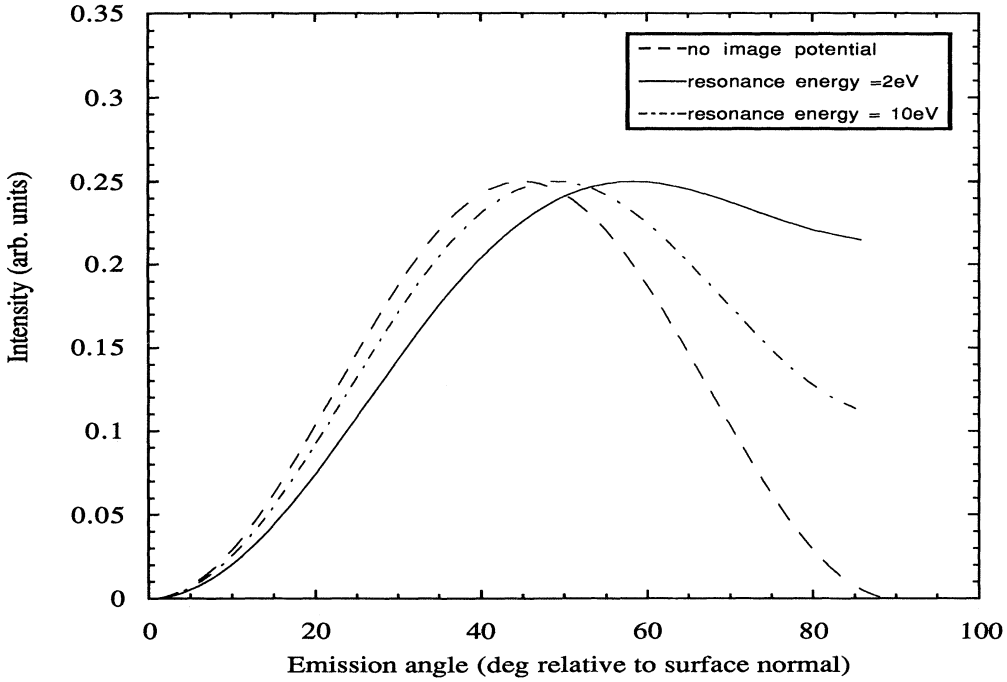

FIG. 34. The angular distribution of 2 eV (solid line) and 10 eV (dashed line) electrons emitted into a $d\pi$ wave by the adsorbed molecule, incorporating refraction by the image potential. For comparison the angular profile in the absence of the image potential is also shown (dot-dashed line).

small emission angles relative to the surface normal. As we shall see in the next section, there is, in fact, a much stronger scattering mechanism in operation at these electron energies.

c. *The molecule on the surface: multiple elastic scattering*

In addition to the long-range image interaction discussed in the previous section, the electron which forms the negative ion is also subject to a shorter-range interaction with the atoms and molecules that constitute the surface. When an electron is inelastically ejected from an adsorbed molecule, it can make its way to the detector along various paths. These paths may include coherent scattering events which involve the substrate atoms and, in the case of a dense overlayer, the coadsorbed molecules as well. Similarly, electrons injected into the crystal from the electron gun may undergo elastic multiple scattering prior to forming a negative-ion resonance. We note, however, that the inelastic event breaks the coherence between the incoming and outgoing paths. It is well known that in the energy range within which resonances are typically observed (<20 eV) the elastic-scattering cross section of an atom or molecule is similar to, and often greater than, its physical dimension. Indeed, all adequate descriptions of electron emission from surfaces within this energy range, such as those describing angle-resolved photoemission (Pendry, 1978; Liebsch, 1978), low-energy electron diffraction (LEED; Pendry, 1974; Van Hove *et al.*, 1979), and impact scattering in HREELS (Ibach and Mills, 1982), take account of the strong elastic multiple scattering of electrons that occurs at these low energies. A similar treatment is necessary in order to interpret correctly the measured angular distribution of electrons emitted from a negative-ion resonance within a molecular overlayer.

Rous and co-workers (Rous, Palmer, and Willis, 1989a) have established the multiple-scattering theory needed to calculate these angular distributions. Although their treatment assumes that the mechanism of electron capture, molecular vibrational excitation, and electron emission is that of the isolated molecule described by Davenport *et al.* (1978) and discussed earlier (Sec. V.A.1.a), the theory can readily incorporate the changes in the intrinsic molecular ion state induced by the molecule-surface interaction. The perturbation of the resonant state by multiple scattering between the molecule and the surface, investigated in the model calculations of Gerber and Herzenberg (1985), is, in fact, automatically included in this treatment. Indeed the theory effectively incorporates a development of Gerber and Herzenberg's calculation, in the sense that it goes beyond the simple barrier potential used by these authors to describe the surface.

In order to calculate the angular emission profiles it is necessary to describe the interference of electron waves as they propagate through the surface. This can be done

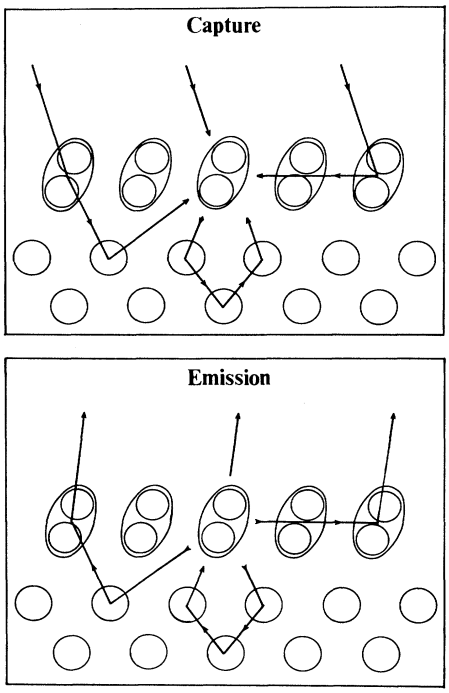

FIG. 35. A schematic diagram of the multiple-scattering paths followed by electrons prior to and after the formation of a negative ion of a molecule with a dense molecular overlayer. Rous, Palmer, and Willis (1989).

by summing the multiple-scattering paths by which an electron is injected into the crystal by the electron gun, captured within a molecular negative-ion resonance, and subsequently emitted from the resonant state to travel to the detector. Some of these paths are illustrated schematically in Fig. 35. We can split this process into three stages. First we sum all elastic multiple-scattering paths by which an electron can arrive at the molecule. Next we consider the capture of a proportion of these incident electrons by the molecule and their subsequent emission. Since the probability for electron capture is sensitive to the wave field of the impinging electron, multiple scattering of the incident electrons will affect the extent to which the molecular resonance is populated; however, when a single partial wave dominates the capture/emission process, multiple scattering of the incident electrons does not influence the angular distribution of detected electrons (Davenport *et al.*, 1978). Finally, we sum all the paths by which the emitted electrons can be elastically scattered by the overlayer molecules and substrate atoms before they reach the detector. At this stage we consider each adsorbed molecule as an incoherent source of inelastically scattered electrons; in other words, electrons emitted from different molecules do not interfere.

In considering electron scattering after emission from the resonant state, it is important that we consider paths by which an electron returns to be scattered again (elasti-

cally) by the molecule from which it was emitted. Similarly, we consider paths by which the incident electron is scattered (elastically) by a particular molecule before being captured by that same molecule. Including these closed paths is crucial because in doing so one automatically includes the process by which multiple scattering breaks the molecular symmetry and effectively mixes forbidden partial waves into the resonance.

We now lay out a formal treatment of the multiple-scattering theory needed to calculate the angular distribution of electrons emitted from a molecular resonance. For simplicity we shall assume that the surface consists of a substrate covered by a monolayer of a single molecular species in which the negative-ion resonance is excited, although the method can be generalized.

We take as our starting point the generalization of Davenport's formula for the angular distribution of electrons emitted from an *isolated,* oriented molecule:

$$\frac{d\sigma}{d\Omega}=\left|\sum_{lm}\sum_{l'm'}A_{lm}(\hat{\mathbf{k}})F^{\nu\nu'}_{lm,l'm'}A_{l'm'}(\hat{\mathbf{k}}')\right|^2 . \tag{39}$$

Here A_{lm} denotes the amplitudes of the spherical partial waves in the wave field of an incident electron with wave vector $\mathbf{k}$, expanded in an angular momentum representation about the center of mass of the molecule,

$$\psi_0(\mathbf{r})=\sum_{lm}A_{lm}j_l(\kappa r)Y_{lm}(\hat{\mathbf{r}}) . \tag{40}$$

Although Eq. (39) describes the coupling of an incident and emitted partial wave, time-reversal symmetry allows us to formulate this equation in terms of the spherical wave amplitudes for two incident plane waves—the actual incident wave $\mathbf{k}$ and the time-reversed emitted wave $\mathbf{k}'$ (see Rous *et al.*, 1989a). Similar matrix elements to that of Eq. (39) may be found in related electron-emission problems, such as photoemission (Pendry and Liebsch, 1978), low-energy electron diffraction (LEED; Pendry, 1974; Van Hove *et al.*, 1979), and impact scattering in HREELS (Ibach and Mills, 1982).

In the case of the isolated molecule, the probe electron arrives at and leaves the molecule in pure plane-wave states, $\mathbf{k}$ and $\mathbf{k}'$,

$$\psi_0(\mathbf{r})=e^{i\mathbf{k}\cdot\mathbf{r}}=\sum_{lm}A_{lm}j_l(\kappa r)Y_{lm}(\hat{\mathbf{r}}) , \tag{41}$$

so that

$$A_{lm}(\hat{\mathbf{k}})=4\pi i^{-l}Y_{lm}(\hat{\mathbf{k}}) . \tag{42}$$

If we were to insert Eq. (42) into Eq. (39), then we would recover Davenport's description of the differential cross section for resonance scattering from an isolated, oriented molecule [Eq. (33)].

For the case of an *adsorbed* molecule the effect of multiple elastic scattering has to be included. To do this we recognize that the elastic multiple scattering of the incident electron means that the electron no longer arrives at the molecule in a pure plane-wave state. Multiple scattering through the substrate and overlayer distorts the probe electron's wave function and is reflected in a change of the spherical wave amplitudes A_{lm}. To calculate these spherical wave amplitudes we need to sum the multiple-scattering paths of the probe electron as it travels to the molecule from the electron gun. Rous *et al.* employed conventional LEED methods (Rous *et al.*, 1989a) and obtained the amplitudes directly from a standard LEED calculation suitably modified to treat a molecular overlayer.

The importance of multiple scattering in altering the angular distribution of emitted electrons is graphically illustrated in Fig. 36, which shows the result of a model calculation of the angular distribution of electrons detected in the scattering plane after inelastic scattering by a single domain of the ζ phase of O_2 on graphite. The electron beam has an energy of 8.5 eV and is incident at an angle of 65 degrees from the normal in the plane which contains the $\langle 11 \rangle$ direction of the physisorbed O_2 monolayer. The molecules' axes are tilted at 25 degrees from the normal to the surface. In the calculations shown, scattering by the graphite substrate was neglected, so that only intermolecular scattering within the O_2 overlayer was included (at this particular electron energy the graphite reflectivity is sufficiently small that it may be neglected).

The profiles shown in Fig. 36 were calculated assuming resonant emission/capture via three different partial

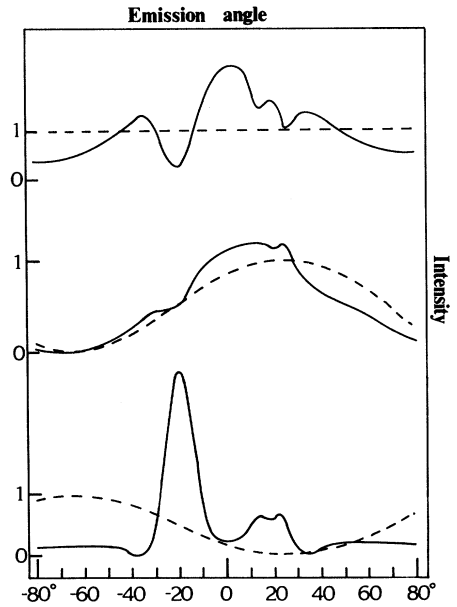

FIG. 36. Comparison of the angular distribution of electrons emitted into three different partial waves from molecular oxygen within a dense overlayer corresponding to a single domain of the $\zeta 2$ phase of O_2 on HOPG graphite. Results with (solid line) and without (dashed line) multiple scattering are shown. Top panel: *s*-wave emission; center panel: $p\sigma$ emission; lower panel: $p\pi$ emission. The molecule tilts at 25° from the surface normal.

waves: $p\sigma$ and $p\pi$ partial waves corresponding to the formation of the $^4\Sigma_u$ and $^2\Pi_u$ negative-ion resonances, respectively, of O_2, and an s wave, which might be expected if the molecule inversion symmetry were strongly broken upon physisorption. For comparison, we also show the corresponding no-scattering angular distributions, where the detected intensities become simple $\cos^2$, $\sin^2$, or constant ($=1$) functions.

From this figure we can immediately see the role that multiple elastic scattering plays in determining the angular profiles at an energy of 8.5 eV. Indeed, for some profiles the intensity is enhanced by a factor of 2 or 3 at certain emission angles. We see a sharpening of peaks in k space and additional structure that is not present in the profiles for which multiple scattering was omitted, general trends which have also been observed in other electron-emission profiles such as those seen in angle-resolved photoemission (Pendry, 1978; Liebsch, 1978). We note that multiple scattering has a particularly important influence upon the $p\pi$ profile; in this case electrons are predominantly ejected directly into the O_2 monolayer. In contrast, the angular distribution of electrons emitted into the $p\sigma$ partial wave remains relatively unperturbed, since electrons are ejected predominantly away from the overlayer. Figure 36 serves to emphasize that, in order to interpret quantitatively the angular distributions obtained in an experiment, we need a method of calculating the angular distributions which incorporates a proper treatment of multiple scattering.

Finally, we note that the theoretical approaches we have described have a number of limitations. First, in common with the models of Teillet-Billy and Gauyacq (1991) and Gerber and Herzenberg (1985), it is assumed that the molecular core is not distorted upon adsorption, so that the resonant state is not perturbed by the formation of molecule-surface bonds. Secondly, one must be careful when applying standard multiple-scattering methods, and in particular the muffin-tin approximation, at the electron energies at which resonances are typically observed ($E<20$ eV). The muffin-tin approximation makes the assumption that the atomic ion cores do most of the scattering and that the interstitial potential is sufficiently slowly varying that it may be averaged to a constant. This approximation becomes less accurate as the electron energy approaches the vacuum level, but is nevertheless highly successful even at band energies, where it forms the basis of the KKR (Korringa *et al.*, 1947; Kohn and Rostocker, 1954) and the SW-Xα methods (Messmer, 1979) for the evaluation of the electronic structure of solids and molecules. Where the muffin-tin approximation is least accurate is in the treatment of the molecular scattering, because in molecules such as N_2, CO, and O_2 a substantial fraction of the total electronic charge density resides between the ion cores.

d. The molecule on the surface: selection rules

Although it has been shown that a complete multiple-scattering analysis can successfully determine both the complete adsorption geometry and resonance symmetry, it is possible to gain some insight into these parameters without resorting to a full calculation of electron scattering in the surface. Rous and Palmer (1989; Rous *et al.*, 1990) have demonstrated the existence of selection rules for resonance scattering by adsorbed molecules which give rise to nodes in the angular distribution of inelastically scattered electrons at fixed angles relative to the surface normal. The presence (or absence) of these extinctions then provides some information about the adsorption site and resonance symmetry.

Our starting point in explaining this phenomenon is, once again, the isolated, oriented molecule. A common feature of all negative-ion resonances is that the electrons ejected from the resonance are emitted into one or more partial waves, which match onto the quasibound molecular orbital in which the electron was trapped. As has been shown by Davenport *et al.* (1978), in the case of the isolated, oriented molecule this gives rise to a characteristic angular distribution of inelastically scattered elec-

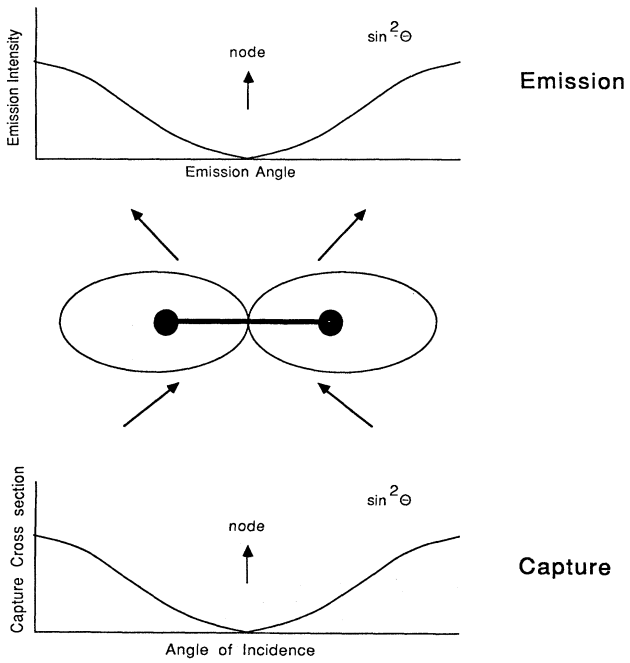

FIG. 37. Schematic diagram of resonance electron scattering by an *isolated oriented* homonuclear diatomic molecule, showing the existence of nodes in the differential cross sections for capture and emission: (a) electron emission into a $p\sigma$ partial wave for which a node exists in the angular distribution of electrons perpendicular to the molecular axis. The angular distribution of emitted electrons is the $\sin^2\theta$ profile expected for emission into a pure p wave. (b) Electron capture by the homonuclear diatomic molecule shown in (a). Electrons are captured through a $p\sigma$ partial wave, producing a node in the differential capture cross section perpendicular to the molecular axis. The paths contributing to the capture cross section are the time reversal of those shown in the case of emission (a), and so the differential capture cross section is the $\sin^2\theta$ profile expected of capture into a pure $p\sigma$ state.

trons, which manifests the symmetry of the negative-ion state. This situation is illustrated schematically in Fig. 37, which shows electrons being emitted into a $p\sigma$ partial wave, as might be the case in the decay of, say, a $^2\Sigma_u$ resonance in a homonuclear diatomic molecule. In this case electrons are emitted predominantly along the molecular axis, but, more importantly for the present discussion, no electrons are emitted at emission angles corresponding to the nodes of the molecular orbital. For an isolated, oriented molecule this gives rise to extinctions in the angular emission profiles. When a molecule is adsorbed on a surface, multiple elastic scattering of the probe electron distorts the angular distribution of electrons relative to the isolated molecule, as we have seen. However, Rous and co-workers (1989a) have shown that in many cases these extinctions are preserved.

The argument is facilitated by the particular example of an adsorbed homonuclear diatomic molecule which emits into a $p\sigma$ partial wave, as shown schematically in Fig. 38. In the absence of the substrate there is a node of emitted intensity normal to the molecular axis—a consequence of the $\sin^2\theta$ dependence of the emitted intensity. Now let us consider adsorbing this molecule with its axis parallel to a surface. The emitted electrons can now make their way to the detector along a variety of paths, which involve scattering among the atoms within the substrate. These paths interfere and radically alter the angular distribution of detected electrons compared with the case of the isolated molecule. Suppose, however, that the center of symmetry of the adsorbed molecule lies in a mirror plane of the surface, which in Fig. 38 occupies the zy plane. We find that the node still exists, *independent of the extent of the multiple scattering.* This selection rule occurs because the $p\sigma$ partial wave into which the resonance decays lies across the mirror plane, so that electrons emitted into the half-space $x>0$ and $x<0$ have opposite phase. For every electron path which starts with emission into the $x>0$ half-space and terminates with detection along the surface normal there is an equivalent path which starts with emission into the $x<0$ half-space with opposite phase. These pairs of scattering paths interfere destructively, producing a node in the emitted intensity along the surface normal, shown schematically in the upper panel of Fig. 38. An identical argument holds for the differential capture cross section. In this case the incident electrons follow paths that are time reversed with respect to those illustrated in Fig. 38: for normal incidence the resonance cannot be populated.

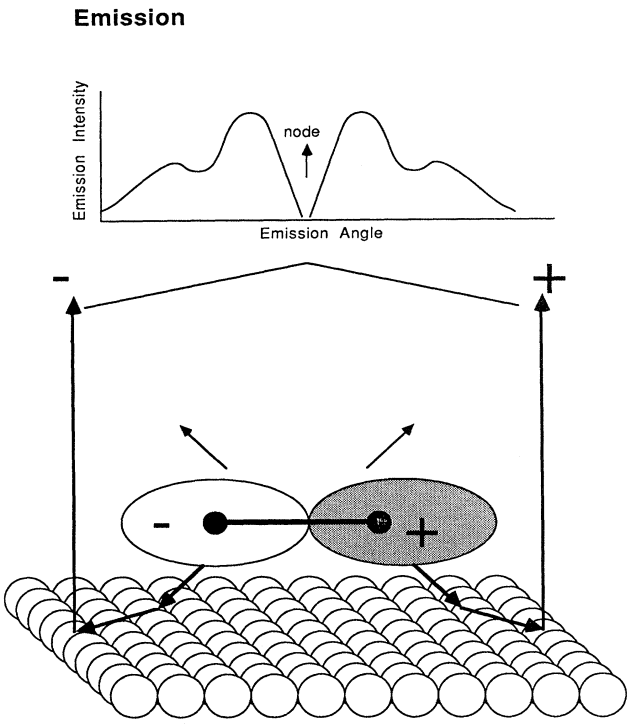

FIG. 38. Schematic diagram of electron emission into a $p\sigma$ partial wave by a homonuclear diatomic molecule oriented by adsorption across a mirror plane of a single-crystal surface. Instead of traveling directly to the detector, the emitted electrons undergo multiple elastic scattering by the substrate or adjacent molecules (not shown). Although, compared to the isolated molecule shown in Fig. 37, the emission profile is perturbed by interference between these paths, the node remains. This is because electrons emitted with opposite phase into opposite lobes of the p wave interfere destructively along the surface normal.

Although this discussion concerns a specific example, it is clear that the presence of these selection rules is a quite general phenomenon, which will occur for other resonance symmetries and adsorption geometries. For example, in the presence of a substrate containing a 180° rotation axis passing through the center of the molecule, a resonance with $p\pi$ symmetry in an upright homonuclear diatomic molecule cannot be populated at normal incidence and always yields a node in the emitted intensity along the surface normal. In contrast, if the rotation axis is the only symmetry element present, then a resonance with $p\sigma$ symmetry in an upright homonuclear diatomic molecule can be populated for all angles of incidence and will emit electrons across the entire backscattering hemisphere.

A more general formulation of this selection rule may be obtained by representing the effect of multiple elastic scattering of the emitted electrons by a matrix $O_{l'm',lm}$ (Hock and Palmer, 1992):

$$B_{l'm'}=\sum_{lm} O_{l'm',lm}\, A^0_{lm} \ . \tag{43}$$

Here A^0_{lm} is the initial amplitude of electrons emitted into the partial wave (l,m) by the resonance, and $B_{l'm'}$ is the amplitude of partial waves arriving at the detector after multiple scattering through the surface. The matrix O contains all the details of the multiple-scattering events undergone by the emitted electron as it propagates through the surface. We note that the matrix O depends only upon the scattering potential of the surface and is, in

general, a sparse matrix that can only couple together partial waves in a manner compatible with the surface symmetry. In particular, if the surface has an nth-order rotation axis through the adsorbed molecule, then the only elements of $O_{l'm',lm}$ that are nonzero are those for which $|m-m'|=n$. For example, if a diatomic molecule lies across a mirror plane of the surface ($n=2$) and the resonance decays into a $p\pi(l=1,|m|=1)$ partial wave, the scattered wave field at the detector can only contain the partial waves for which $m=\pm1,\pm3,\ldots$. Thus the scattered intensity has a node *line* parallel to the mirror plane, independent of the extent of multiple scattering.

2. Experimental results and analysis

The first substantial measurements of the angular distributions of electrons scattered via the resonant states of adsorbates were conducted in Cambridge on the O_2/graphite system. The O_2/graphite phase diagram is presented in Fig. 39. Because graphite is available in high-surface-area forms dominated by the easy-cleavage basal plane, a number of bulk techniques, such as neutron scattering, x-ray and neutron diffraction, and magnetic susceptibility measurements, in conjunction with low-energy electron diffraction (LEED) measurements on single-crystal graphite substrates, have enabled detailed phase diagrams of this type to be obtained (see, for example, Toney and Fain, 1987). For the purposes of investigating molecular resonances, this rich phase diagram may be regarded as a laboratory for preparing ordered films of oriented molecules. Thus, in particular, in the δ phase, which has a centered rectangular unit cell, diffraction measurements in conjunction with molecular packing arguments suggest that the molecular axes of the physisorbed O_2 molecules are oriented at least approximately parallel to the surface, whereas in the higher-coverage (but still monolayer) ζ phase similar arguments suggest that the molecules stand approximately upright on the surface. The δ and ζ phases therefore provide a means of preparing "lying down" and "standing up" molecules, but note that these two phases feature different crystalline ordering as well as different molecular orientations.

The earliest reports of inelastic electron scattering by the O_2/graphite system (Palmer *et al.*, 1986, 1987; Palmer, Wilkes, and Willis, 1988) included the observation of a resonance centered at approximately 9 eV in the cross sections for vibrational excitation. Comprehensive angular distribution measurements, from what was believed to be the monolayer ζ phase, were reported for the first time, and showed (Fig. 40) a broad, structured distribution peaked at large angles from the specular direction and largely unaltered, with respect to the surface, by a change in the direction of the incident-electron beam. These results seemed to substantiate the notion of "memory loss" in resonance scattering described by Davenport *et al.* (1978). Clearly the angular distributions bore no particular relation to the specular direction. Palmer and co-workers interpreted the data in terms of resonance scattering by the negative-ion states of O_2 near

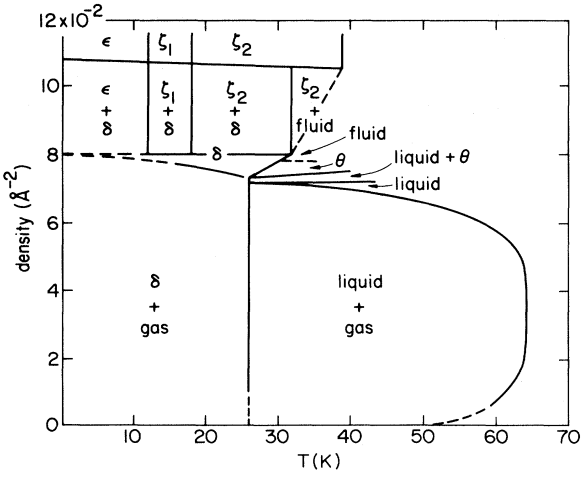

FIG. 39. Phase diagram for O_2 physisorbed on graphite at low temperatures. After Toney and Fain (1987).

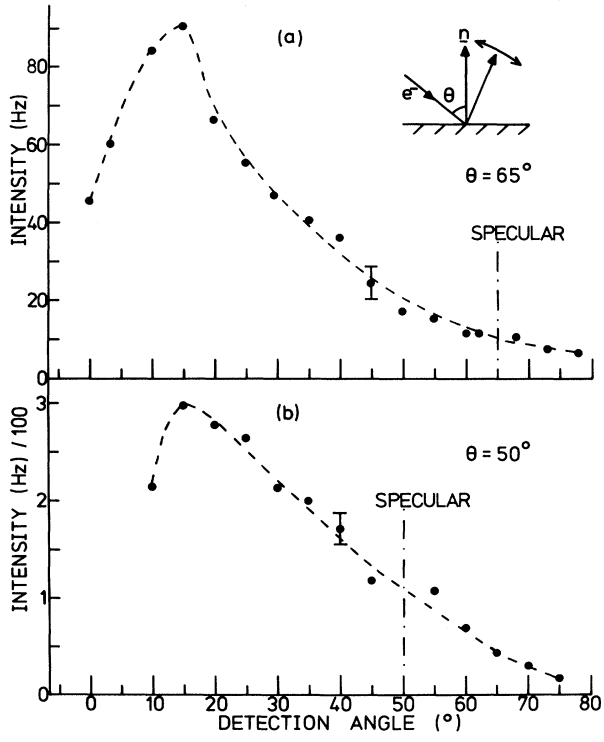

FIG. 40. Angular distribution of electrons detected after resonance scattering by O_2 physisorbed on graphite. The graphs show the number of electrons collected after exciting the $v=0$–1 vibrational transition of O_2 as a function of detector position with respect to the normal to the surface. The electron energy is 8.5 eV. Note the similarity between the angular distributions obtained for two different angles of incidence. Palmer, Rous, and Willis (1988).

9 eV, notably the $^4\Sigma_u$ shape resonance. It was noted (Palmer *et al.*, 1987) that the angular distributions observed were too sharp to result from a mere average over adsorbate domains of the simple partial-wave profiles expected in resonance scattering from isolated, oriented molecules. It was pointed out that multiple elastic scattering of electrons emitted by the molecular resonance before reaching the detector would introduce new structure into the emission patterns. Calculations of the angular distributions embodying LEED-style theory as described in Sec. V.A.1.c were presented in conjunction with the experimental angular distributions by Palmer, Rous, *et al.* (1988; Palmer, Rous, and Willis, 1988; Rous, Palmer, and Willis, 1989). The authors found that on the assumption (based on a preparation prescription derived from thermal desorption measurements) that they were observing the ζ phase, it was not possible to fit the experimental distributions with a resonance of $p\sigma$ symmetry (as expected of the $^4\Sigma_u$ state), but that a good fit could be obtained if a resonance of $p\pi$ symmetry, consistent with the $^2\Pi_u$ state, was invoked. The best match was then obtained with a molecular axis tilt of 25 degrees from the vertical, consistent with the intermolecular spacing derived from the LEED measurements of Toney and Fain (1984).

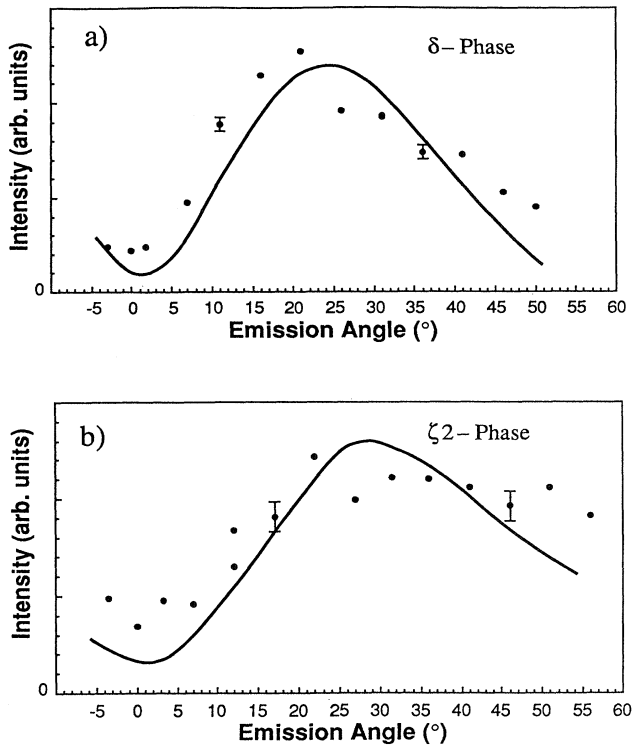

FIG. 41. Angular distributions of electrons detected after resonance scattering by (a) the δ phase and (b) the $\zeta 2$ phase of O_2 physisorbed on graphite: ●, experimental; solid curves, theoretical. The emission angle is given with respect to the surface normal. The electron-impact energies are 8.5 eV in (a) and 6.5 eV in (b), with an angle of incidence of 60 degrees in each case. The calculations assume electron capture and emission in a $p\sigma$ partial wave in the δ phase (and a molecular tilt of 15 degrees from the surface), and capture and emission in a $p\pi$ wave in the $\zeta 2$ phase (and a molecular tilt of 15 degrees from the normal). Jensen *et al.* (1990a).

Subsequent work in Cambridge by Jensen *et al.* (1990c), incorporating low-energy electron-diffraction measurements, showed that the monolayer phase that Palmer *et al.* had been investigating, produced by the thermal desorption method, was in fact the δ phase rather than the ζ phase, and called for a revaluation of the angular distributions and energy-dependent cross sections which the earlier work had obtained. With the structural phase now pinned down, it was found that an equally good fit to the experimental angular distributions could be obtained provided that the original resonance assignment, the $^4\Sigma_u$ state with $p\sigma$ symmetry, was restored. The best fit, Fig. 41(a), was then obtained with a small tilt (about 20 degrees) of the molecular axis from the surface in the δ phase. Of course, the unexpected result that a satisfactory fit to the experimental angular distributions could be obtained with two quite different models, i.e., the ζ phase with a $p\pi$ partial wave or the δ phase with a $p\sigma$ partial wave, is not without its lessons regarding the effectiveness of such measurements as a structural probe:

(i) Angular distributions in resonance scattering are not a good probe of *long-range* crystallographic order, although they sample it, and a diffraction or real-space method is really needed to determine the center-of-mass order as an input to simulations of these distributions.

(ii) Angular distribution measurements are well suited to a determination of *either* the orientation of the molecule on the surface or the symmetry of the resonant state, but *not both* at once. If one is known the other can be derived with some confidence.

Jensen and Palmer (1990; Jensen *et al.*, 1990d) extended the measurement of the angular distributions of electrons scattered by physisorbed molecules from the O_2/graphite system to the CO/graphite system, which has a similarly rich phase diagram. They observed resonances in the excitation function for the CO stretch mode at 1.6 eV and 18 eV (Fig. 42), which they assigned to the molecular $^2\Pi$ and $^2\Sigma$ shape resonances isolated in the gas phase at similar energies. The angular distributions that were reported, recorded at a beam energy, 17.5 eV, near the center of the $^2\Sigma$ resonance, served to confirm the validity of the selection rules discussed in Sec. V.A.1.d. At low coverages and temperatures the CO monolayer orders into a "herringbone" structure in which it has been thought that the molecular axes lie parallel to the surface. The angular distribution of electrons scattered by this phase after exciting the $v=0-1$ mode of CO is shown in Fig. 43 and may be compared with the angular distribution obtained from electron scattering by the δ phase of O_2 via the $^4\Sigma_u$ negative ion, Fig. 41(a). Both the

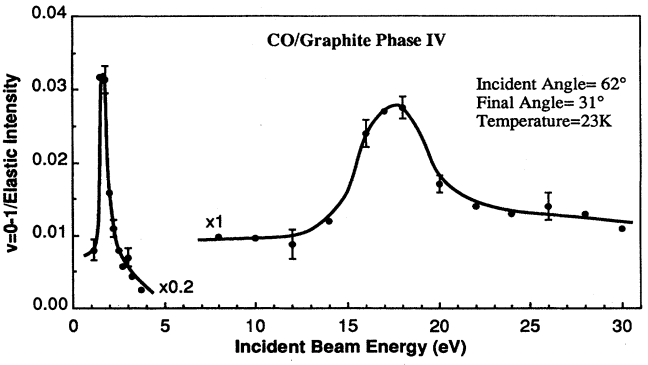

FIG. 42. Cross section for excitation of the $v=0-1$ mode of CO physisorbed on graphite (phase IV) as a function of incident-electron energy (away from the specular direction). Two resonances are observed, at 1.6 eV and 18 eV, attributed to the $^2\Pi$ and $^2\Sigma$ shape resonances, respectively. Jensen and Palmer (1990).

angular distributions show a characteristic minimum in the direction normal to the surface. The leading term in the partial-wave expansion of the CO $^2\Sigma$ resonance, obtained from gas-phase studies, is the $f\sigma$ wave, which, like the $p\sigma$ wave in the O_2 $^4\Sigma_u$ resonance, produces a node along the surface normal if the molecule is exactly flat and if the molecular site symmetry conforms to that required for operation of the selection rules, Sec. V.A.1.d. In phase I of CO, as in the δ phase of O_2, appropriate symmetry elements are present (e.g., a mirror plane). The characteristic minimum in the CO angular distribution (Fig. 43) can be viewed, as with the O_2 case, as an approximate realization of these selection rules. Tilting (e.g., dynamical tilting) of the CO molecules away from the surface would account for the weak violation of the selection rule, as would the mixing into the resonance of certain other partial waves; even in the gas phase, the CO $^2\Sigma$ resonance appears to contain a $d\sigma$ component. Jensen *et al.* were able to show that in phase IV of the CO/graphite system, in which there is an ordered mixture of molecular orientations, the characteristic minimum in the angular distributions was lost.

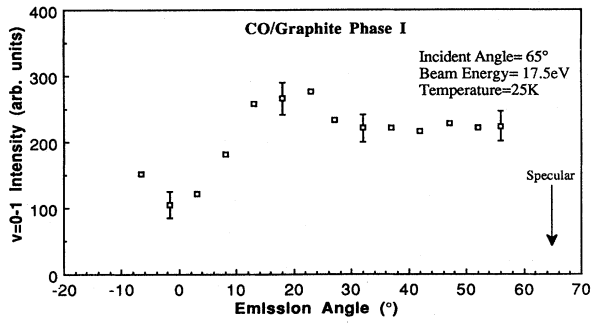

FIG. 43. Angular distribution of electrons scattered via the $^2\Sigma$ resonance of CO physisorbed on graphite in phase I. The graph shows the number of electrons collected after exciting the $v=0-1$ vibrational transition of CO, as a function of emission angle with respect to the surface normal. Note the minimum in intensity in the direction of the surface normal, also observed in the δ phase of O_2, Fig. 41(a). Jensen and Palmer (1990).

The first report of substantial measurements of the angular distributions in resonance electron scattering by chemisorbed molecules was made by Jones and Richardson at Liverpool (1988, 1989; Jones, Ashton, and Richardson, 1989). They investigated the adsorption of the formate species (HCOO) on the Ni(110) surface. The (off-specular) cross section for the excitation of the symmetric O-C-O stretching mode (relative to the O-C-O deformation) showed a resonance centered at a beam energy of 14 eV (Fig. 44). This is an example of mode-selective vibrational excitation, which we shall discuss in more detail in Sec. VI. The first and second overtones of the O-C-O symmetric stretch were also detected in the HREELS spectrum. Given that the formate species was strongly bound to the surface, the authors looked to other spectroscopic investigations of the species on the surface to help identify the resonant state. They pointed out that a σ shape resonance is a common feature in near-edge x-ray-absorption fine structure (NEXAFS) studies (see Sec. VII) of chemisorbed CO and molecules containing the CO group. In the case of the formate species on Cu(110) and Cu(100), this resonance is located about 15

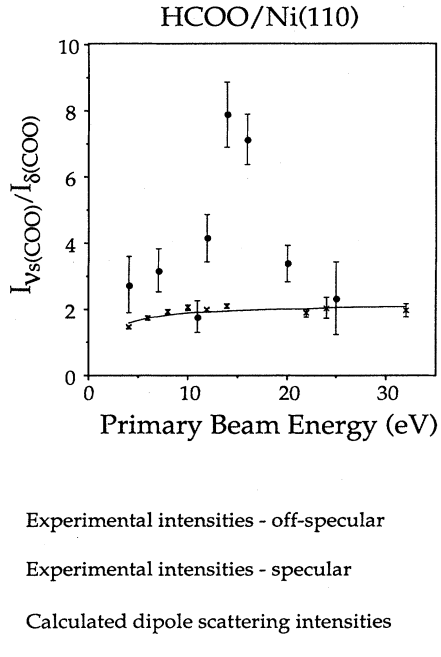

FIG. 44. Cross section for excitation of the symmetric C-O-O stretch mode, relative to the C-O-O deformation, in the formate species HCOO, chemisorbed on Ni(110) as a function of electron-impact energy. The solid line is the calculated dipole scattering cross section and accounts for the data obtained in the specular direction (crosses). A resonance is evident in the excitation function obtained 10 degrees away from the specular direction (solid circles). Jones and Richardson (1988).

eV above the Fermi level. If the presence of the core hole in NEXAFS experiments stabilized the molecular resonance by about 4 eV, then one could (overlooking the change of substrate) match the energy of the resonance observed in the electron-scattering cross section with that observed in NEXAFS studies (Fig. 45); assuming a work function of about 5 eV, the NEXAFS resonance is about 10 eV above the vacuum level, 4 eV below the electron-scattering resonance.

The angular distribution of electrons scattered by the formate resonance is of particular interest in the context of the present discussion. The O-C-O stretch mode is dipole active, and its intensity was found to peak in the specular direction, but, relative once again to the (also dipole-active) O-C-O deformation, it was found to have very strong intensity far away from the specular direction, with a relative maximum at 60–80 degrees from the surface normal (Fig. 46). This angle correlated quite well with the orientation of the C-O groups with respect to the normal and was suggestive of strong resonance scattering in a direction close to that of the C-O bond. If, as in gas-phase CO, the resonance is primarily of $f\sigma$ character, then such scattering would be expected, provided that distortions due to multiple scattering were modest. As we have seen in Sec. V.A.1.c, multiple-scattering effects are likely to be weakest in the case of a lobe of electrons projected like a searchlight away from the surface and towards the detector. Jones and Richardson were also able to obtain some information

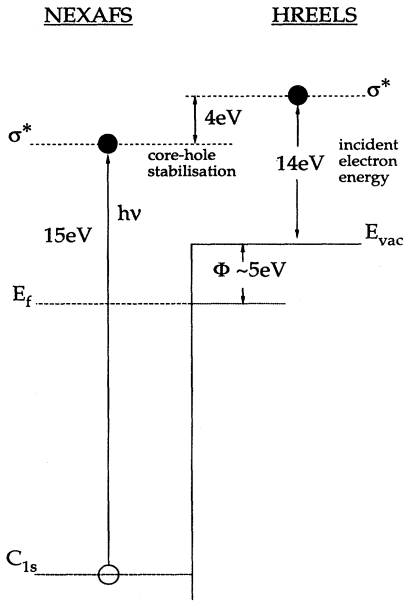

FIG. 45. Energy-level diagram proposed to relate the resonance seen in electron scattering (HREELS) of HCOO/Ni(110) to that seen in near-edge x-ray-absorption fine structure (NEXAFS) measurements of HCOO/Cu(110). The resonance observed in the x-ray-absorption experiment is stabilized by the presence of a core hole. Jones and Richardson (1989).

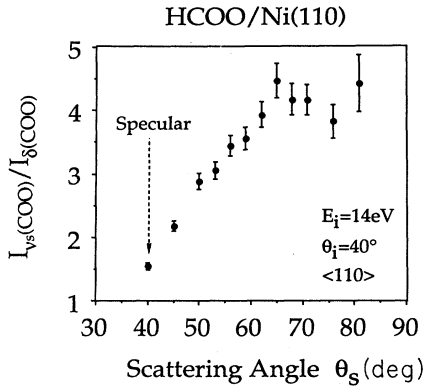

FIG. 46. Angular distribution of the intensity of the symmetric C-O-O stretch mode, relative to the C-O-O deformation, obtained at the resonance energy in HCOO/Ni(110), as a function of emission angle with respect to the surface normal. The electron-scattering plane is aligned along the ⟨110⟩ azimuth of the surface. The substantial (relative) enhancement well away from the specular direction correlates approximately with the direction of the CO bonds in the formate species. Jones and Richardson (1988).

about the azimuthal distribution of electrons scattered via the resonance. The resonant enhancement of the symmetric O-C-O stretch was obtained when the scattering plane contained the surface normal and the ⟨110⟩ azimuth of the Ni(110) surface, the plane in which the formate species is believed to lie. Measurements obtained along the perpendicular ⟨100⟩ azimuth did not show the resonant behavior, a result consistent with strongly diminished electron emission and capture at large angles away from the direction of the C-O bond.

Having isolated a resonance understood to be localized on the O-C-O group in the chemisorbed formate species, the Liverpool group went on to consider electron scattering by chemisorbed CO itself (Jones, Ashton, Ding, and Richardson, 1989; Richardson and Jones, 1990; Jones and Richardson, 1990). They investigated the CO/Ni(110) system, and, as expected, they found strong dipole scattering in the specular direction. However, at large angles away from specular the cross section for excitation of the C-O stretch mode showed a clear resonance centered at about 18 eV (Fig. 47), and Jones *et al.* identified this resonance with the "σ shape resonance" of CO well known from other electron spectroscopies and observed in electron scattering by gas-phase (Tronc *et al.*, 1980), condensed (Sanche and Michaud, 1984b), and physisorbed (Jensen and Palmer, 1990; Fig. 42) CO. This resonance is the $^2\Sigma$ negative-ion state created by adding one electron to the unoccupied $2p\sigma^*_u$ orbital of the CO molecule. The energy of the observed resonance, 18 eV, was remarkably similar to that in the gas phase, 19.5 eV, in the condensed phase, 19 eV, and in the physisorbed CO molecule on graphite, 18 eV, despite the

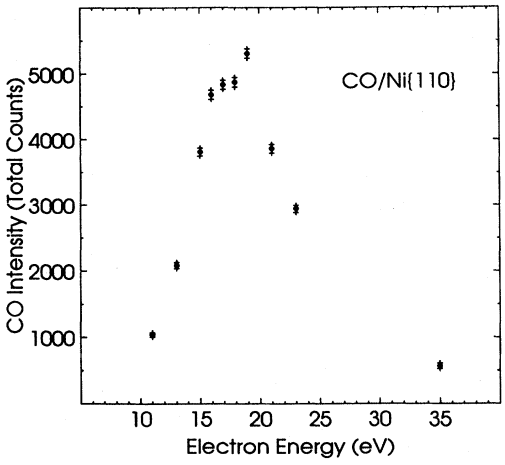

FIG. 47. Cross section for excitation of the stretch mode of CO chemisorbed on Ni(110) as a function of electron-impact energy, obtained by detecting electrons emitted along the surface normal. The resonance corresponds to that seen in CO physisorbed on graphite, Fig. 42. Jones, Ashton, *et al.* (1989).

chemisorption interaction with the substrate on the Ni(110) surface. Jones and co-workers also reported angular distribution measurements (well away from specular) that showed the CO stretch intensity rising as the analyzer was moved to the surface normal (Fig. 48). Such a distribution is qualitatively consistent with electron emission in an $f\sigma$ partial wave, assuming that the

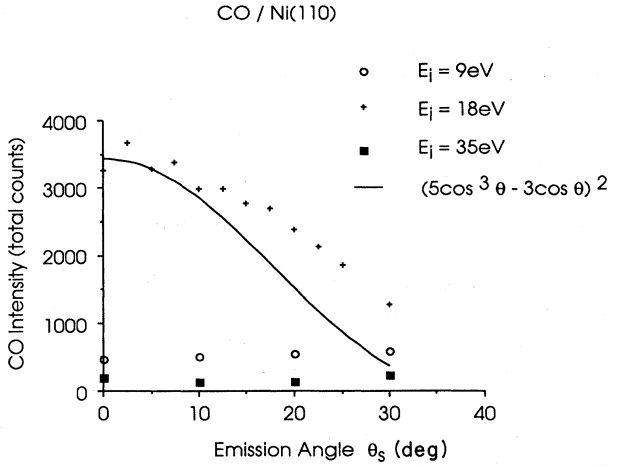

FIG. 48. Angular distribution of electrons scattered via the resonance in CO chemisorbed on Ni(110). The graphs show the intensity of the C-O stretch mode as a function of emission angle with respect to the surface normal. Data obtained at three incident-beam energies are shown: 18 eV (the resonance energy), and 9 eV and 35 eV (away from the resonance in both cases). The "maximum" in intensity along the surface normal at 18 eV correlates with the orientation of the CO axis on the surface. The solid line shows the angular distribution expected of electron emission in an undistorted $f\sigma$ wave. Jones, Ashton, *et al.* (1989).

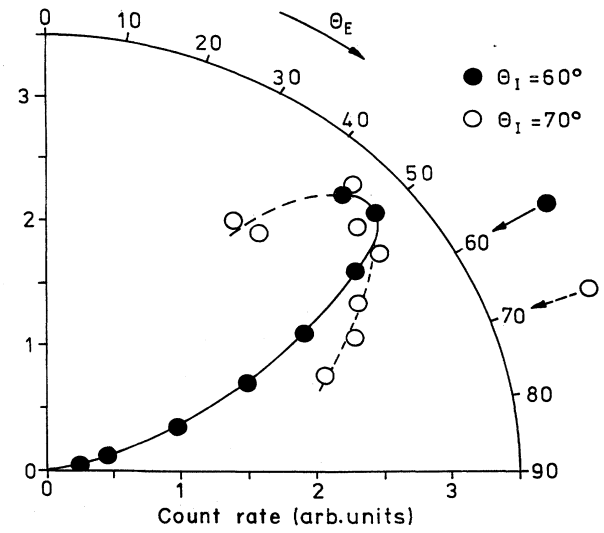

FIG. 49. Angular distribution of electrons scattered via the low-energy shape resonance in N_2 physisorbed on Al(111). The figure shows a polar plot of the intensity of the N_2 stretch mode as a function of emission angle with respect to the surface normal. Note the similarity between the angular distributions obtained for two different angles of incidence, also evident in Fig. 40. Jacobi, Bertolo, *et al.* (1990).

molecule stands upright on the surface. Regarding the interpretation of the specific form of the angular distribution, Jones *et al.* noted the need to account for dynamic oscillation of the molecule about the vertical—one should not regard an adsorbate as static—but the possible contributions of partial waves other than the $f\sigma$ term to the resonance (as in the gas phase) prevented a quantitative analysis of the results. Of course such an analysis would also require a treatment of multiple elastic scattering of the electrons in the surface region *en route* to the detector.

Further measurements of the angular profile of scattered electrons were reported by Jacobi and co-workers (Jacobi, Bertolo, *et al.*, 1990; Jacobi, Bertolo, and Hansen, 1990), who measured the angular distribution of electrons inelastically scattered by N_2 physisorbed on Al(111) at an impact energy corresponding to the $^2\Pi_g$ resonance. They found that the emission cross section (Fig. 49) peaked at an angle of about 50 degrees from the surface normal for two different angles of incidence, 60 degrees and 70 degrees, manifesting once more the "memory loss" effect originally observed in the O_2/graphite system.

B. Differential capture cross sections

Only a few measurements of the differential capture, as opposed to emission, cross sections have been reported. Our discussion of the theory of the differential cross sections, Sec. V.A, implies that the capture cross section should have exactly the same form as the emission cross

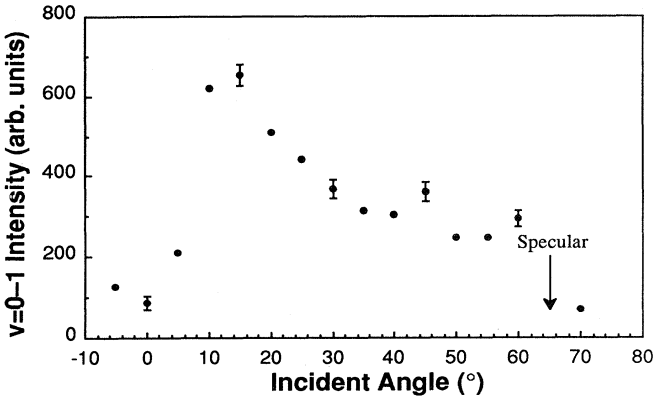

FIG. 50. Differential electron-capture cross section in resonance scattering by O_2 physisorbed on graphite in the δ phase. The graph shows the number of electrons collected at a fixed emission angle (65 degrees with respect to the surface normal) after exciting the $v=0-1$ vibrational transition of O_2, as a function of the direction of the incident-electron beam relative to the surface normal. Note the similarity between this distribution and the differential emission cross section, Fig. 41. Jensen *et al.* (1990c).

section. This notion is substantiated by the available data (Palmer *et al.*, 1987; Rous, Palmer, and Willis, 1989; Jensen *et al.*, 1990c). Figure 50 shows the differential capture cross section for the δ phase of O_2 on graphite at 8.5 eV. Comparison with the emission cross section for the same system, Fig. 41(a), indicates how similar these angular profiles are. The minimum in intensity normal to the surface in the capture cross section, like that in the emission cross section, is consistent with an approximate realization of the selection rules discussed in Sec. V.A.1.d.

C. Apparent shifts of the resonance energy in oriented molecules

When molecules are oriented in an ordered molecular array on the surface of a solid, a new phenomenon occurs that does not occur either in the gas phase or in the case of disordered molecular adsorption, namely, the modulation of the measured excitation function of the resonance, which may lead to an apparent shift of the resonance energy. We use the word "apparent" here because the resonance shift is not an intrinsic molecular shift in the energy of the virtual orbital in which the electron is trapped. Instead it arises from the effect of multiple scattering upon the probe electron before and after the formation of the resonance. Since coherent scattering causes this effect, just as it causes the distortion of the angular distributions, it seems appropriate to examine this phenomenon in the context of the present discussion. We begin by laying out the theoretical basis of this effect, and then see how it is manifest in the experiments.

1. Theoretical model

The way in which the phenomenon in question arises can seen from Eq. (39),

$$\left.\frac{d\sigma(E)}{d\Omega}\right|_{\text{surf}} = \left|\sum_{lm}\sum_{l'm'} A_{lm}(\hat{\mathbf{k}},E)F^{vv'}_{lm,l'm'}(E)A_{l'm'}(\hat{\mathbf{k}}',E)\right|^2 , \tag{44}$$

in which we have included explicitly the energy dependence of each of the terms that contribute to the energy-dependent differential cross section. This is the function that one measures, with a particular scattering geometry, in order to obtain the resonance energy in the surface experiments. This equation is to be compared with that of Davenport *et al.* (1978) for the differential cross section of an *isolated* oriented molecule:

$$\left.\frac{d\sigma(E)}{d\Omega}\right|_{\text{iso}} = \left|\sum_{lm}\sum_{l'm'} Y_{lm}(\hat{\mathbf{k}})F^{vv'}_{lm,l'm'}(E)Y_{l'm'}(\hat{\mathbf{k}}')\right|^2 , \tag{45}$$

from which we would obtain the intrinsic resonance energy of the isolated molecule. By comparing these equations, we see that the energy dependence of the differential cross section will, in general, not be the same for the isolated and the adsorbed molecule. In particular, the peak in the cross section (the *observed* resonance energy) need not be in the same location for the adsorbed and the isolated molecule, a consequence of multiple elastic scattering, which distorts the wave field of electrons incident upon and emitted from the adsorbed molecule. This is because, for an adsorbed molecule, the spherical wave amplitudes A_{lm}, which appear in Eq. (44) for the differential cross section, are functions of the incident-electron energy. This energy dependence is a result of coherent interference between all the multiple-scattering paths by which an incident electron may arrive at and leave the adsorbed molecule. If the energy dependence of the A_{lm}'s is strong, then we expect that the observed resonance profile will not match that of the intrinsic (isolated) molecular scattering; in particular, multiple scattering may modulate or shift the observed resonance profile. Equation (44) simplifies if it is assumed that each electron that undergoes resonant scattering is captured from and emitted into a *single* partial wave (l,m) (Rous *et al.*, 1989a). In this case the equation reduces to

$$\left.\frac{d\sigma(E)}{d\Omega}\right|_{\text{surf}} \propto \rho(E)\left.\frac{d\sigma(E)}{d\Omega}\right|_{\text{iso}} , \tag{46}$$

$$\rho(E) = \frac{|A_{lm}(\hat{\mathbf{k}},E)A_{lm}(\hat{\mathbf{k}}',E)|^2}{|Y_{lm}(\hat{\mathbf{k}})Y_{lm}(\hat{\mathbf{k}}')|^2} . \tag{47}$$

Thus, in the case of an adsorbate system, the identity of detected electrons factorizes into two terms, the intrin-

sic resonance profile of the adsorbed molecule and the quantity $\rho(E)$, which describes the energy dependence of the multiple scattering of electrons propagating to and from the molecule—what we might term the "multiple-scattering cross section" or "feeding function." $\rho(E)$ modulates the intrinsic resonance profile of the adsorbed molecule and therefore implies that the observed resonance behavior is, in essence, a convolution of the surface multiple scattering with the intrinsic molecular profile.

2. Experimental results and analysis

The experimental study that exposed the modulation of the molecular resonance profile as a consequence of multiple elastic scattering was the investigation of the electronic excitation of O_2 on graphite reported by Rous, Jensen, and Palmer (1989; Palmer *et al.*, 1990). The low-lying $^3\Sigma_g \rightarrow {}^1\Delta_g$ spin-flip excitation observed in gas-phase electron scattering by the O_2 molecule proceeds via the $^2\Pi_g$ negative-ion shape resonance of O_2 (Chang, 1977; Noble and Burke, 1986; the earlier gas-phase resonance assignment, $^2\Pi_u$, appears to be erroneous). The excitation functions for this transition obtained from electron scattering by the δ and ζ phases of O_2 on graphite are presented in Fig. 51. In the δ phase the resonance peaks at 6 eV, and in the ζ phase at 8 eV. In both cases the angular distributions can be matched (Jensen *et al.*, 1990b) with a partial wave of $d\pi$ symmetry (Fig. 52), consistent with the $^2\Pi_g$ state. How then can we account for the energy shift between the two phases? The lowering of the resonance energy in the δ phase by 1–2 eV compared with the gas phase is consistent with an image-potential shift, but given that both the δ and the ζ phases are monolayer structures, one cannot envisage a difference in the image-potential shift between the two structures of more than a few tenths of an eV. In order to explain the result, Rous, Jensen, and Palmer invoked the multiple-scattering cross section discussed in the previous section.

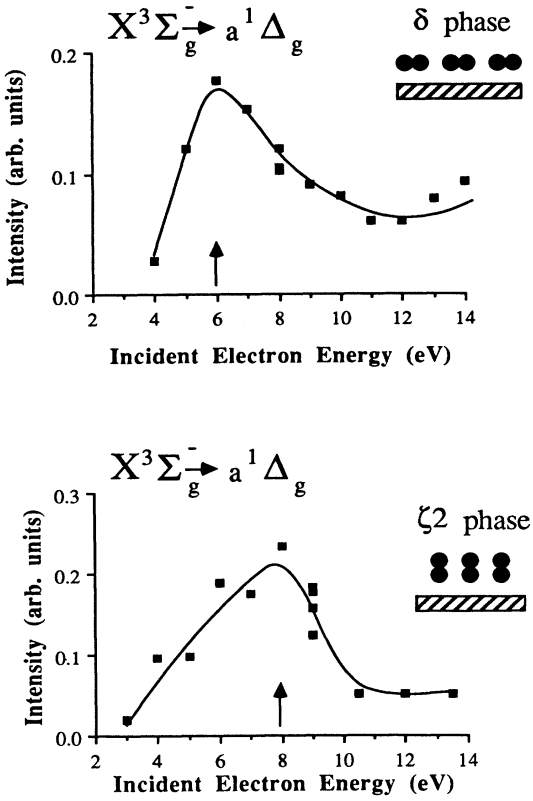

FIG. 51. Excitation functions for the $X^3\Sigma_g^- \rightarrow a^1\Delta_g$ electronic excitation of O_2 physisorbed on graphite in δ and $\zeta 2$ phases, obtained with the same scattering geometry in each case (angle of incidence 60 degrees, emission angle 40 degrees). The energy of the resonance shifts significantly between the two phases, attributed to the modulation of the cross section by coherent multiple elastic electron scattering. Rous, Jensen, and Palmer (1989).

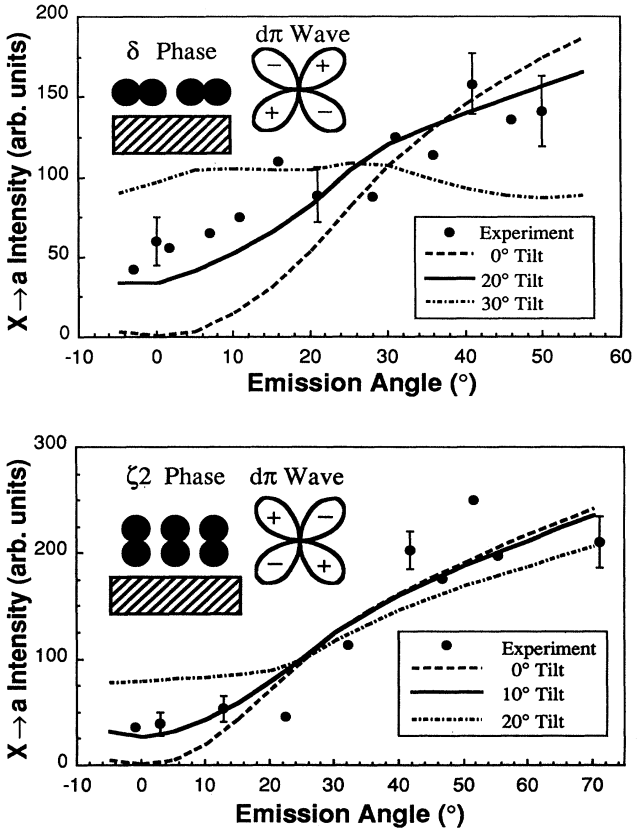

FIG. 52. Angular distribution of electrons detected after the $X^3\Sigma_g^- \rightarrow a^1\Delta_g$ electronic excitation of O_2 physisorbed on graphite in the δ and $\zeta 2$ phases. The experimental results are shown, together with calculated angular distributions, for various orientations of the molecular axis, which assume resonance capture/emission via a $d\pi$ wave in both phases. These calculations suggest that the symmetry of the resonant state is the same in both phases and also illustrate the sensitivity of the angular distributions in resonance scattering to the orientation of the adsorbed molecule. Jensen *et al.* (1990b).

In particular, they pointed out that the excitation function observed on the surface is the product of two terms:

(i) the intrinsic molecular resonance cross section, as perturbed on the surface by the image potential, etc.,

(ii) the multiple-scattering cross section, the "feeding function" which describes how much of a particular partial wave is provided to the target molecule and collected by the detector.

Multiple-scattering cross sections or "feeding functions" $\rho(E)$ calculated for various partial waves in the δ and ζ phases are plotted in Fig. 53(a), for the scattering geometry used in the experiment. The relevant multiple-scattering cross sections for scattering via the $^2\Pi_g$ state are those for the $d\pi$ wave. One can see that in the δ phase the $d\pi$ cross section is a fairly smooth function of energy, but that in the ζ phase it shows sharp structure with a peak near 10 eV. If the hypothesis is true, that the shift in resonance energy between the δ and ζ phases is due to the difference in the multiple-scattering cross sections, then the molecular resonance profiles that can be recovered from the equation

$$\left.\frac{d\sigma(E)}{d\Omega}\right|_{\text{iso}} = \frac{1}{\rho(E)} \left.\frac{d\sigma(E)}{d\Omega}\right|_{\text{surf}} \tag{48}$$

should be similar. Here the measured excitation function for the molecule on the surface is divided by $\rho(E)$, the calculated multiple-scattering cross section ("feeding function") for the $d\pi$ wave in each phase. Figure 53(b) shows the molecular resonance profiles derived by this procedure; they show a remarkable level of similarity (except at higher energies, possibly due to another resonant state), confirming the hypothesis. This phenomenon is expected to be quite general. In every case where an excitation function is measured for an ordered molecular array we expect the molecular resonance profile to be modulated by the multiple-scattering cross section.

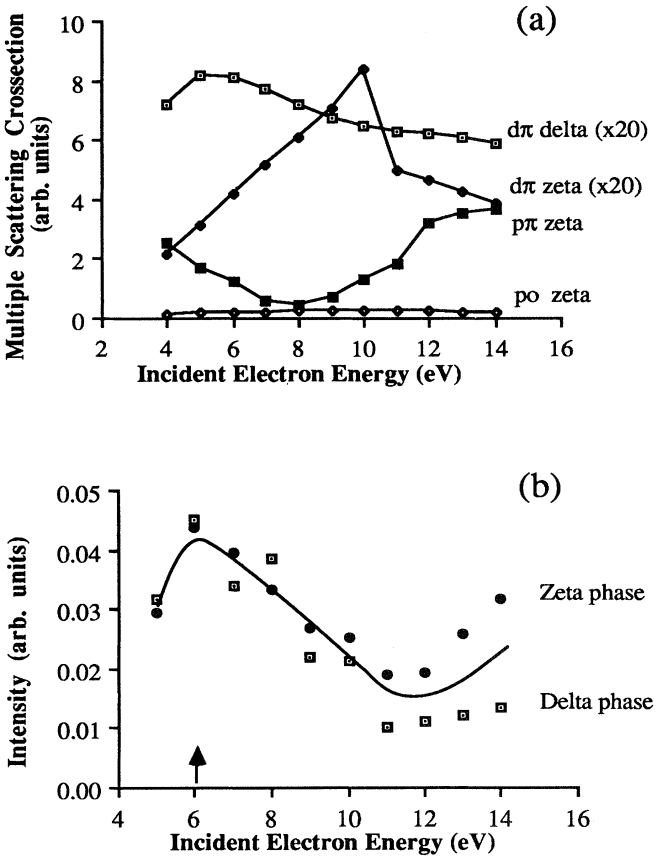

FIG. 53. The effect of multiple scattering upon the observed resonance profile of the monolayer $\zeta 2$ and δ phases of O_2 on graphite: (a) Calculated effective multiple-scattering cross sections ("feeding functions") $\rho(E)$ for capture/emission via the $d\pi$ partial wave, assuming molecules tilt at angles of 25 and 75 degrees from the surface normal in the $\zeta 2$ and δ phases, respectively. Cross sections for the $p\sigma$ and $p\pi$ partial waves are shown for comparison. The angle of incidence is 60 degrees, the emission angle is 40 degrees. (b) The intrinsic O_2 molecular resonance profile obtained by removing the energy variation of multiple scattering from the measured resonance profiles of Fig. 51. We assume that emission and capture occur through the $d\pi$ partial wave. The angle of incidence was 60 degrees, the detection angle 40 degrees from normal. Rous, Jensen, and Palmer (1989).

D. Selective resonance population in oriented molecules

In this section we discuss another phenomenon that arises when a molecule is oriented by adsorption on the surface of a solid. Suppose that a molecule has two resonant states of similar energy but different symmetry. In a gas-phase electron-scattering experiment all of these states will be populated and thus contribute to the scattering cross sections because of the random orientations of the molecules there. However, when a molecule is aligned on a surface, it becomes possible to choose a scattering geometry such that one state is populated in preference to the other. This effect has been termed "selective resonance population" (Jensen *et al.*, 1990a). The degree to which one state is populated over the other depends on the differential cross sections for electron capture and emission, so that the effect of multiple elastic scattering must again be considered.

1. Theoretical model

In simplest terms the phenomenon of selective resonance population is a consequence of the surface's acting as a template to orient the adsorbed molecule. If we ignore the electron-surface interaction, then we know that the differential cross section for resonance electron scattering reflects the symmetry of the negative ion. In particular, electrons are emitted preferentially in directions corresponding to lobes of the resonant-state wave function and are not emitted along directions in which the wave function of the resonant state has a node. Simi-

larly, the differential cross section for electron capture is maximal for angles of incidence in directions corresponding to lobes of the resonant-state wave function and vanishes along directions in which the wave function of the resonant state has a node. Thus we can never observe resonant excitation if either the electron detector or the electron gun points into a node of the wave function of the resonant state.

Now suppose that an adsorbed molecule possesses two distinct resonant states of similar energy but different symmetry. Clearly, a consequence of orientation is that the *relative* probability of forming these two negative-ion states is a function of the scattering geometry. Consider, for example, a molecule that has a resonance of $p\sigma$ symmetry and a resonance of $p\pi$ symmetry and that is oriented normal to the surface, and assume that we can ignore the electron-surface interaction. If the electron beam is incident normal to the surface (along the molecular axis), then only the $p\sigma$ state is populated. If the electron beam comes in at glancing incidence, then only the $p\pi$ resonance can be seen. If the molecule lies flat on the surface, then the reverse behavior would be observed. This is the basic description of the phenomenon of selective resonance population.

Inclusion of the surface-electron interaction complicates the picture given above, since the differential cross sections for electron capture and emission are modified, as we have seen already. However, it is clear that the probabilities of populating two resonances with different symmetries, given an arbitrary scattering geometry, are still not, in general, going to be equal. Further, it may still be possible to choose a scattering geometry in which the ratio of probabilities markedly favors populating one of the two states. So, while the modulation of the angular distributions because of adsorption on the surface determines the precise differential cross sections for populating each resonance, the phenomenon of selective resonance population is preserved.

Another way of looking at selective resonance population in adsorbed molecules arises from the discussion of Sec. V.C, where we saw how the observed energy of a resonance in an adsorbed molecule could be shifted because of multiple elastic scattering of the probe electron prior to and after formation of the negative ion. The cause of this effect was the energy-dependent interference between the elastic multiple-scattering paths contributing to the electron wave field surrounding the molecule on the surface, and was summarized by the "feeding function" $\rho(E)$, which modulated the intrinsic resonance profile of the adsorbed molecule. In the multiple-scattering regime, selective resonance population occurs as a result of the $\mathbf{k}$ dependence of the "feeding function" $\rho(E)$. Thus the selective population of a resonance occurs when the scattering geometry is such that the multiple-scattering paths represented by ρ interfere to enhance the capture and emission cross sections of one negative ion, and suppress the capture and emission cross sections of the other resonant state(s).

2. Experimental results and analysis

The phenomenon of selective resonance population was revealed by the investigations of vibrational excitation in the O_2/graphite system reported by Jensen *et al.* (1990a). In the δ phase, a resonance in the $v=0-1$ cross section was seen, centered at 8.5 eV [Fig. 54(a)]. The angular distributions, Fig. 41(a), obtained with a beam energy corresponding to the peak of the resonance, were satisfactorily modeled with calculations that assumed a partial wave of $p\sigma$ symmetry, compatible with the $^4\Sigma_u$ shape resonance, as discussed in Sec. V.A.2. In the ζ phase, again identified with LEED measurements, the energy of the resonance peak was found to shift substantially downwards, to 6.5 eV [Fig. 54(b)]. The angular distributions, Fig. 41(b), measured at this energy were not now consistent with a $p\sigma$ partial wave, but could be matched by a calculation assuming the $p\pi$ partial wave consistent with the $^2\Pi_u$ Feshbach resonance of the O_2 molecule. In

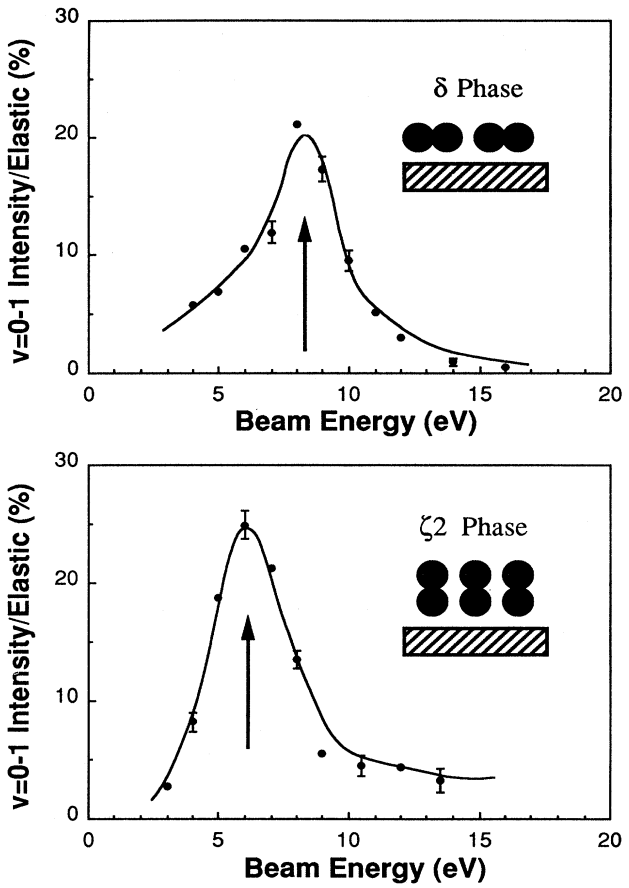

FIG. 54. Excitation functions for the $v=0-1$ vibrational transition of O_2 physisorbed on graphite: (a) the δ phase; (b) the $\zeta 2$ phase. The angle of incidence is 60 degrees from the normal in each case; the detection angle is 20 degrees in (a) and 40 degrees in (b). The energy of the resonance shifts significantly between the two phases, attributed to the population of different resonant states in the two phases. Jensen *et al.* (1990a).

short, the $^4\Sigma_u$ resonance is observed in the δ phase; the $^2\Pi_u$ resonance is observed in the ζ phase. The results suggest that the single broad resonance observed in gas-phase electron-molecule scattering experiments (Wong *et al.*, 1973), centered at 9.5 eV and assigned, on energy grounds, to the $^4\Sigma_u$ state with a possible contribution from the $^2\Pi_u$ state, involves both states—the individual contributions are not resolved because of the average over molecular orientations in the gas-phase case.

But why should one negative-ion resonance be seen in the δ phase and the other in the ζ phase? A comprehensive answer to this question requires a knowledge of the individual cross sections for vibrational excitation via the two resonant states in the gas phase, which is not at present available. Nevertheless, two possible factors can be isolated.

(i) It might be the case that each resonance couples to the surface or to its neighbors in a way that depends on the adsorbate orientation and/or structure. One could then envisage that the $^4\Sigma_u$ resonance is quenched by interaction with the surface in the ζ phase, while the $^2\Pi_u$ is quenched in the δ phase. This hypothesis, however, requires a degree of interaction with the surface in the case of physisorbed species which appears rather to conflict with the insights that have been obtained into the resonance lifetime in such species, discussed in Sec. IV.A.

(ii) Another possibility is that the probability of the probe electrons coupling into the respective resonance states and then being detected is a function of the adsorbate orientation, for a given scattering geometry and energy. One way of looking at this issue is to consider how much of the $p\sigma$ ($p\pi$) partial wave, required to populate the $^4\Sigma_u$ ($^2\Pi_u$) negative-ion resonance, is supplied to the adsorbed O_2 molecules in the two phases. Jensen *et al.* (1990c) presented calculations, for the geometries used in their experiment and over a range of electron-beam energies, of the partial wave "feeding functions," which couple the incident electron beam to the detected beam via a partial wave of given symmetry in the expansion of the wave function about the target molecule. The results of this calculation are shown in Fig. 55. In the δ phase the $p\pi$ partial wave is always suppressed relative to the $p\sigma$ wave, while the reverse is true in the ζ phase. This phenomenon, selective resonance population, leads to (relatively) enhanced scattering, via the $^4\Sigma_u$ state in the δ phase, and via the $^2\Pi_u$ state in the ζ phase, as observed. Another way of looking at the same effect is to consider the differential capture cross sections in the two phases, which will look just like the differential emission cross section in Fig. 41(a). Consider the δ phase by way of example. The ideal angle of incidence and also of detection for scattering via the $^4\Sigma_u$ state is around 20 degrees from the surface normal, whereas to populate the $^2\Sigma_u$ state one would want (according to calculations of Jensen *et al.*, 1990c) both the incident beam and the detected beam to be in the direction of the surface normal. The experimental geometries chosen by Jensen *et al.* thus favor the

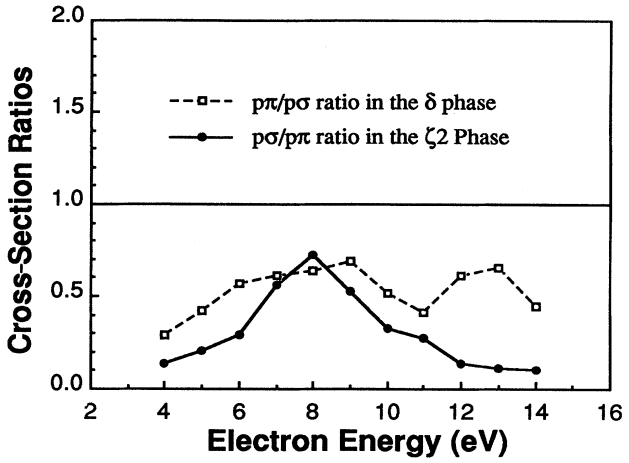

FIG. 55. Calculation of the relative weights of the $p\sigma$ and $p\pi$ partial waves coupling to the O_2 molecule physisorbed on graphite in the δ and ζ2 phases, for an angle of incidence of 60 degrees and an emission angle of 40 degrees. The results illustrate the preferential coupling to the *ps* symmetry resonance in the *d* phase, and the *ppi* symmetry resonance in the ζ2 phase, for this scattering geometry, an example of "selective resonance population." Jensen *et al.* (1990c).

$^4\Sigma_u$ state. The converse argument holds in the ζ phase.

If (ii) is correct, then an appropriate choice of the scattering geometry should allow the $^2\Pi_u$ state to be selected in the δ phase, rather than the $^4\Sigma_u$ state, and vice versa in the ζ phase. Figure 56 shows excitation functions recently observed by Barnard and Palmer (1992a) for O_2/graphite which graphically confirm this

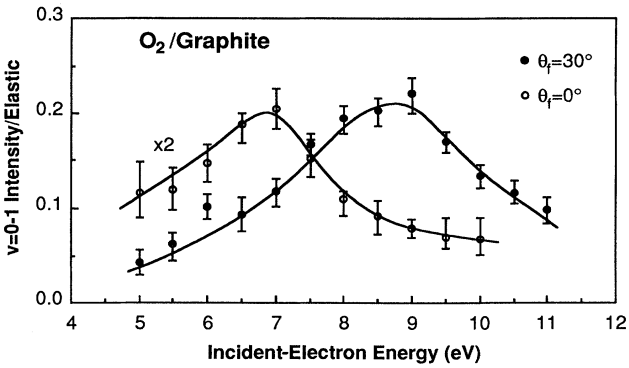

FIG. 56. Cross sections for excitation of the $v=0-1$ mode of a physisorbed monolayer of O_2 on graphite, produced by melting the δ phase, as a function of incident-electron energy, obtained with an angle of incidence of 60 degrees and two different emission angles, 30 degrees and 0 degrees, relative to the surface normal. The different resonance profiles obtained in these two cases are attributed to the collection of electrons scattered via two resonant states of different symmetry, the $^4\Sigma_u^-$ state (at 9 eV) and the $^2\Pi_u$ state (at 7 eV), respectively. Barnard and Palmer (1992).

prediction. For the scattering geometry ($\theta_{in}=60°$, $\theta_{out}=30°$) a resonance is seen in the melted δ phase at approximately 9 eV ($^4\Sigma_u$), as Jensen *et al.* (1990c) found. However, for the scattering geometry ($\theta_{in}=60°$, $\theta_{out}=0°$) the resonance energy is shifted to 6.5 eV, indicating that the $^2\Pi_u$ state is now being populated. Note that the $^4\Sigma_u$ resonance is stronger than the $^2\Pi_u$ state, as anticipated in view of the fact that the broad gas-phase resonance, which must be an average over both states, has a peak at 9.5 eV.

VI. RESONANCE DECAY CHANNELS

In this section we discuss the various channels by which a negative-ion resonance of an adsorbed molecule can decay and, in particular, the different types of vibrational mode that can be excited via resonance scattering. The range of possible resonance decay channels is substantially increased when a molecule is adsorbed on a surface, in comparison with the gas phase, because of the coupling of the molecule to the surface and to coadsorbed molecules. We shall see that the mechanism by which, for example, molecule-surface modes can be excited on the surface is fundamentally similar in character to the mechanism of mode-selective vibrational excitation in polyatomic gas-phase molecules, because in one sense the molecule-surface complex can be viewed as a kind of giant polyatomic molecule. Thus, after outlining the theory of these effects, we begin our treatment of the relevant experimental work by showing that mode-selective vibrational excitation is preserved when polyatomic molecules are adsorbed on a surface, and then move on to discuss the excitation of vibrational modes which have their origin in the adsorption of the molecule on the surface, such as intermolecular vibrational modes and the vibration of the molecule against the surface. We then give a brief review of the resonant excitation of rotational modes in adsorbed molecules and end the section with a short discussion of the branching ratios between competing decay channels in resonance decay.

One resonance decay channel that this review does not address, since it is concerned with electron *scattering* by adsorbed molecules, is dissociative attachment (i.e., molecular dissociation induced by electron attachment). For reviews of the work in this area, pioneered by Sanche and co-workers, the reader is referred to the articles by Sanche himself (1989, 1990). This work has concentrated on dissociative attachment in condensed molecules on polycrystalline substrates; similar investigations of dissociative attachment in molecules adsorbed on single-crystal surfaces may be an important area of future investigation.

A. Theoretical models

1. Mode-selective vibrational excitation

The enhancement of the vibrational excitation cross section when a temporary negative ion is formed occurs because of the change in the molecular potential-energy surface, which drives the motion of the nuclei during the lifetime of the molecular ion and results in the vibrational excitation of the neutral molecule after electron detachment. In the case of a diatomic molecule, the potential-energy surface is a function of only one internuclear coordinate vector. On the other hand, the potential-energy surface of a polyatomic molecule is a multidimensional function of several coordinates. Thus various vibrational modes may in principle be excited by the creation of a short-lived negative ion in a polyatomic molecule. It turns out, however, that the symmetry of the vibrational modes that can be excited depends on the symmetry of the electronic state of the negative ion that is formed.

To see how this occurs we need to consider the dynamics of the intramolecular motion during the lifetime of the negative ion. Whilst the probe electron resides within the molecule the intramolecular bonds are distorted. This motion of the nuclei can be decomposed into one or more of the normal mode coordinates of the molecule, each of which corresponds to a distinct vibrational mode of the molecule. Clearly, only those modes which are needed to describe the intramolecular motion during the lifetime of the ion will be excited when the electron detaches. Put simply, only those vibrational modes which are compatible with the symmetry of the resonant state can be excited by resonance formation. For all other vibrational modes, resonance electron scattering does not lead to vibrational enhancement. So a selection rule is operating, and the resulting phenomenon has come to be called *mode-selective vibrational excitation.*

When a molecule is adsorbed on a surface new modes of vibration are created as a consequence of the coupling between the molecule and the atoms in the substrate. In one sense, we can view the molecule-surface system as a giant polyatomic molecule. Thus, we expect that the formation of a negative-ion resonance may lead to the enhanced excitation of these new modes, just as the temporary localization of an electron in an unoccupied orbital of a particular functional group of a polyatomic molecule may lead to the excitation of various modes of vibration of that molecule. Also, we expect that the constraints on the symmetry of the vibrational modes into which a resonance can decay in a polyatomic molecule will also determine whether or not a particular mode can be excited by a resonance.

Ibach (1982) has formulated rigorously the selection rule describing mode-selective vibrational excitation using group theory. Suppose that the quasibound molecular orbital in which the electron is trapped belongs to a representation G of the surface point group of the *adsorbed* molecule. For example, for CO adsorbed on a top site of a fcc(111) surface the point group is C_{3v}. For adsorption on a bridge site the point-group symmetry is C_{2v}. The irreducible representations of the charge distribution $|\psi|^2$ of the trapped electron are the irreducible representations of G taken in direct product with itself.

For nondegenerate representations, the character of the irreducible representation of $|\psi|^2$ is $+1$. This reflects the fact that the charge distribution of the trapped electron, $|\psi|^2$, is symmetric. Thus, for surface point groups that have nondegenerate representations, only totally symmetric vibrations can be excited by negative-ion formation. It is only these vibrational modes that are compatible with the symmetry of the quasibound orbital into which the probe electron is captured. For degenerate representations, it is necessary to evaluate the irreducible representation for the point group. In this way one obtains the representation of those vibrational modes which can be excited through resonance electron scattering involving a particular quasibound molecular orbital.

2. Resonant excitation of molecule-surface vibrational modes

The precise mechanism by which molecule-surface modes may be excited in resonance scattering deserves some attention. The phenomenon was predicted first by Gadzuk (1985), who treated the excitation of the molecule-surface vibration on a metallic surface (Fig. 57). He argued that, when the negative molecular ion is formed, the molecule can be attracted towards the surface by the image charge within the metal which is "switched on" when the electron attaches to the molecule. This attraction causes the center of mass of the molecule to move towards the surface whilst the electron remains attached, thereby compressing the molecule-surface bound. When the electron detaches, the molecule finds itself in a nonequilibrium position relative to the surface; hence a molecule-surface vibration can be excited. The probability of exciting this vibration clearly depends upon the lifetime of the resonance. From a semiclassical viewpoint, the longer the lifetime of the negative ion (in the short-lifetime limit), the greater the compression of the surface-molecule bond and the higher the probability of exciting the molecule-surface mode. Gadzuk (1985, 1988) estimated the probability of exciting this vibration for typical resonance lifetimes and vibrational frequencies. For $\tau=10^{-15}$ s, the probability of exciting the molecule-surface mode is $P_{0\to1}\approx0.002$, but for $\tau=10^{-14}$ s, $P_{0\to1}\approx0.17$. These numbers suggested that, for long-lived resonances, the observation of the excitation of molecule-surface vibrations was a possibility. As we describe in the following section, the first observations of the excitation of such modes via resonance electron scattering have now been made.

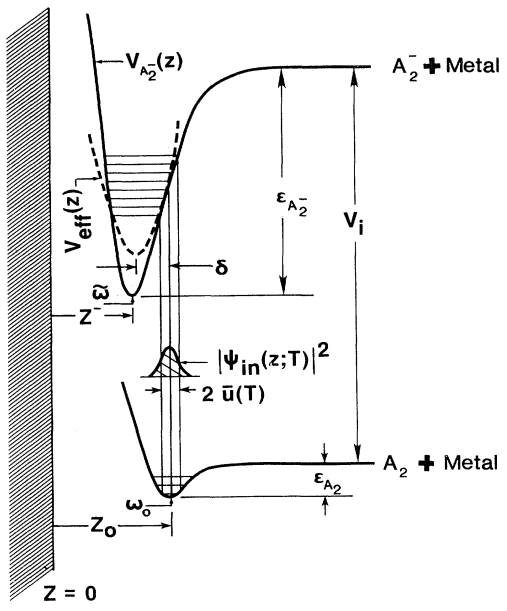

FIG. 57. Potential-energy curves for a chemisorbed neutral molecule and its negative ion. The structure labeled $|\Psi(z;T)|^2$ represents the initial-state charge distribution of the wave packet, which propagates over the potential-energy surface of the negative ion and leads to vibrational excitation of the surface-molecule bond. Gadzuk (1988).

B. Experimental results and analysis

1. Mode-selective intramolecular vibrational excitation in polyatomic molecules

The observation of resonances on surfaces was first extended into the regime of polyatomic species by Liehr *et al.* (1985a, 1985b), who explored the adsorption of formic acid (HCOOH) on an oxidized Al(110) surface. The HREELS spectra obtained were understandably rather rich, but the authors were able to isolate two vibrational modes whose excitation functions (Fig. 58), deviated measurably from dipole scattering theory. The cross section for the CH stretch mode showed a resonance, centered at about 6 eV, superimposed on the dipole prediction. The cross section for the asymmetric stretch mode of the O-C-O group featured a similar resonance at about 3.5 eV. The authors suggested that the unoccupied π_3^* orbital of formic acid, localized on the OCO group, might be the origin of the resonance in the O-C-O cross section, consistent with the mode selectivity observed. Liehr and co-workers also noted the presence of another unoccupied (σ^*) molecular orbital in the gas-phase molecule just above the vacuum level, to which they assigned the enhancement in the CH stretch mode. Curiously, Liehr *et al.* (1985a) attributed an observed increase in intensity of the CH mode relative to the O-C-O symmetric stretch (presumably used as a normalization) at large angles from the specular direction to "impact" scattering, though since this data was taken at a beam energy for which the "resonant" enhancement was observed, it seems to us that the angular data is also quite compatible with resonant, rather than impact, excitation of the CH mode.

The preservation of mode selectivity in resonance

scattering by molecules on surfaces was confirmed by the studies of benzene (C_6H_6, and deuterated benzene, C_6D_6) chemisorbed on the Pd(100) surface reported by Kesmodel (1984) and Waddill and Kesmodel (1985, 1986a, 1986b). They found a resonance in the cross section for the symmetric CH stretch mode ($\nu 1$) located at about 2.7 eV and another in the cross section for the ring stretching mode, $\nu 13$, at about 5 eV (Fig. 59). $\nu=0-2$ and $\nu=0-3$ overtones of the CH stretch were observed, together with combination bands involving this mode, and the $\nu=0-2$ cross section tracked that of the fundamental. The authors suggested that the 2.7 eV resonance might arise from an image-potential shift of the broad resonance centered at 4.8 eV in the gas phase and assigned to the $^2b_{2g}$ negative ion of the benzene molecule (Wong and Schulz, 1975). We note that subsequently Cloutier and Sanche (1989) observed a resonance in the excitation function of the $\nu 1$ mode of condensed C_6H_6 which was also centered between 2 and 3 eV. Waddill and Kesmodel (1985) presented angular distribution measurements over a limited range and showed that the intensity of the $\nu 1$ and $\nu 13$ modes held up at small angles from specular, in contrast with the dipole excited modes of the molecule. On Pd(111) the authors found a similar resonance at 2–3 eV in the $\nu 1$ mode (Waddill and Kesmodel, 1985, 1986a, 1986b), but the resonance in the $\nu 13$ mode was not reproduced, causing the authors to reflect that the excitation mechanism of the $\nu 13$ mode might be impact scattering on both Pd(100) and Pd(111).

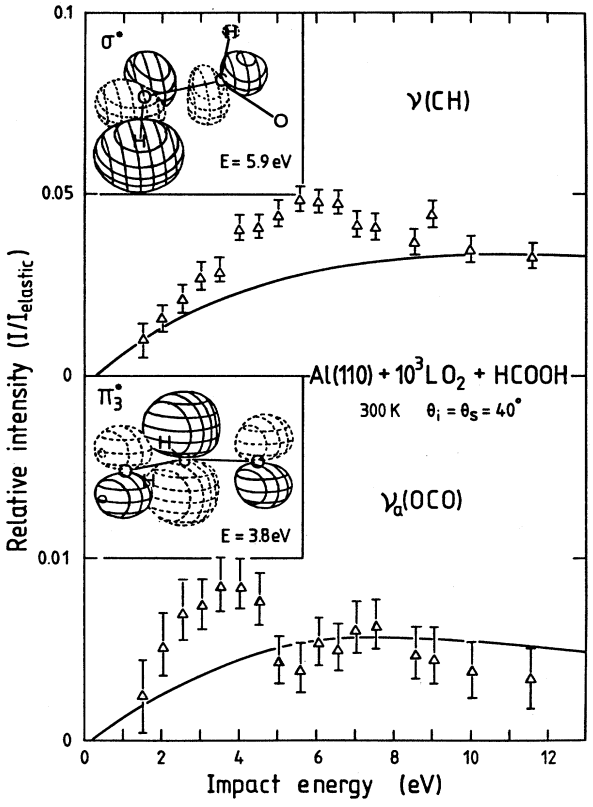

FIG. 58. Cross sections for excitation of the CH stretch mode ν(CH), and the asymmetric stretch of the OCO group, ν_a(OCO), of the formate species chemisorbed on an oxidized Al(110) surface as a function of electron-impact energy in specular scattering. The insets show the molecular orbitals of formic acid from which the resonances observed in the ν(CH) cross section at about 6 eV and in the ν_a(OCO) cross section at about 3.5 eV may be derived. The solid lines are the predictions of the dipole scattering theory upon which the resonances are superimposed. Liehr *et al.* (1985a).

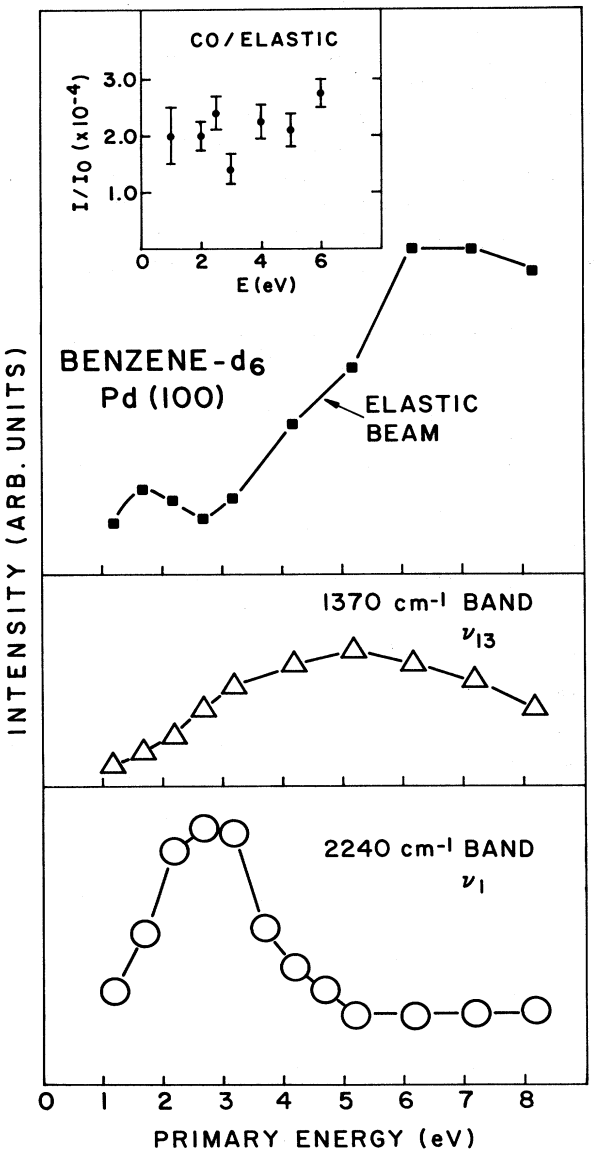

FIG. 59. Excitation functions for the $\nu 1$ and $\nu 13$ vibrational modes of (deuterated) chemisorbed benzene (C_6D_6) on Pd(100), showing resonance structures centered at about 3 eV in the $\nu 1$ cross section and about 5 eV in the $\nu 13$ cross section. The excitation functions are not normalized, and the elastic reflectivity is shown for comparison. The inset shows the normalized excitation function of the stretch mode of chemisorbed CO, which is used as a calibration. Kesmodel (1984).

We note that a possible complication in resolving such an issue arises in this case because the excitation functions presented by Waddill and Kesmodel were not normalized, and there was substantial structure in the recorded energy dependence of the elastic-scattering count rate which might in principle contain an instrumental component. Finally, the excitation functions of the $\nu 10$ CH (CD) bending mode on Pd(111) [Pd(100)] were also found to be compatible with a resonant contribution at 2–3 eV, like that observed in the CH stretch ($\nu 1$) cross section, although resonant excitation of the $\nu 10$ mode via the $^2b_{2g}$ resonance was not observed in the gas phase (Wong and Schulz, 1975).

If a negative-ion resonance is localized on a particular functional group, then one might expect the resonance to be evident in various molecules bearing the same functional group. This notion was explored by the investigation by Waddill and Kesmodel (1986a) of pyridine and cyclohexane adsorption on the Pd(111) surface. In the case of pyridine (C_5H_5N), which features a six-membered ring structure similar to the benzene molecule, a resonance in the cross section for the CH stretch mode was observed at about 3 eV, just as in benzene (Fig. 60). On the other hand, no such enhancement was seen in the case of adsorbed cyclohexane (C_6H_{12}). These results are consistent with the gas-phase data, insofar as pyridine, like benzene, has a resonance in the CH stretch cross section at around 4.6 eV (Azria and Schulz, 1975). In these molecules the resonance invoked involves the trapping of an electron in a π^* molecular orbital localized on the unsaturated ring. Because the cyclohexane ring is saturated, such a resonance cannot exist in that molecule.

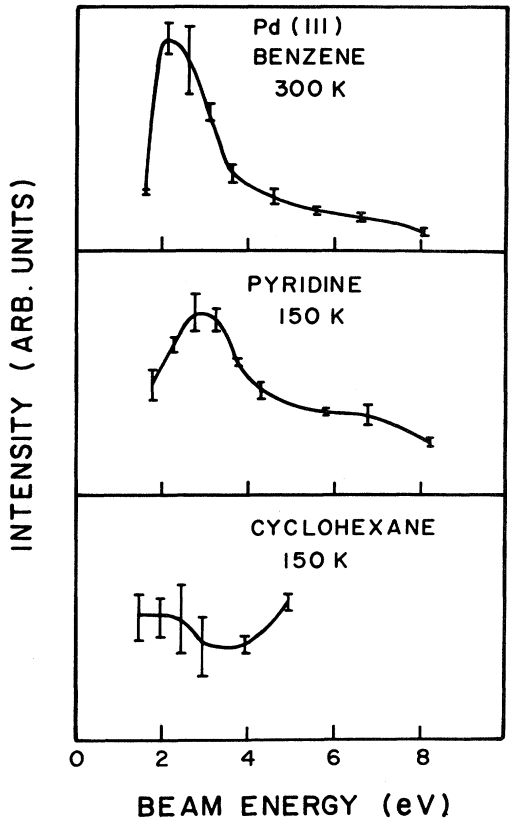

FIG. 60. Excitation functions of the C-H stretch mode in benzene, pyridine, and cyclohexane chemisorbed on Pd(111). The resonance observed in the unsaturated benzene and pyridine molecules is absent in the saturated cyclohexane molecule, suggesting that the resonance involves electron trapping in the π^* molecular-orbital system common to the two ring molecules. Waddill and Kesmodel (1986a).

Mode-selective vibrational excitation in electron scattering by adsorbed polyatomic (organic) molecules was again observed by Timbrell *et al.* (1988), in their study of acetylene (C_2H_2) adsorption on the Pd(111) surface. As the electron-beam energy was lowered to the minimum value used (3 eV), the intensity of the symmetric CH bend mode in the specular HREELS spectrum rose sharply (relative to the elastic peak), while the intensities of the other vibrational modes observed in the spectrum, the antisymmetric CH bend, the CC stretch, and the CH stretch, barely rose. Timbrell *et al.* pointed out that, given the mirror plane symmetry of the adsorbed C_2H_2 molecule, resonant excitation of the antisymmetric CH bend mode was forbidden (Sec. VI.A), whereas the other three modes were allowed. The fact that only the symmetric CH bend was enhanced must then be attributed to the different degrees of coupling between the particular charge distribution of the temporary negative ion and the various vibrational modes. The authors noted that in gas-phase C_2H_2 resonant excitation of the CC stretch mode was observed and attributed to temporary occupation of the lowest unoccupied π^* orbital, 2.6 eV above the vacuum level. This adsorption system thus appears to represent a prime example of the (radial) distortion of the molecule's electronic structure by chemisorption in resonance electron scattering. Indeed, the authors speculated that the resonant state was actually localized on the metal-adsorbate bond.

An interesting example of mode selectivity in physisorbed species was provided by the study of vibrational excitation of CO_2 on the Ag(111) surface conducted by Sakurai *et al.* (1987a). These authors observed loss peaks in the HREELS spectra, obtained at various coverages, at frequencies close to those of the symmetric stretch, asymmetric stretch, and bending modes of the gas-phase CO_2 molecule. A number of other loss peaks were also observed and assigned to overtones of the symmetric stretch and to multiple losses of the type (n10), where (010) represents the fundamental of the bending mode and (n00) represents a $\nu=0$-n excitation of the symmetric stretch vibration. As a function of electron-impact energy, the cross section for the symmetric stretch obtained (slightly) away from the specular direction showed a distinctive peak near 9 eV and a shoulder near 5 eV; in the gas phase there is a negative-ion resonance at 10.8 eV (Tronc *et al.*, 1979). The cross sections for the asymmetric stretch and the bending mode appeared to be con-

sistent with dipole scattering. The intensity of these modes peaked sharply on specular, whereas that of the symmetric mode was more diffuse. The excitation of the higher-order (n10) and (n00) modes was especially strong at electron impact energies of 1.5–2 eV; there is another resonance in the gas-phase CO_2 molecule at 3.8 eV. Thus it seems that both the low-energy gas-phase resonances persist in the physisorption of CO_2 on Ag(111), and that the distinctive mode-selective resonant enhancement observed in the gas phase, an enhancement that is a consequence of the particular charge distribution of the negative ion (Sec. VI.A), is also preserved.

Sakurai *et al.* (1987b) also investigated vibrational excitation of CH_4 on the Ag(111) surface and obtained results compatible with, if not proof of, negative-ion resonance electron scattering. The excitation function of the infrared active v4 mode showed a sharp minimum at 8 eV, which could be correlated with a similar structure in the elastic reflectivity (assigned to a surface wave resonance feature). Such a correlation is indicative of dipole scattering. The excitation function of the Raman-active $\nu 2$ mode did not show this correlation, so that in this case the excitation mechanism was thought to be impact or resonance scattering. Arguably, one could describe the excitation function of the $\nu 2$ mode as showing a broad resonance centered at approximately 8 eV, but this is one of a number of cases in which the measurement of an excitation function away from the specular direction might be illuminating, especially since the intensity of the $\nu 2$ mode was found to remain high off specular.

A number of studies have also isolated mode-selective vibrational intensity enhancements in polymers on surfaces. For example, in their investigation of a monolayer Langmuir-Blodgett film composed of long chainlike barium behenate molecules, Wandass and Gardella (1987) measured the (normalized) cross sections for excitation of the C-H, C-C, and CH_2 stretching modes as a function of primary beam energy (in the specular direction) and found resonances in the C-C and CH_2 cross sections centered at about 5.5 eV. These authors did not attempt to assign this resonance structure to the occupation of particular molecular orbitals, but Apai and McKenna (1991) have noted that resonances of similar energy in formic acid on alumina (Liehr *et al.*, 1985a, 1985b), and in their own study of polycarbonate films, may be ascribed to σ^* states. On the other hand, these studies were seeing enhancement of the C-H stretch mode at the resonance energy, the very mode that does not appear to be enhanced in the Langmuir-Blodgett film. Wandass and Gardella (1986) found another effect compatible with mode-selective resonant vibrational excitation in their study of stearic acid films on Ag; in this case, particular energy-loss features were enhanced relative to other modes in the HREELS spectrum at specific film thicknesses, an effect that the authors suggested might be due to changes in the electronic structure of the film with increasing thickness, and thus in the resonance parameters. A further result consistent with resonance scattering by polymers may be seen in the excitation function for the stretching modes in films of deposited hexatriacontane reported by Pireaux *et al.* (1986), which shows a clear peak at a beam energy of about 3 eV. It is worth bearing in mind that all these studies have been confined to specular scattering, and, on the whole, to a modest set of primary energy points; it would be rather helpful, if possible, to obtain a more comprehensive set of excitation functions at a variety of scattering angles in order to explore fully the richness of resonance scattering in this type of system.

In Sec. V.A.2, we saw that the σ symmetry shape resonance of the CO molecule was also manifest in the CO group of the formate species, and this suggests that it may be possible to look at a complex molecule as a sequence of connected functional groups, each manifesting its distinctive resonant states. The investigation of electron scattering by polycarbonate films between 2 and 12 eV reported by Apai and McKenna (1991) accords with this notion. They found (Fig. 61) the following features in the excitation functions:

(i) The cross section (relative to the elastic peak) of the aromatic C-H stretch modes (i.e., the stretch mode of a

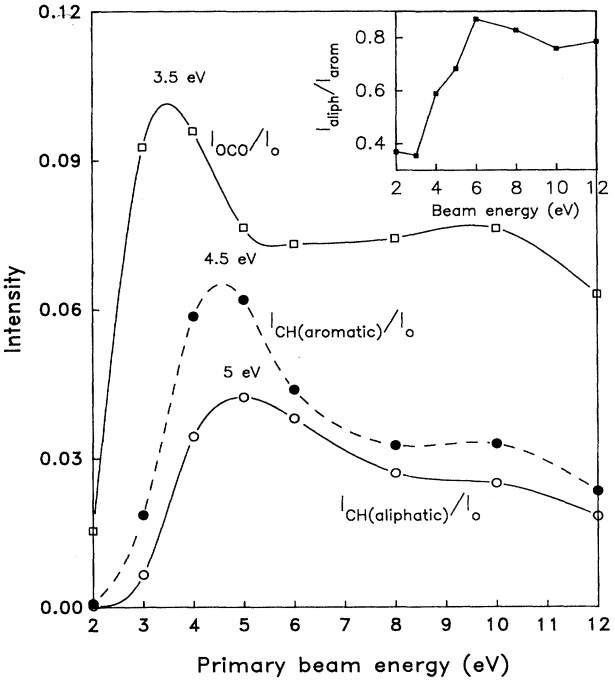

FIG. 61. Excitation functions for various vibrational modes of a polycarbonate film on graphite, showing resonances that may be compared with those in smaller molecules containing the constituent functional groups of the polymer. Resonances are seen in the cross section for the aromatic C-H stretch modes, at 4.5 eV (compare Fig. 60), and for the aliphatic C-H stretch modes and the carbonate (O-C-O) stretch mode, at 5 eV and 3.5 eV, respectively (compare Fig. 58). Apai and McKenna (1991), reprinted courtesy of the Eastman Kodak Company.

CH group on a benzene-type ring) showed a resonance with a peak at around 4.5 eV.

(ii) The intensity of the methyl group C-H stretching modes peaked at about 5 eV.

(iii) The intensity of the O-C-O vibrations of the carbonate was at a maximum at about 3.5 eV.

These three resonances align in a remarkable fashion with those observed in simpler molecules. Specifically,

(i) the C-H stretch mode in gas-phase benzene shows a resonance at 4.8 eV (Wong and Schulz, 1975), assigned to occupation of the $^2b_{2g}$ antibonding orbital;

(ii) the resonance in the C-H stretch of the surface formate species on aluminum oxide observed by Liehr *et al.* (1985a, 1985b) is located at about 6 eV (Fig. 58) and attributed to a σ^* molecular orbital;

(iii) the resonance in the asymmetric O-C-O stretch mode in the same species is located at about 3.5 eV (Fig. 58) and assigned to population of the π_3^* molecular orbital. Other vibrational modes in the polycarbonate spectrum also appeared to be enhanced at specific electron-impact energies, but limitations of resolution prevented the mapping out of cross sections for these modes.

2. Resonant excitation of intermolecular modes

One intriguing possibility in the study of resonances in molecules on surfaces is that new decay channels open up. Michaud and Sanche (1987; Sanche, 1988) found evidence for this phenomenon in their study of amorphous ice. Here they observed not only intramolecular vibrational modes in the HREELS spectrum, but also intermolecular (librational) modes due to the coupling between hydrogen-bonded neighbors. The cross sections for excitation of these intermolecular modes (Fig. 62) were found to display resonant structure (at 7–8 eV, the same energy as the intramolecular stretch modes), which the authors associated with molecular anion states known in the gas phase. The presence of the trapped electron modifies the charge density of the (global) system and thus also the potential-energy surfaces on which all of the nuclei in the coupled system move, as discussed in Sec. VI.A.

Another means by which one can excite modes of vibration that are specific to the structure in which the molecule is adsorbed or condensed (e.g., intermolecular modes or molecule-surface modes) is the creation of a resonance localized on a bond which itself only arises from placing a molecule in a particular structural environment. Sanche and Michaud (1984a) drew attention to this possibility in their investigation of condensed NO. The vibrational spectra which the authors obtained were assigned to dimerized NO, and resonances in the cross sections for excitation of the dimer modes were assigned to molecular resonant states of the dimer arising from the overlap of unfilled NO orbitals. A similar notion was employed by de Paola and Hoffmann (1984), in attempting to account for the angular distribution of electrons scattered after exciting two C-O stretch vibrations in the CO/K/Ru(001) system. This angular profile was broad, indicating a short-range electron-molecule interaction, whereas those for the single loss and first vibrational overtone were sharply peaked in the specular direction. The authors speculated that formation of a bimolecular negative-ion state might favor decay into two CO fundamentals. The measurement of a resonance in the cross section for electron stimulated desorption of atomic O on Pt at low energy, reported by Hoffman *et al.* (1989), assigned to a resonant state localized on the O-surface bond and discussed further in Sec. VIII, is another example of this type of phenomenon.

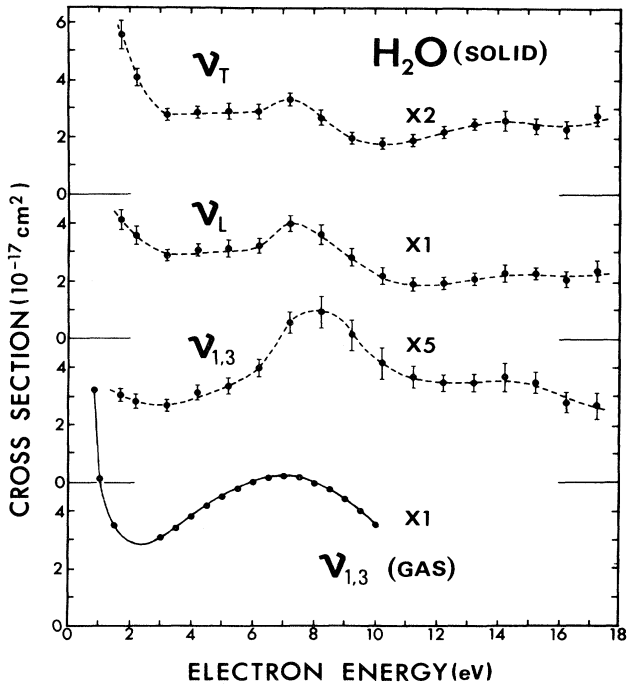

FIG. 62. Cross sections for excitation of the frustrated translational (ν_T), librational (ν_L), and intramolecular stretching ($\nu_{1,3}$) modes of solid H_2O (amorphous ice) as a function of incident-electron beam energy. A resonance is seen in the cross section for each mode at about 7 eV and may be compared with the gas-phase resonance profile of the $\nu_{1,3}$ mode, also shown. Michaud and Sanche (1987).

3. Resonant excitation of molecule-surface modes

In their study of N_2 on Al(111), with higher-energy resolution than used in their previous study of this system (Secs. IV.A.2 and V.A.2), Jacobi and Bertolo (1990; Jacobi, Bertolo, and Hansen, 1990) isolated for the first time a resonance in the cross section for the excitation of a molecule-surface mode, as postulated by Gadzuk (1985).

Figure 63 shows an enlargement of the line shape of the $\nu=0-1$ vibrational mode of monolayer N_2, obtained

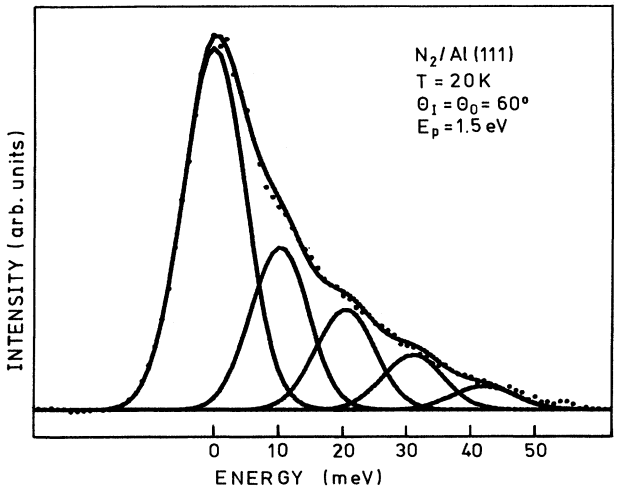

FIG. 63. Detailed line shape of the $\nu=0-1$ vibrational excitation of N_2 physisorbed on Al(111), showing the asymmetry attributed to the simultaneous excitation of molecule-surface vibrational transitions ($\nu=0-n$), modeled by the solid lines shown. Jacobi and Bertolo (1990).

with a beam energy of 1.5 eV. The energy-loss scale on the graph is given with respect to the N_2 stretch mode frequency of 290 meV. The significantly asymmetric line shape was interpreted as corresponding to the excitation of the molecule-surface vibration and its overtones in addition to the N_2 intramolecular stretch mode. Jacobi and Bertolo modeled the line shape by the superposition of Gaussians spaced apart by 10.5 meV, an energy which then corresponds to the frequency of the N_2-surface vibrational mode (this frequency was too low for the pure molecule-surface mode to be resolved from the quasielastic peak in the HREELS spectrum). By contrast, the line shape of the CO fundamental vibration, also obtained at 1.5 eV and in the specular direction, appeared symmetric, consistent with the lack of resonance scattering for that molecule under these conditions. It is of interest to note in the context of discussing the line shape, that the shape of the physisorbed O_2 line recorded by Imbihl and Demuth (1986) in their earlier EELS study of O_2 on Pd(111) appears to show the same asymmetry that Jacobi and Bertolo were later to highlight.

The first explicit observation of the resonant excitation of a molecule-surface mode on a metallic surface was reported recently by Ha and Sibener (1991). They assigned an energy-loss peak at 37.5 meV in the HREELS spectrum of CO chemisorbed on Ni(111), obtained far from the specular direction, to a frustrated rotation of the bridge-bonded molecule. The excitation functions of this mode and the C-O stretch mode (also obtained far from specular, towards the surface normal) showed a resonance centered at 18 eV, attributed to the familiar $^2\Sigma$ negative-ion resonance of the CO molecule. The angular distribution of the intensity of the frustrated rotational mode of the upright CO molecule was also consistent with the $^2\Sigma$ resonance; the intensity increased monotonically as the detector was moved towards the surface normal, just as Jones and co-workers (Jones *et al.*, 1989) found in the case of the $^2\Sigma$ resonance of (upright) CO on Ni(110) (Sec. V.A.2).

4. Resonant excitation of rotational modes

While most studies of resonance electron scattering by adsorbed molecules have been concerned with vibrational excitation, the rotational states of the H_2 molecule can be observed in HREELS as a consequence of the smallness of the molecule's moment of inertia, which pushes the rotational excitation energies away from the quasielastic peak in which the rotational states of most other molecules are buried. A number of studies (Avouris *et al.*, 1982; Andersson and Harris, 1982, 1983; Palmer and Willis, 1987) have detected rotational excitations in physisorbed H_2. In each system investigated, the rotational frequencies turned out to be very similar to those of the gas-phase molecule, indicating that in each case the rotation of the molecule was not strongly hindered by the surface. Although the cross sections for rotational excitation as a function of electron-impact energy were not reported in these experiments, the impact energies at which all the spectra were recorded are compatible with resonant rotational excitation via the $^2\Sigma_u^+$ negative-ion resonance of H_2, observed in the rotational excitation of the molecule in the gas phase (Wong and Schulz, 1974) and also in the cross section for vibrational excitation of physisorbed H_2 (Demuth *et al.*, 1981). These results suggest the possibility of observing resonant excitation of the low-frequency hindered rotational modes which arise when molecules are adsorbed on surfaces, in addition to the low-frequency molecule-surface vibrational modes discussed in the previous section. Indeed, the results of Ha and Sibener, also discussed in the previous section, appear to represent a first observation of this phenomenon.

5. Branching ratios in resonance decay

An interesting feature of the results for condensed O_2 obtained by Sanche and Michaud (1981), discussed in Sec. IV.A.2, was the observation that the excitation functions of the various O_2 overtones showed maxima at different energies; the peaks shifted to higher energy as the quantum number of the overtone increased (Fig. 64). The authors speculated that this effect might have its origin in the two negative-ion resonances, the $^2\Pi_u$ state and the $^4\Sigma_u$ state, which, according to calculations, intercept the Franck-Condon region at 6–8 eV and 8–12 eV, respectively (Das *et al.*, 1978). Then, if the relative cross sections for exciting the series of O_2 overtones differ from one resonance to another, an effect like the one observed could occur. Subsequent studies of (monolayer) phy-

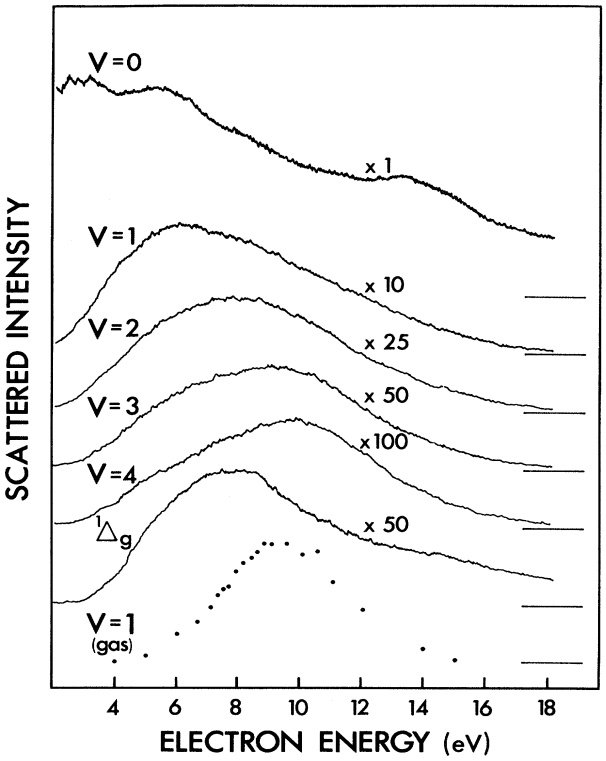

FIG. 64. Excitation functions for the $v=0-n$ vibrational transitions (and the $X^3\Sigma_g^- \rightarrow a\,^1\Delta_g$ electronic transition) of O_2 condensed in a multilayer film. The peak energy of the resonance in the vibrational transition cross sections shifts as a function of n, the resonance decay channel. The elastic reflectivity ($v=0-0$) of the film and the excitation function of the $v=0-1$ transition in the gas phase are also shown for comparison. Sanche and Michaud (1981a).

sisorbed O_2 on graphite (Barnard and Palmer, 1992b) failed to reproduce this effect, but it is possible that the effect is a function of the degree of order and molecular orientation in the film in question. It may be worth remarking that a result of the kind reported by Sanche and Michaud could arise spuriously, if the transmission function of the electron analyzer varied with the electron energy loss.

VII. FUTURE DIRECTIONS

A. Unrecognized resonances?

In assessing how the field of resonance electron scattering by molecules on surfaces may develop in the future, it is helpful to take stock of the number of systems in which one might expect to see such resonances. It is worth bearing in mind that the majority of the numerous HREELS studies of adsorbed molecules reported in the literature have been concerned with electron scattering in or near the specular direction. The prime focus of many of these studies has been a determination of the vibrational frequencies of the adsorbed species, with a view to deriving information about the structure and chemical state of the adsorbate. For the same reason, the energy dependence of the vibrational mode intensities has often been of little concern. The investigations of the angular distributions in resonance electron scattering reviewed in this article make it plain that the specular direction has no special place in the resonance scattering cross sections. In general, then, the resonance scattering cross section will reach a maximum at some angle (possibly far) away from the specular direction. The observation of resonances also requires, of course, that one searches through the electron-impact energy till one finds the energy of the resonance. The observations of resonances in electron scattering by both physisorbed and chemisorbed molecules which we have discussed suggest to us that resonance scattering by molecules on surfaces may be an extremely widespread phenomenon, and that it might be observable, for example, in very many of the adsorption systems that have already been investigated by HREELS in studies having other priorities. A good example of the support for this idea is the resonance reported in the chemisorbed CO molecule at 18 eV (Jones, Ashton, Ding, and Richardson, 1989; Richardson and Jones, 1990; Jones and Richardson, 1990) and reviewed in Sec. V.A.2. There have been very many studies of chemisorbed CO with HREELS, but these have largely been confined to near-specular scattering, and the work of Jones and coworkers shows the need to move far away from the specular direction, both to sieve out the dipole contribution to the electron-scattering cross section and to find the maximum in the resonance scattering cross section at the energy of the resonance. Thus, in considering what remains to be learnt about the nature of resonance scattering by molecules on surfaces and how resonance scattering might be exploited as an analytical tool, it is our contention that resonances may be observable in numerous surface systems, provided that one has the capability to tune through the electron-impact energy and to detect electrons scattered through a wide angle.

B. Development of the theoretical models

The theoretical models described in this review article represent a description of resonance scattering that is still in its infancy, and the limitations of the current approaches have been indicated in the text. A particular comparison one might make in the future is between these descriptions of resonant states on surfaces and the state-of-the-art computational approaches to the calculation of the valence levels of adsorbed molecules and surface electronic structure. Clearly, there is a need to begin to apply the types of approaches employed for the evaluation of electronic structure of occupied states at surfaces to unoccupied or quasibound states which encompass the type of resonance phenomena we have described. A particularly desirable goal would be to couple the type of calculations now available for the description of resonances in free molecules (Burke *et al.*, 1977) to those of

surface electronic structure (e.g., the Layer-KKR approach).

The development of a more comprehensive theoretical description of the resonance scattering process would hopefully throw more light onto a number of unresolved issues pertaining to resonance scattering from adsorbates:

(i) To what extent do the current theories of resonance scattering from adsorption represent a universal picture of resonant states at surfaces? We feel that the apparent universality of lifetime reduction and resonance energy shifting may be more a function of the similarity of the theoretical models, rather than an intrinsic feature of resonance electron scattering. It is our belief that there is considerable motivation to begin a study of the effect of the form of the metallic band structure upon adsorbate resonant states.

(ii) To what extent does the formation of a strong bond between the surface and the molecule influence the resonant state and the excitation of vibrations? Such a study would be especially relevant to resonances in chemisorbed molecules.

(iii) Under what circumstances can a resonance be quenched? In particular, one might ask whether quenching always requires the direct distortion of the molecular electronic structure or whether a weakly bound system can be subject to quenching by short-range multiple-scattering effects and/or the long-range image potential.

(iv) What is the effect of coadsorbates upon resonance electron scattering? In particular, one may wish to study coadsorbate interactions through long-range electrostatic fields and the direct interaction of molecular orbitals. We anticipate that cases involving polar coadsorbates may be of particular interest.

C. Applications of resonance electron scattering

1. Vibrational states

While most studies of vibrational excitation via resonance electron scattering reported so far have dealt with intramolecular vibrational modes, the recent studies of the excitation of intermolecular and molecule-surface modes reviewed in Secs. VI.B.2 and VI.B.3 indicate that new vibrational decay channels open on the surface. The enhanced excitation of the low-frequency vibrational modes of an adsorbed molecule, i.e., molecule-surface modes and intermolecular modes, in resonance electron scattering suggests an important area of application for the "technique," since these low-frequency modes, which exist only when the molecule is adsorbed on the surface, play a significant role in various surface dynamical processes, such as molecular diffusion over the surface and desorption. The latest generation of HREELS spectrometers, capable of energy resolution down to around 1 meV and very high signal levels, are ideally equipped to exploit the resonance scattering mechanism in determining the frequencies, anharmonicities, and temperature dependent populations of such vibrational modes.

The cross sections for the excitation of vibrational overtones in resonance scattering are relatively large, and this suggests another contribution that resonance scattering can make to vibrational spectroscopy. Apart from the measurement of the frequencies of the overtones, which has already been used to measure the anharmonicity of the intramolecular potential well in adsorbed molecules (Schmeisser *et al.*, 1982; Demuth *et al.*, 1983), we have the prospect of using the new generation of high-resolution spectrometers to make accurate measurements of the line shapes of these high-lying vibrational modes. High-resolution infrared absorption experiments have been used to analyze the line shapes of dipole active $\nu=0-1$ vibrational transitions, providing insights into, for example, the relaxation dynamics of the vibrationally excited state and dephasing mechanisms resulting from vibrational mode coupling on the surface (Chabal, 1988). We suggest that resonance scattering with high resolution may be used to derive similar information about the higher-lying vibrational states which are inaccessible in infrared measurements and which are important in probing the higher-lying reaches of the potential-energy surface.

2. Electronic structure

Resonance electron scattering is a probe of surface electronic structure as well as vibrational properties. While one can hardly compare the scale of what might be learnt about electronic states at the surface from resonance scattering with what can be learnt from techniques like photoemission and inverse photoemission, it seems to us that there is a niche in which resonance scattering can make a helpful contribution. This contention arises from the fact that the numerous molecular resonances that have been observed in gas-phase experiments are, at least in many cases, extremely well characterized, both experimentally and theoretically. The properties (energy, lifetime, symmetry, decay channels) of the resonances that can be observed in electron scattering by adsorbed molecules can be compared with the well-documented properties of the gas-phase model, so that one can, in effect, take a well-defined "model" molecular electronic state, bring it up to the surface, and investigate how it is perturbed. This offers the advantage over inverse photoemission, perhaps the best known probe of the unoccupied electronic states of molecules on surfaces, of allowing one to choose the same decay channel, e.g., intramolecular vibrational excitation, used to characterize the resonance in the gas phase (recall that the resonance profile is, in general, a function of the decay channel).

3. Geometric structure

In Secs. V.A and V.B we saw that the angular distributions in resonance scattering are a sensitive function of

the orientation of the molecule on the surface. Indeed, the first theoretical treatment of resonance scattering by (isolated) oriented molecules by Davenport *et al.* (1978) speculated that the angular distributions might be used to determine adsorbate molecular orientation. One thing that is clear from the studies reported is that one cannot simply read off the molecular orientation from the form of the measured angular distribution. Apart from the fact that the angular distributions also depend on the symmetry of the molecular resonance in question, which one therefore has to be sure of, we have seen that multiple elastic electron scattering by the surface modulates the angular distributions expected of an isolated, oriented molecule. Nevertheless, in cases where the symmetry of a corresponding gas-phase resonance is known and is not too strongly perturbed on the surface, and with the guidance of the symmetry selection rules discussed in Sec. V.A, it appears that the orientation of the molecule can be quantitatively determined in a useful fashion by comparison of the measured angular distribution with model calculations. In the cases where this procedure has been carefully implemented (Sec. V.A.2), the results obtained have been consistent with those expected on the basis of molecular packing arguments. But numerous experimental probes of surface structure have now been developed, and one has to make an evaluation of whether resonance scattering has a genuine future as a structural probe in competition with these techniques.

Low-energy electron diffraction (LEED) has developed into the most widely used surface structural tool, but the number of molecular overlayers whose structure has been determined by this method is limited (Rous, 1991b). There are two reasons for this. The first is that molecular overlayer systems produce an enormous parameter space over which the LEED structure analysis must search. Secondly, LEED is not species specific, in that the LEED experiment collects electrons scattered by all the atoms and molecules in the surface region. The virtue of resonance electron scattering as a probe of molecular orientation is that the angular distributions obtained by detecting electrons scattered with a characteristic energy loss (arising from, say, the excitation of a molecular vibrational mode) necessarily reflect the orientation of the particular molecular species (or bond) in which the resonance is localized. Additionally, the selection rules governing the angular distributions observed in resonance scattering by molecules adsorbed in structural configurations of high symmetry, which may be used to home in on the orientation of the molecule prior to a detailed multiple-scattering calculation of the full angular distribution, have no parallel in LEED. These advantages, i.e., molecule specificity and the existence of selection rules to simplify the interpretation (in favorable cases), do have a parallel in the technique of near-edge x-ray-absorption fine structure (NEXAFS) measurement (Woodruff, 1986). Indeed, one may argue that NEXAFS is a superior technique to resonance electron scattering in that the analysis of the angular distributions obtained in NEXAFS depends purely upon the symmetry of the resonant states to which the core electron is excited, i.e., there is no multiple scattering with which to contend. In sum, our belief is that resonance electron scattering may be a useful probe of the molecular orientation of adsorbed molecules for those who have ready access to a laboratory-based HREELS spectrometer but not to the synchrotron needed for NEXAFS measurements.

One interesting idea, which arises from considering the influence of multiple elastic scattering on the angular distribution of scattered electrons in resonance scattering, is the possibility of using these angular distributions to determine the local crystallographic structure of a molecular array with high density but without long-range order. The inelastic mean free path of electrons with an energy in the range where resonances are commonly observed (<30 eV) is typically not more than a few lattice spacings. This mean free path determines the range of the coherent scattering which distorts the angular distribution expected of an isolated, oriented molecule. Consequently, the angular distributions observed in resonance scattering are, in effect, a probe of the local crystal structure. The recent work of Barnard and Palmer (1992a), who explored the local structure of the fluid phases of O_2 on graphite, is an example of the application of resonance scattering to this type of problem.

D. Resonances in electron scattering by atoms on surfaces

This review has been concerned with resonances in electron scattering by molecules on surfaces. We still await the first report of resonances in electron scattering by adsorbed atoms, of the kind well known in gas-phase studies (Schulz, 1973a). These resonances manifest themselves in the cross sections for elastic scattering and for electronic excitation of the atom. In the case of an atom on a surface, it might be difficult to observe a resonance in the elastic channel, because of contributions to the elastic-scattering signal from diffraction and diffuse elastic scattering by the surface. On the other hand, a resonance in the cross section for electronic excitation of the atom might be easier to see. Moreover, when an atom is adsorbed on a surface, new decay channels open up into which the atomic resonance might decay. In particular, one might see a resonance in the cross section for excitation of the vibration of the atom against the surface. This decay channel would parallel the decay of a molecular resonance into the vibration of the molecule against the surface, reviewed in Sec. VI.B.3. Further credence is lent to this notion by the experiments of Hoffmann *et al.* (1989), who measured the cross section for electron stimulated desorption of atomic oxygen chemisorbed on Pd(111) and found a resonance at an electron-impact energy of about 10 eV, which they attributed to the formation of an atomic negative ion. It could be that there are many similar resonances waiting to be observed in the

cross sections for excitation of atom-surface vibrational modes.

REFERENCES

Allan, M., 1989, J. Electron Spectrosc. Relat. Phenom. **48**, 219.
Andersson, S., 1979, Surf. Sci. **89**, 477.
Andersson, S., and J. W. Davenport, 1978, Solid State Commun. **28**, 677.
Andersson, S., and J. Harris, 1982, Phys. Rev. Lett. **48**, 545.
Andersson, S., and J. Harris, 1983, Phys. Rev. B **27**, 9.
Apai, G., and W. P. McKenna, 1991, Langmuir **7**, 2266.
Avouris, Ph., and J. E. Demuth, 1984, Annu. Rev. Phys. Chem. **35**, 49.
Avouris, Ph., D. Schmeisser, and J. E. Demuth, 1982, Phys. Rev. Lett. **48**, 199.
Azria, R., and G. J. Schulz, 1975, J. Chem. Phys. **62**, 573.
Barnard, J. C., and R. E. Palmer, 1992a, Surf Sci. (in press).
Barnard, J. C., and R. E. Palmer, 1992b, unpublished.
Baro, A. M., and H. Ibach, 1981, Surf. Sci. **103**, 248.
Birtwistle, D. T., and A. Herzenberg, 1971, J. Phys. B **4**, 53.
Burke, P. G., I. Mackey, and I. Shimamura, 1977, J. Phys. B **10**, 2497.
Chabal, Y. J., 1988, Surf. Sci. Rep. **8**, 211.
Chang, E. S., 1977, J. Phys. B **10**, L677.
Christophorou, L. G., 1984, Ed., *Electron-Molecule Interactions and Their Applications* (Academic, Orlando).
Cloutier, P., and L. Sanche, 1989, Rev. Sci. Instrum. **60**, 1054.
Cohen-Tannoudji, C., B. Diu, and F. Laloë, 1977, *Quantum Mechanics* (Wiley Interscience, New York), see p. 564ff.
Danese, J. B., and J. W. D. Connolly, 1974, J. Chem. Phys. **61**, 3063.
Das, G., A. C. Wahl, W. T. Zemke, and W. C. Stwalley, 1978, J. Chem. Phys. **68**, 4252.
Davenport, J. W., W. Ho, and J. R. Schrieffer, 1978, Phys. Rev. B **17**, 3115.
Demuth, J. E., Ph. Avouris, and D. Schmeisser, 1983, J. Electron Spectrosc. Relat. Phenom. **29**, 163.
Demuth, J. E., D. Schmeisser, and Ph. Avouris, 1981, Phys. Rev. Lett. **47**, 1166.
de Paola, R. A., and F. M. Hoffmann, 1984, Phys. Rev. B **30**, 1122.
Farrell, H. H., J. A. Schaefer, J. Q. Broughton, and J. C. Bean, 1985, in *The Structure of Surfaces,* edited by M. A. Van Hove and S. Y. Tong (Springer, Berlin), p. 163.
Gadzuk, J. W., 1983, J. Chem. Phys. **79**, 3982.
Gadzuk, J. W., 1985, Phys. Rev. B **31**, 6789.
Gadzuk, J. W., 1987, in *Vibrational Spectroscopy of Molecules on Surfaces,* edited by J. T. Yates, Jr., and T. E. Madey (Plenum, New York), p. 49.
Gadzuk, J. W., 1988, Annu. Rev. Phys. Chem. **39**, 395.
Gadzuk, J. W., S. Holloway, C. Mariani, and K. Horn, 1982, Phys. Rev. Lett. **48**, 1288.
Gadzuk, J. W., L. J. Richter, S. A. Buntin, D. S. King, and R. R. Cavanagh, 1990, Surf. Sci. **235**, 317.
Gasiorowicz, S., 1974, *Quantum Physics* (Wiley, New York).
Gerber, A., and A. Herzenberg, 1985, Phys. Rev. B **31**, 6219.
Ha, J. S., and S. J. Sibener, 1991, Surf. Sci. **256**, 281.
Hansen, W., M. Bertolo, and K. Jacobi, 1991, Surf. Sci. **253**, 1.
Haochang, P., T. C. M. Horn, and A. W. Kleyn, 1986, Phys. Rev. Lett. **57**, 3035.
Hock, K. M., and R. E. Palmer, 1992, unpublished.
Hoffman, A., X. Guo, J. T. Yates, Jr., J. W. Gadzuk, and C. W. Clark, 1989, J. Chem. Phys. **90**, 5793.
Holloway, S., and J. W. Gadzuk, 1985, J. Chem. Phys. **82**, 5203.
Ibach, H., 1982, J. Mol. Struct. **79**, 129.
Ibach, H., 1990, in *Interaction of Atoms and Molecules with Surfaces,* edited by V. Bortolani, N. H. March, and M. P. Tosi (Plenum, New York), p. 338.
Ibach, H., 1991, *Electron Energy Loss Spectroscopy: The Technology of High Performance,* Springer Series in Optical Sciences, Vol. 63 (Springer, Berlin).
Ibach, H., and D. L. Mills, 1982, *Electron Energy Loss Spectroscopy and Surface Vibrations* (Academic, New York).
Imbihl, R., and J. E. Demuth, 1986, Surf. Sci. **173**, 395.
Jacobi, K., C. Astaldi, P. Geng, and M. Bertolo, 1989, Surf. Sci. **223**, 569.
Jacobi, K., and M. Bertolo, 1990, Phys. Rev. B **42**, 3733.
Jacobi, K., M. Bertolo, P. Geng, W. Hansen, and C. Astaldi, 1990, Chem. Phys. Lett. **173**, 97.
Jacobi, K., M. Bertolo, and W. Hansen, 1990, J. Electron Spectrosc. Relat. Phenom. **54/55**, 529.
Jensen, E. T., and R. E. Palmer, 1990, Surf. Sci. **233**, 269.
Jensen, E. T., R. E. Palmer, and P. J. Rous, 1990a, Phys. Rev. Lett. **64**, 1301.
Jensen, E. T., R. E. Palmer, and P. J. Rous, 1990b, Chem. Phys. Lett. **169**, 204.
Jensen, E. T., R. E. Palmer, and P. J. Rous, 1990c, Surf. Sci. **237**, 153.
Jensen, E. T., R. E. Palmer, and P. J. Rous, 1990d, J. Electron Spectrosc. Relat. Phenom. **54/55**, 519.
Jones, T. S., M. R. Ashton, and N. V. Richardson, 1989, J. Chem. Phys. **90**, 7564.
Jones, T. S., M. R. Ashton, M. Q. Ding, and N. V. Richardson, 1989, Chem. Phys. Lett. **161**, 467.
Jones, T. S., and N. V. Richardson, 1988, Phys. Rev. Lett. **61**, 1752.
Jones, T. S., and N. V. Richardson, 1989, Surf. Sci. **211/212**, 377.
Jones, T. S., and N. V. Richardson, 1990, Vacuum **41**, 240.
Kesmodel, L. L., 1984, Phys. Rev. Lett. **53**, 1001.
Kohn, W., and N. Rostocker, 1954, Phys. Rev. **94**, 1111.
Korringa, J., 1947, Physica **13**, 392.
Liebsch, A., 1978, in *Photoemission and the Electronic Properties of Surfaces,* edited by B. Feuerbacher, B. Fitton, and R. F. Willis (Wiley, New York), p. 167.
Liehr, M., P. A. Thiry, J. J. Pireaux, and R. Caudano, 1985a, Phys. Rev. B **31**, 42.
Liehr, M., P. A. Thiry, J. J. Pireaux, and R. Caudano, 1985b, J. Vac. Sci. Technol. A **3**, 1645.
Messmer, R. P., 1979, in *The Nature of The Surface Chemical Bond,* edited by T. N. Rhodin and G. Ertl (North-Holland, Amsterdam).
Michaud, M., and L. Sanche, 1987, Phys. Rev. Lett. **59**, 645.
Michaud, M., and L. Sanche, 1990, J. Electron Spectrosc. Relat. Phenom. **51**, 237.
Nilsson, A., 1991, private communication.
Nilsson, A., and N. Mrtensson, 1989, Phys. Rev. Lett. **63**, 1483.
Nishijima, M., K. Edamato, Y. Kubota, S. Tanaka, and M. Onchi, 1986, J. Chem. Phys. **84**, 6458.
Noble, C. J., and P. G. Burke, 1986, J. Phys. B **19**, L35.
Nordlander, P., and J. C. Tully, 1990, Phys. Rev. B **42**, 5564.
Otto, A., T. Bornemann, U. Erturk, I. Mrozek, and C. Pettenkofer, 1989, Surf. Sci. **210**, 363.

Palmer, R. E., 1992, Prog. Surf. Sci (to be published).
Palmer, R. E., J. F. Annett, and R. F. Willis, 1986, J. Electron Spectrosc. Relat. Phenom. **38**, 317.
Palmer, R. E., E. T. Jensen, and P. J. Rous, 1990, Vacuum **41**, 740.
Palmer, R. E., P. J. Rous, J. L. Wilkes, and R. F. Willis, 1988, Phys. Rev. Lett. **60**, 329.
Palmer, R. E., P. J. Rous, and R. F. Willis, 1988, in *Electron-Molecule Scattering and Photoionization,* edited by P. G. Burke and J. B. West (Plenum, New York), p. 123.
Palmer, R. E., J. L. Wilkes, and R. F. Willis, 1987, J. Electron Spectrosc. Relat. Phenom. **44**, 229.
Palmer, R. E., J. L. Wilkes, and R. F. Willis, 1988, Vacuum **38**, 271.
Palmer, R. E., and R. F. Willis, 1987, Surf. Sci. **179**, L1.
Pendry, J. B., 1978, in *Photoemission and the Electronic Properties of Surfaces,* edited by B. Feuerbacher, B. Fitton and R. F. Willis (Wiley, New York), p. 87.
Persson, B. N. J., 1980, Surf. Sci. **92**, 265.
Pireaux, J. J., P. A. Thiry, R. Caudano, and P. Pfluger, 1986, J. Chem. Phys. **84**, 6452.
Plummer, E. W., and T. Gustafsson, 1977, Science **198**, 165.
Richardson, N. V., and T. S. Jones, 1990, Appl. Phys. A **51**, 126.
Rous, P. J., 1991a, in *The Structure of Surfaces III,* edited by M. A. Van Hove and S. Y. Tong (Springer, Berlin), p. 118.
Rous, P. J., 1991b, Surf. Sci. **260**, 361.
Rous, P. J., E. T. Jensen, and R. E. Palmer, 1989, Phys. Rev. Lett. **63**, 2496.
Rous, P. J., and R. E. Palmer, 1989, J. Phys.: Condensed Matter **1**, SB225.
Rous, P. J., R. E. Palmer, and E. T. Jensen, 1990, Phys. Rev. B **41**, 4793.
Rous, P. J., R. E. Palmer, and R. F. Willis, 1989, Phys. Rev. B **39**, 7552.
Roy, D., and D. Tremblay, 1990, Rep. Prog. Phys. **53**, 1621.
Sakurai, M., T. Okano, and Y. Tuzi, 1987a, J. Vac. Sci. Technol. A **5**, 431.
Sakurai, M., T. Okano, and Y. Tuzi, 1987b, Jpn. J. Appl. Phys. **26**, L1651.
Sanche, L., 1988, Radiat. Phys. Chem. **32**, 269.
Sanche, L., 1989, Radiat. Phys. Chem. **34**, 15.
Sanche, L., 1990, J. Phys. B **23**, 1597.
Sanche, L., and M. Michaud, 1981a, Phys. Rev. Lett. **47**, 1008.
Sanche, L., and M. Michaud, 1981b, Chem. Phys. Lett. **84**, 497.
Sanche, L., and M. Michaud, 1983, Phys. Rev. B **27**, 3856.
Sanche, L., and M. Michaud, 1984a, J. Chem. Phys. **81**, 257.
Sanche, L., and M. Michaud, 1984b, Phys. Rev. B **30**, 6078.
Schmeisser, D., J. E. Demuth, and Ph. Avouris, 1982, Phys. Rev. B **26**, 4857.
Schulz, G. J., 1973a, Rev. Mod. Phys. **45**, 378.
Schulz, G. J., 1973b, Rev. Mod. Phys. **45**, 423.
Schulz, G. J., 1976, in *Principles of Laser Plasmas,* edited by G. Bekefi (Wiley, New York), Chap. 2.
Schulz, G. J., 1979, in *Electron-Molecule Scattering,* edited by S. C. Brown (Wiley, New York), p. 1.
Smith, N. V., and D. P. Woodruff, 1986, Prog. Surf. Sci. **21**, 295.
Sporken, R., P. A. Thiry, J. J. Pireaux, R. Caudano, and A. Adnot, 1985, Surf. Sci. **160**, 443.
Stucki, F., J. Anderson, G. J. Lapeyre, and H. H. Farrell, 1984, Surf. Sci. **143**, 84.
Teillet-Billy, D., and J. P. Gauyacq, 1990, Surf. Sci. **239**, 343.
Teillet-Billy, D., and J. P. Gauyacq, 1991, Nucl. Instrum. Methods **B58**, 393.
Thiry, P. A., M. Liehr, J. J. Pireaux, and R. Caudano, 1987, Phys. Scr. **35**, 368.
Timbrell, P. Y., A. J. Gellman, R. M. Lambert, and R. F. Willis, 1988, Surf. Sci. **206**, 339.
Toney, M. F., and S. C. Fain, Jr., 1984, Phys. Rev. B **30**, 1115.
Toney, M. F., and S. C. Fain, Jr., 1987, Phys. Rev. B **36**, 1248.
Tronc, M., R. Azria, and Y. Le Coat, 1980, J. Phys. B **13**, 2327.
Tronc, M., R. Azria, and R. Paineau, 1979, J. Phys. Lett. **40**, L323.
van den Hoek, P. J., and E. J. Baerends, 1989, Surf. Sci. **221**, L791.
Van Hove, M. A., W. H. Weinberg, and C.-M. Chan, 1986, *Low Energy Electron Diffraction* (Springer, Berlin).
Waddill, G. D., and L. L. Kesmodel, 1985, Phys. Rev. B **32**, 2107.
Waddill, G. D., and L. L. Kesmodel, 1986a, Chem. Phys. Lett. **128**, 208.
Waddill, G. D., and L. L. Kesmodel, 1986b, J. Vac. Sci. Technol. A **4**, 1303.
Wandass, J. H., and J. A. Gardella, Jr., 1986, Langmuir **2**, 543.
Wandass, J. H., and J. A. Gardella, Jr., 1987, Langmuir **3**, 183.
Willis, R. F., 1980, in *Vibrational Spectroscopy of Adsorbates,* edited by R. F. Willis, Series in Chemical Physics No. 15 (Springer, Berlin), p. 23.
Woodruff, D. P., 1986, Rep. Prog. Phys. **49**, 683.
Wong, S. F., M. J. W. Boness, and G. J. Schulz, 1973, Phys. Rev. Lett. **31**, 969.
Wong, S. F., and G. J. Schulz, 1974, Phys. Rev. Lett. **32**, 1089.
Wong, S. F., and G. J. Schulz, 1975, Phys. Rev. Lett. **35**, 1429.
Xu, M-L., B. M. Hall, S. Y. Tong, M. Rocca, H. Ibach, S. Lehwald, and J. E. Black, 1985, Phys. Rev. Lett. **54**, 1171.
Zangwill, A., 1988, *Physics at Surfaces* (Cambridge University, Cambridge, U.K.), Chapters 8 and 9.
Zhou, X.-L., X.-Y. Zhu, and J. M. White, 1991, Surf. Sci. Rep. **13**, 73.

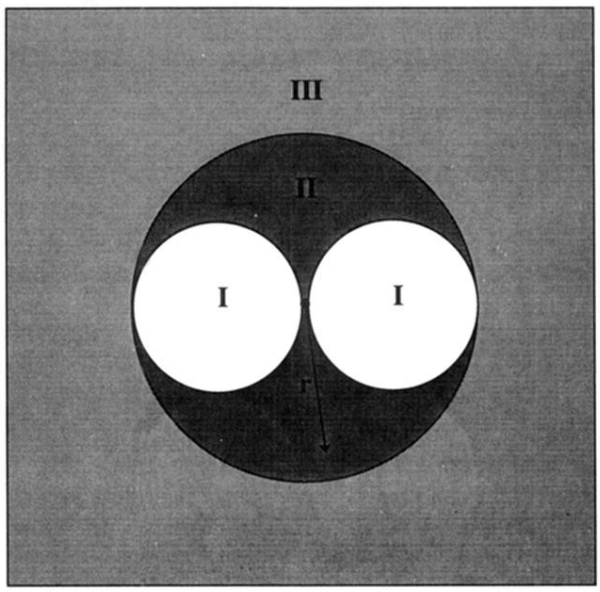

FIG. 28. A schematic diagram of the partitioning of the molecular potential of a diatomic molecule into three nonoverlapping regions, used by Davenport (1978) to evaluate the differential cross section from resonance electron scattering from oriented molecules. Region I, the atomic spheres. Region II, the interstitial potential (averaged to a constant). Region III lies beyond the outer sphere.

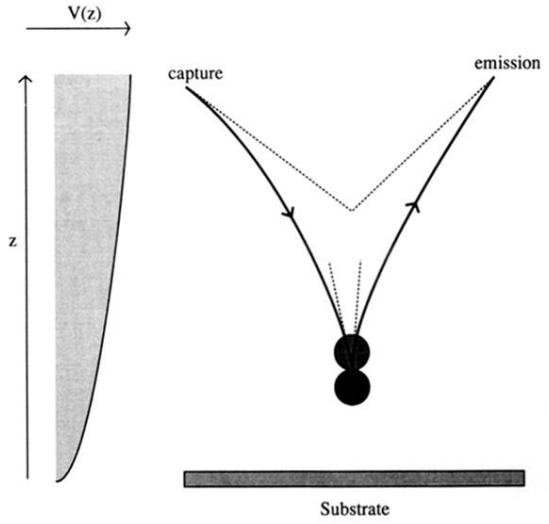

FIG. 32. Schematic diagram of the classical trajectory followed by the probe electron through a classical image potential before and after the formation of a molecular negative ion.